



# Lawrence Berkeley Laboratory

UNIVERSITY OF CALIFORNIA

## Materials & Molecular Research Division

RECEIVED  
LAWRENCE  
BERKELEY LABORATORY

MAY 17 1983

LIBRARY AND  
DOCUMENTS SECTION

THE MAGNETORESISTANCE, ELECTRICAL CONDUCTIVITY  
AND HALL EFFECT OF GLASSY CARBON

Dennis Frank Baker  
(Ph.D. Thesis)

February 1983

### TWO-WEEK LOAN COPY

*This is a Library Circulating Copy  
which may be borrowed for two weeks.*

*For a personal retention copy, call  
Tech. Info. Division, Ext. 6782.*



LBL-13652 <sup>c2</sup>

## DISCLAIMER

This document was prepared as an account of work sponsored by the United States Government. While this document is believed to contain correct information, neither the United States Government nor any agency thereof, nor the Regents of the University of California, nor any of their employees, makes any warranty, express or implied, or assumes any legal responsibility for the accuracy, completeness, or usefulness of any information, apparatus, product, or process disclosed, or represents that its use would not infringe privately owned rights. Reference herein to any specific commercial product, process, or service by its trade name, trademark, manufacturer, or otherwise, does not necessarily constitute or imply its endorsement, recommendation, or favoring by the United States Government or any agency thereof, or the Regents of the University of California. The views and opinions of authors expressed herein do not necessarily state or reflect those of the United States Government or any agency thereof or the Regents of the University of California.

LBL-13652

**THE MAGNETORESISTANCE, ELECTRICAL CONDUCTIVITY  
AND HALL EFFECT OF GLASSY CARBON**

Dennis Frank Baker

Ph.D. Thesis

Materials and Molecular Research Division  
Lawrence Berkeley Laboratory  
University of California  
Berkeley, California 94720

February 1983

This work was supported by the Director, Office of Energy Research,  
Office of Basic Energy Sciences, Material Sciences Division of the  
U.S. Department of Energy under Contract No. DE-AC03-76SF00098.

TABLE OF CONTENTS

Abstract . . . . .	v
Acknowledgements . . . . .	xiii
I. Introduction . . . . .	1
II. Experimental . . . . .	10
III. Results . . . . .	11
IV. Discussion . . . . .	13
A. Magnetoresistance . . . . .	13
B. Electrical Conductivity . . . . .	22
C. Hall Effect . . . . .	25
D. Correlation with Microstructure . . . . .	26
V. Conclusions and Recommendations . . . . .	29
References . . . . .	33
Figure Captions . . . . .	49
Figures . . . . .	55
Appendices . . . . .	109
A. Experimental Detail . . . . .	109
1. Specimen Preparation . . . . .	109
2. Phenomenological Theory, Experiment Design and Instrumentation . . . . .	113
3. Cryogenic Procedures . . . . .	124
References for Appendix A . . . . .	130
Figures Captions for Appendix A . . . . .	132
Figures for Appendix A . . . . .	133

B.	Electrical Conductivity Mechanisms . . . . .	.138
1.	Metallic Conductivity . . . . .	.138
2.	Variable Range Hopping . . . . .	.140
	References for Appendix B . . . . .	.144
C.	Hall Effect Mechanisms . . . . .	.149
	References for Appendix C . . . . .	.153
D.	Curie-Pauli Negative Magnetoresistance Parameters . . .	.155
E.	Kobayashi Model Parameters . . . . .	.157
F.	Bright Model Parameters . . . . .	.159
G.	Electrical Conductivity Model Parameters . . . . .	.160

THE MAGNETORESISTANCE, ELECTRICAL CONDUCTIVITY  
AND HALL EFFECT OF GLASSY CARBON

ABSTRACT

The magnetoresistance, electrical conductivity and Hall effect of glassy carbon heat treated for three hours between 1200 and 2700°C was measured at temperatures from 3 to 300°K in magnetic fields up to 5 tesla.

The magnetoresistance was generally negative and saturated with reciprocal temperature, but still increased as a function of magnetic field. The maximum negative magnetoresistance measured was 2.2% for 2700°C material. Several empirical models based on the idea that negative magnetoresistance is proportional to the square of the magnetic moment were attempted; the best fit was obtained for the simplest model combining Curie and Pauli paramagnetism for heat treatment temperatures greater than 1600°C. The proportionality parameters increased approximately linearly with heat treatment temperature. Positive magnetoresistance was found only in less than 1600°C treated glassy carbon for low measurement temperatures.

The electrical conductivity, of the order of 200 (ohm-cm)<sup>-1</sup> at room temperature, can be empirically written

$$\sigma = A + B \exp(-CT^{-1/4}) - DT^{-1/2}$$

where the first term is a strongly scattering metallic component the second term is attributed to variable range hopping, and the third and new term is a negative correction to the metallic conductivity associated with one-dimensionality. All of the constants A, B, and C were insensitive to heat treatment temperature; the constant D decreased with increasing temperature until it disappeared at about 2200°C.

The Hall coefficient was independent of magnetic field, insensitive to temperature, but was a strong function of heat treatment temperature, crossing over from negative to positive at about 1700°C and ranging from -0.048 to 0.126 cm<sup>3</sup>/coul.

The idea of one-dimensional filaments in glassy carbon suggested by the electrical conductivity is compatible with the present consensus view of the microstructure constructed through such means as lattice imaging in transmission electron microscopy, and x-ray diffraction and small angle scattering.

### ACKNOWLEDGEMENTS

Thanks are in order to the Lawrence Berkeley Laboratory Materials and Molecular Research Division technical staff in Building 62, especially Jim Severns, Glen Baum, Herb Riebe, and Weyland Wong, for their help in fixing, patching, and maintaining the cryostat, the electronic instruments associated with the experiment, and in the preparation of the specimens. I would also like to thank Dick Wolgast, Don Hunt, and Ming Hui for their work on the design of the rebuilt cryostat insert, and Bill Lee and Frank Maxwell for its construction. Thanks are also in order to Dr. William S. Gilbert for his advice and help regarding the superconducting magnet. I would like to acknowledge Gloria Pelatowski for drafting the line drawings and Sharon Kerst for typing the manuscript. Again I would like to thank Dr. A. S. Rao for preparing the transmission electron microscope specimens and Dr. Ron Gronsky for his lattice imaging work.

Special thanks are due to the members of my research group, Leo G. Henry, Bhola Mehrotra, Tony Pearson, and Jeff Hoyt, for their comments and questions on this work during its preparation as well as their contribution to the understanding of glassy carbon through the study of its microstructure, and to Professor Marshal F. Merriam during Professor Bragg's leave of absence. Bhola Mehrotra deserves special thanks for doing the bulk of the heat treating of the specimens and for doing the survey of the thermoelectric power.

Finally, but not lastly, I want to give special recognition to my academic committee, Professors Robert H. Bragg, Eugene E. Haller, and Andrew R. Neureuther, for their critical reading of the manuscript and their comments to the end of making this a better work. I want to thank Professor Bragg as my research supervisor for his infinite patience and support and constructive criticism during the long period of time that this work was in progress.

This work was supported by the Director, Office of Energy Research, Office of Basic Sciences, Materials Sciences Division of the U.S. Department of Energy under Contract Number DE-AC03-76SF00098.

## INTRODUCTION

Carbons that do not easily graphitize but require both high temperatures and high pressures for graphitization are known as hard carbons because they are mechanically hard. Hard carbons have two morphologies, fibrous and bulk.

Bulk hard carbons, of which glassy carbon can be considered a prototype, are made from thermosetting resins such as phenol-formaldehyde, phenol-benzaldehyde, polyfurfuryl alcohol, polyvinylidene chloride, resorcinol-formaldehyde, p-p-dihydroxy-biphenyl-formaldehyde, and 1,5-naphthalenediol-formaldehyde, and from cellulose, pits, sucrose, and some other organic precursors.<sup>1</sup> These precursors are marked by the fact that they are capable of cyclization or ring fusion, or chain coalescence at the onset of carbonization. Many hard carbons or chars have open pore structures and are good gas adsorbers or molecular sieves.<sup>2</sup> High density ( $>1.3 \text{ g/cm}^3$ ) glassy carbon can be made with a completely closed very fine ( $<50 \text{ \AA}$ ) pore structure. Glassy carbon, or glass-like or vitreous carbon as it is otherwise called, is notable for its high temperature stability. Its principal commercial use today is as a material for high temperature crucibles and susceptors. It is hard ( $1-3 \text{ GN/m}^2 \text{ DPH}$ )<sup>1,3</sup>, strong ( $40-60 \text{ MN/m}^2$  ultimate tensile strength)<sup>1,4-6</sup>, but unfortunately brittle ( $K_{Ic} = 10.5 \text{ M-m}^{-3/2} \times 10^{-5}$ )<sup>7,8,9</sup>. The impermeability ( $10^{-6} - 10^{-12} \text{ cm}^2/\text{sec}$  He)<sup>10,11,12</sup> and its even greater chemical inertness and oxidation resistance than graphite<sup>1,13,14,15</sup> has been used to advantage by applying glassy carbon as a glaze to cheaper impure carbon or graphite and refractory parts.<sup>16</sup> Glassy carbon is nearly always superior to

graphite as an electrolysis electrode,<sup>17</sup> but this application at present is not economically feasible. Other proposed applications are as medical prostheses,<sup>1</sup> electron gun element or filament<sup>18</sup> replacing tungsten, and as a standard material for small angle scattering apparatuses.<sup>19,20</sup>

The structure of glassy carbon has been the subject of numerous investigations since it was first manufactured, beginning with the work of Bragg and Hammond.<sup>21</sup> The first method used was x-ray diffraction<sup>22-29</sup> which produced patterns dominated by small angle scattering and diffuse peaks corresponding to 00 $\ell$  reflections and hk bands in graphite. The small angle scattering portion has been analyzed.<sup>21,28-34</sup> Glassy carbon obeys the Porod law for heat treatment temperatures greater than about 2000°C. All of these x-ray studies concur with the model proposed by Jenkins, Kawamura and Ban,<sup>23</sup> illustrated in Figure I.1. According to this model, glassy carbon consists of ribbons or laths of highly strained and defective turbostratic carbon of apparent crystallite size 15-50 Å which twist, turn, split and join, and interlace with each other to form closed split shaped pores of 10-20 Å in size. Of course, in dense glassy carbon where the pore size has been kept to a minimum, these details are not resolved in optical microscopes or even in scanning electron microscopes.<sup>35,36</sup>

Transmission electron micrographs also support this model. Lattice images of glassy carbon using the 002 reflections were observed by Bose, Dahmen, Bragg, and Thomas;<sup>37</sup> Kaae;<sup>38</sup> Jenkins, Kawamura and Ban,<sup>23</sup> and Phillips.<sup>39</sup> Whittaker<sup>40</sup> and Saxena<sup>41</sup> found that

flake specimens prepared by grinding gave spot patterns corresponding to chaoite, diamond, graphite, and other allotropes; however no such patterns have been found in specimens thinned by ion milling. Figures I.2 through I.5 are recent glassy carbon lattice images obtained by Dr. Ron Gronsky from specimens prepared by A. S. Rao. Images were not obtained until the heat treatment temperatures exceeded 1800°C. None of the other investigators reported lattice fringes in glassy carbon heated at temperatures less than this. However, Ban, Crawford, and Marsh<sup>42</sup> observed lattice fringes in polyvinylchloride carbonized at 530°C. Both polyvinylchloride and glassy carbon are hard carbons, so it appears that factors other than heat treatment temperature, notably the precursors, affect the structure of the resulting hard carbon product.

Many attempts to discover the bonding in glassy carbon have been made. The most numerous have been by performing a Fourier transform from scattering vector reciprocal space of x-ray diffraction patterns to direct lattice real space to get a radial distribution of electrons.<sup>22,25,26,28,43,44</sup> They have not been particularly informative, showing that carbon in glassy carbon is mostly trigonally bonded, but that there is a spectrum of bond lengths consistent with the presence of other carbon-carbon bonds. Analysis of the Compton scattering of glassy carbon<sup>45</sup> drew the conclusion that the carbon atoms are more nearly in a free state than in a state similar to that in graphite or diamond. The conclusion from carbon K-emission studies on glassy carbon was that the electrons in carbon atoms were bound at energy levels somewhere between those of diamond and graphite.<sup>46</sup> Nakamizo,

Kammereck and Walker performed Raman spectroscopy on glassy carbon.<sup>47</sup> They found only two peaks which became increasingly sharper with heat treatment temperature: one at  $1355\text{ cm}^{-1}$  which was associated with the bonding of benzene rings, and one at  $1580\text{ cm}^{-1}$  which corresponds to a vibrational mode of graphite. No peaks corresponding to C-H bonds were reported.

Electrical properties have been measured in a vast array of carbon materials. Values have been measured over the whole range of electrical conductivities measured on all other materials. Spain<sup>48</sup> has recently published an excellent review on the subject.

On a scale of a few unit cells, the structure of glassy carbon resembles that of graphite. The Slonczewski-Weiss<sup>49</sup> model has seven parameters calculated from crystal potentials using a single electron tight-binding approximation in perfect single crystal graphite. A. W. Moore<sup>50</sup> in his recent review of highly oriented pyrolytic graphite gives the best values for experimental work for these parameters; they are extremely sensitive to the potentials and to each other. For prediction purposes, the Slonczewski-Weiss band model is limited to electrical conductivity; anomalies are commonly observed for thermomagnetic properties for both low and high magnetic fields and at low temperatures. The most recent comprehensive review of the model itself is given by Spain.<sup>51</sup>

Magnetoresistance data has been used extensively to measure the band parameters of the Slonczewski-Weiss band model, mostly through oscillations with magnetic field (the Shubnikov-de Haas effect)<sup>51</sup>. Magnetoresistance in good single crystal graphite is always positive

but negative magnetoresistance has been observed in many defective and disordered soft carbons. It is usually a low temperature (liquid helium) phenomenon, and is a complicated function of the magnetic field.<sup>48,52-61</sup> Of course, the Shubnikov-de Haas effect is no longer observed due to the defects in these carbons.

The modified Slonczewski-Weiss band model is limited to perfect single crystal graphite; its finer details are soon washed out in most industrial graphites. In grossly defective graphite, the electrical conductivity increases with temperature as a semiconductor and does not decrease like a semimetal and pure graphite.<sup>62</sup>

The Hall effect in graphite for small magnetic fields and room temperature is negative, but in general and for soft carbons it is sensitive to local strain, temperature, impurities, and heat treatment temperature, and is a function of magnetic field.<sup>57,58,63-75</sup> Work to explain this phenomenon continues on the modified Slonczewski-Weiss theory along the lines of trigonal warping,<sup>76,77,78</sup> wherein the corners of the constant energy Fermi surface become less pointed and more rounded in the presence of a magnetic field.

S. Mrozowski<sup>71</sup> has reviewed and charted the electrical properties of soft carbons from carbonization through graphitization. His proposed band model (Figure I.11) as a function of heat treatment temperature shows the semiconductor behavior of low temperature carbons (<1200°C) and band overlap at high temperature (>2500°C). The band structure in the transition region remains undetermined. The band structure of hard carbons was considered similar to that of soft carbons for low heat treatment temperatures.

Precursors of glassy carbon processed at low temperatures behave as do a number of other organic compounds<sup>79-82</sup> and carbon thin films<sup>83-85</sup> and low temperature chars.<sup>86-89</sup> The conductivity is proportional to  $\exp(-T^{-1/4})$  and is attributed to Mott scattering<sup>90,91</sup> as shown in Figure 12.<sup>90</sup> In the only attempt reported, Bucker<sup>92</sup> could not obtain any Hall measurements on his low-temperature glassy carbon. Phenomena such as ac conductivity<sup>88,89</sup> and high field effects (switching)<sup>93,94</sup> can be anticipated for glassy carbon heat treated below a critical temperature of about 700°C. This temperature marks a nonmetal-metal transition, and is the critical temperature at which the last of the organic radicals have been driven off. This work is concerned with glassy carbon heat treated at temperatures well above this point.

Prior to this work, only three systematic investigations of the electrical properties of glassy carbon in the heat treatment temperature range of 1000 - 3000°C have been reported by Yamaguchi,<sup>95</sup> Tsuzuku and Saito,<sup>96</sup> and Saxena and Bragg.<sup>97,98</sup> Yamaguchi found that the magnetoresistance is negative and that the Hall effect is nearly the same at 20°K, 77°K, and 300°K and is independent of magnetic field up to 1.35 tesla. He found little change in the electrical conductivity, which increased slowly with temperature. Tsuzuku and Saito reported similar electrical conductivity and Hall effect data for magnetic fields up to 2.2 tesla. Saxena and Bragg made measurements of the negative magnetoresistance and electrical conductivity over a continuous range of temperatures above 10°K with a maximum field of 5 tesla, but made few Hall measurements. They were the first to put

forth empirical expressions for the electrical conductivity and magnetoresistance. The electrical conductivity was written as the sum of three components:

$$\sigma = A + B \exp(-(T/T_0)^{-1/4}) + \delta(T) \quad (1)$$

The first component was attributed to metallic states or conduction between extended states and was thought to be dependent on the apparent crystallite size as determined by x-rays. The second term was attributed to variable range hopping or Mott scattering. The last term was a low temperature correction term attributed to a Kondo-like mechanism applicable to glassy carbon heat treated at temperatures less than about 2000°C. The form of the low temperature conductivity correction was thought to be of the form  $\delta(T) = \log(T/T_c)$ ;  $T < T_c$ .

Because of the lowest measurement temperature was still high, this form was chosen based on the existing Kondo theory. The negative magnetoresistance for high temperature heat treated glassy carbon was found to be linear with the square of the magnetic field divided by the absolute temperature ( $H^2/T$ ) for small values of this parameter. For larger values, the negative magnetoresistance continues to increase though at slower rates. Saxena and Bragg, following Toyozawa,<sup>99</sup> proposed that the negative magnetoresistance is proportional to the square of the magnetic moment, but were unable to cite a specific model for a square root inverse temperature moment dependence.

Thus there are empirical formulae for the behavior of the negative magnetoresistance, electrical conductivity and Hall effect for relatively high temperatures and for heat treatment temperatures greater than about 2000°C. For lower measurement temperatures, the negative magnetoresistance fails to increase as rapidly as predicted. Magnetic moment models, especially one based on Curie paramagnetism, would predict that the negative magnetoresistance should saturate with increasing ratio of magnetic field to temperature  $(H/T)$ . The electrical conductivity for high measurement temperature has the same form for all heat treatment temperatures. The largest deviations from this form occur in low heat treatment temperature glassy carbon, the nature of which remains unknown. The Hall effect appears independent of temperature. However, in a great many carbon materials, the Hall effect undergoes erratic behavior for low temperatures as a function of the field. Since the lowest literature measurement temperature for the Hall effect is a relatively high 20°K, such behavior is possible in glassy carbon, though improbable.

Thus when lower temperatures became available, the anticipated extrapolation of the data was that the negative magnetoresistance should saturate, that enough of the decrease of the low temperature low heat treatment temperature glassy carbon conductivity will be observed to better establish an empirical relation for it, and that the Hall effect will remain temperature insensitive.

Therefore, the objectives of this study were to obtain lower measurement temperatures than the 10°K of Saxena and Bragg, to observe the extended low temperature behavior of the conductivity and magnetoresistance, and to make a complete set of Hall effect measurements as a function of heat treatment temperatures greater than 1000°C.

Electrical properties can be extremely sensitive to microstructure, though evidently less so in glassy carbon. Nevertheless, with the achievement of lower measurement temperatures and the full range of heat treatment temperatures, some conclusions describing the microstructural changes in glassy carbon should be drawn from observations of the magnetoresistance, electrical conductivity and Hall effect.

### EXPERIMENTAL

Glassy carbon was heat treated in a graphite furnace under an inert atmosphere to temperatures ranging from 1200 to 2700°C for three hours. It was ground, polished, and cut ultrasonically into four-probe bar shaped specimens. After cleaning, colloidal silver was painted on the contact pads to assure ohmic contacts.

Measurements were made under isothermal conditions in a variable range cryostat from 3 to 100°K with magnetic fields up to five tesla provided by a superconducting magnet. Electrical conductivity measurements were made up to 300°K. The quality of the measurements are dependent on the accuracy and precision of the specimens and instrumentation. When these are taken into account, the accuracy of the electrical conductivity and Hall coefficient is about 3.7% and of the magnetoresistance approximately 0.01%. The relative precision of the electrical conductivity and Hall coefficient is 0.01% and 0.2% respectively.

A more extensive account of such experimental aspects of this work as specimen preparation, phenomenological theory and experiment design and instrumentation, and cryogenic procedures is given in Appendix A.

## RESULTS

The magnetoresistance of glassy carbon is usually negative; in this work only at low temperatures for heat treatment temperatures less than 1600°C is positive magnetoresistance observed as did Hishiyama et. al.<sup>55</sup> The critical temperature at which the magnetoresistance goes from positive to negative is a function of heat treatment temperature, and is approximately 16°K, 10°K, and 8°K for heat treatment temperatures of 1000°C, 1200°C, and 1400°C, respectively as indicated in Figures III.1-3. The negative magnetoresistance increases monotonically with increasing magnetic field and higher increasing heat treatment temperatures, as also was observed by Yamaguchi<sup>95</sup> and Saxena and Bragg<sup>98</sup>, but is observed to saturate with inverse measurement temperature (Figures III.4-10). The largest absolute value measured was -2.2% for 2700°C heat treated glassy carbon.

The electrical conductivity of glassy carbon (Figure III.11-20) is of the order of 200 ( $\Omega\text{-cm}$ )<sup>-1</sup> and is not a strong function of temperature, as the ratio of the conductivities at room temperature and liquid helium temperature is only 12-24%, depending upon heat treatment temperature. For higher temperatures, as Yamaguchi,<sup>95</sup> Tsuzuku and Saito<sup>96</sup> and Saxena and Bragg<sup>97</sup> observed, the conductivity increases monotonically with temperature through room temperature, apparently in a manner independent of heat treatment temperature. At low temperatures, the conductivity reaches a plateau with a shallow minimum for high heat treatment temperature material. The plateau minimum occurs at decreasing temperatures for decreasing heat treatment

temperatures until it no longer remains within the limits of the experiment. For lower heat treatment temperatures than about 2200°C, the conductivity continues to fall off more rapidly with decreasing heat treatment temperature and measurement temperature.

The Hall coefficient (Figure III.21) for all heat treatments is nearly independent of measurement temperature, as is the Hall mobility (Figure III.22). The Hall coefficient is also not a function of magnetic field as is the case in other carbons. However, the Hall coefficient is a strong function of heat treatment temperature (Figure III.23) having an absolute minimum at about 1200°C, crossing from negative to positive at about 1700°C and becoming increasingly positive with increasing heat treatment temperature. These results are similar to those of Yamaguchi<sup>95</sup> and Tsuzuku and Saito<sup>96</sup> (Figure III.24). The Hall coefficient observed in this work is small, and lies between -0.048 cm<sup>3</sup>/coul and 0.126 cm<sup>3</sup>/coul.

The magnetoresistance and electrical conductivity data were fitted using a comprehensive modified Gauss-Newton algorithm for finding an unconstrained minimum of a sum of squares of the residuals for non-linear functions requiring first and second continuous analytical derivatives.<sup>100,101</sup> The Hessian matrix and hence the uncertainties and correlation coefficients of the fitted parameters are available, as well as the sum of the squares, indicating the quality of fit.<sup>102,103</sup>

The fitted functions were chosen by comparison with the data and literature considerations. The fitted parameters are listed in the Appendices D-G.

## DISCUSSION

### A. Magnetoresistance

Magnetoresistance is the relative change of resistance with magnetic field. Approaches to explain the phenomenon usually emphasize the effect of magnetic field on either the carrier mobility or the number of carriers.

Negative magnetoresistance has always been associated with disorder and crystal defects, chiefly because it is never found in highly ordered nearly defect free materials. Negative magnetoresistance is impossible in single carrier systems. It appears in some amorphous semiconductors, heavily doped semiconductors, and chalcogenide glasses.<sup>104</sup>

The negative magnetoresistance in glassy carbon is linear with the square of the magnetic field at low fields and saturates with reciprocal temperature at high fields for high heat treatment temperatures though it still is increasing with magnetic field. The only well worked out theory to describe this phenomenon of negative magnetoresistance for many years was Toyozawa's theory<sup>99</sup> which explained the negative magnetoresistance in dilute metal alloys with ferromagnetic impurities by a spin interaction mechanism. This mechanism predicts that the negative magnetoresistance is proportional to the square of the total magnetic moment. Some moment models have been tested against the data.

The first model tried in an attempt to explain the data was a paramagnetic moment model based on the fact that glassy carbon contains both localized and extended states which would be expected to have

Curie and Pauli moments respectively. Thus the square root of the absolute value of the magnetoresistance has been fitted to a term proportional to a Brillouin function with spin  $1/2$  and a term independent of temperature and linear in magnetic field. These proportionality parameters are plotted as a function of heat treatment temperature in Figures IV.1 & 2 and listed in Appendix D. They are roughly described as linearly increasing with this parameter. The model fits well at the highest heat treatment temperatures, but less well at intermediate values (Figure IV.3-9).

There are some questions concerning the validity of this analysis. Firstly, even though the effective number of Bohr magnetons remains the same for heat treatment temperatures greater than  $1600^{\circ}\text{C}$ , the lower limit of the model, this number is much too large ( $6.2 \pm 0.1$ ) for single carbon atoms. This result is similar to that found in other studies using this idea, such as in doped Ge, InAs, and GaAs.<sup>105</sup> Large moments such as these have also been found in dilute ferromagnetic impurities in palladium determined through electron paramagnetic resonance (EPR)<sup>106</sup> and cold neutron scattering<sup>107</sup> and have been interpreted as long range polarization or localization of the palladium atoms surrounding the impurity.

Another problem with the Curie/Pauli model is that graphite and most carbons have temperature dependent diamagnetic magnetic susceptibilities. Diamagnetism in graphite is anisotropic;<sup>108</sup> in fact the degree of anisotropy in carbon materials has been used as a reliable measure of graphitization.<sup>109,110</sup> Simply put, the diamagnetism of

graphite consists of two components; a small ( $\approx -0.4 \times 10^{-6}$  emu/g) isotropic part due to the ion cores: and a c-axis part inversely proportional to temperature and sensitive to crystallite sizes less than about 150 Å. This latter part is attributed to London diamagnetism associated with the ring structure of graphite and free electron Peierls diamagnetism.<sup>111</sup> The theory of diamagnetism in bulk single crystal graphite has been addressed by McClure.<sup>112,113</sup> Recent developments have produced a theory applicable to both sheet<sup>114,115</sup> and corrugated ribbons of graphite<sup>116</sup> which make up the microstructure of carbon fibers. Though the geometrical model assumptions may be adjusted to better match the microstructure of glassy carbon, the exact calculations themselves are not trivial and require a considerable amount of computer time. However, because the negative magneto-resistance is so well behaved, a moment model proportional to the square of the theoretical diamagnetic moment could be anticipated to compare about as well as do the experimental ribbon and sheet diamagnetic moments to theory.

The only reported magnetic susceptibility measurements of glassy carbon heat treated in the range of interest were done by Fischbach<sup>117</sup> and were used as a measure of the degree of preferential alignment of the laths after high temperature (1600-2900°C) tensile tests. He reported the diamagnetic susceptibility of his starting materials as  $\chi_T = -9 \times 10^{-6}$  emu/g for a heat treatment temperature of 2000°C and  $\chi_T = -16 \times 10^{-6}$  emu/g for 3000°C, where  $\chi_T$  is one

third of the trace of the magnetic susceptibility tensor. He implied linear interpolation of the magnetic susceptibility between these two extremes.

Paramagnetic moments have been measured in a glassy carbon precursor<sup>118</sup> heat treated at temperatures less than 800°C. The effective number of Bohr magnetons measured was 6.6, comparable to the number derived from the present magnetoresistance measurements, but it is unknown whether this is due to impurities (iron) intentionally introduced in solution in the carbon matrix or to the carbon itself. Paramagnetic moments have been found in a number of carbon,<sup>82,119-123</sup> but usually in those heat treated at temperatures less than 1500°C, leading to the conclusion or at least strong implication that paramagnetism due to unpaired electrons, free organic radicals, and other defects is annealed out at higher temperatures.

A number of studies on the electron spin resonance (ESR) have been done on hard carbons or their precursors.<sup>92,124-128</sup> High heat treatment temperature studies of glassy carbon were done by Toyoda et al.<sup>129</sup> and Orzeszko and Yang.<sup>130</sup> The study by Orzeszko and Yang is particularly interesting because by using a method derived by S. Mrozowski,<sup>131</sup> they were able to differentiate between free electron spins (concentration temperature independent) and localized spins (Curie temperature dependence) as shown in Figure IV.10.

Recently a magnetic moment model having the same characteristics as the square root absolute magnetoresistance data was published by S. Kobayashi et al.<sup>132</sup> It was developed to describe the magnetization

of silicon atoms in heavily phosphorus doped silicon. The total magnetization moment is given as follows:

$$M = \frac{N(0) \mu_B \sinh X}{\beta Z} \ln \left( \frac{(\cosh X) + Z}{(\cosh X) - Z} \right) \quad (2)$$

where  $X = \beta g \mu_B H$

$\beta = (kT)^{-1}$ ,  $T$  = temperature,  $k$  = Boltzman's Constant

$\mu_B$  = Bohr magneton

$g$  = effective moment Bohr magnetons

$H$  = magnetic field induction

$Z = (\cosh^2 X - P)^{1/2}$

$P = e^{-U/T}$

$U$  = intra-state correlation energy/ $k$

This moment model behaves very similarly to the Curie-Pauli model. If the intra-state correlation energy is zero, the moment magnetism behaves like Pauli paramagnetism. If the intra-state correlation energy is nonzero, at high magnetic fields the moment shows Curie-like behaviour, saturating with inverse temperature. The model was fitted to the present data; the proportionality parameter  $Q$  and intra-state correlation energy  $U$  are tabulated in Appendix E and plotted in Figure IV.11 and 12 as functions of heat treatment temperature where

$$Q = \frac{N(0) \mu_B \sinh X}{\beta Z} \quad ; \quad M = Q \ln \left( \frac{(\cosh X) + Z}{(\cosh X) - Z} \right) \quad (3)$$

and where  $g$  has been found to be independent of heat treatment temperature and nearly the same as in the Curie-Pauli model. The linear

parameter  $Q$  increases with heat treatment temperature as did the other linear parameters in the Curie-Weiss model above. However,  $U$  increases with heat treatment temperature until  $2200^{\circ}\text{C}$  where it appears to reach a plateau. The fit of this model compared with the Curie-Pauli model is only slightly inferior and as with Curie-Pauli model, is worse at intermediate heat treatment temperatures.

Saxena and Bragg<sup>98</sup> found that the square root of the absolute value of the negative magnetoresistance is linear with the magnetic field divided by the square root of the temperature for lower values of this parameter. Bright<sup>133</sup> has used this data in this way to support his model of overlapping localized and extended states for negative magnetoresistance in pregraphitic carbons. He assumes that the broadening of the Landau levels is Gaussian, and that the standard deviation of the broadening distribution is proportional to the zero-field carrier drift mobility. This model predicts that near equilibrium (low fields less than 1.5 tesla), the negative magnetoresistance is proportional to  $\mu^4 H^2$ , where  $\mu$  is the drift mobility and  $H$  is magnetic field, and thus that the drift mobility is proportional to the inverse fourth root of temperature. The proportionality constant is plotted as a function of heat treatment temperature in Figure IV.C.13 and listed in Appendix F. It increases roughly linearly with temperature. This model, as with the previous models introduced, fits increasingly worse for decreasing temperatures (Figures IV.C.14-20). Furthermore, as seen in Figure III.22, the Hall mobility, while not necessarily the carrier mobility, is nearly independent of measurement temperature and does not have a definite inverse fourth root temperature dependence.

Other theories of negative magnetoresistance exist. One approach is that the magnetic field aligns the spins of a disordered material, eliminating scattering centers and thus increasing the effective mobility.<sup>134</sup> Another approach is that localized carriers with low mobilities are induced from an impurity band into the conduction band where the mobility is higher, thus effectively increasing the number of carriers and the conductivity.<sup>135-138</sup> Most of these theories have been developed for application to specific materials (semiconductors) and for limiting cases of low fields. None seem to fit the present data as well as the moment models.

Positive magnetoresistance was observed for heat treatment temperatures less than 1600°C and for temperatures less than 20°K in glassy carbon. The temperature at which the magnetoresistance goes from negative to positive decreases as the heat treatment temperature increases.

The classical case of positive magnetoresistance<sup>139</sup> is applicable to metals, semiconductors, and other materials where a band model has been used to successfully describe the electronic structure. The magnetoresistance is given by

$$\frac{\Delta\rho}{\rho} = \frac{\frac{a}{b} \left(\frac{b+1}{a+b}\right)^2 \mu_h^2 H^2}{1 + \left(\frac{a-b}{a+b}\right)^2 \mu_h^2 H^2} \approx c' H^2$$

for small fields such that  $\mu_h^2 H^2 \ll 1$ .

$a = n_e/n_h$  , the ratio of carrier concentrations

$b = \mu_h/\mu_e$  , the ratio of carrier inabilities

Considering that the negative magnetoresistance dominates at high temperatures, the positive magnetoresistance must disappear with increasing temperature, which implies that the mobility is inversely proportional to temperature. A positive component was added to the present empirical Curie/Pauli model describing the negative magnetoresistance in high temperature glassy carbon in an attempt to produce an empirical model for the whole range of heat treatment temperatures. This was unsuccessful.

Magnetoresistance for hopping conduction between localized states without interaction with extended states is positive and highly sensitive to magnetic field,<sup>140</sup> at least for low fields as

$$\frac{\Delta\rho}{\rho} \propto \exp H^2$$

Hishiyama et al.<sup>55</sup> considers this mechanism as responsible for positive magnetoresistance observed at low temperatures for low temperature heat treated glassy carbon. Examination of Figures III.1-3 show that the above is not an adequate description of the experimental behaviour of the positive magnetoresistance observed in glassy carbon.

Of the models discussed above, the moment models for negative magnetoresistance fit the full range of data for high temperature heat treated glassy carbon best. Unfortunately they are also the most ambiguous in that the proportionality constant linking the negative magnetoresistance to the square of the moment is unknown but is expected to be a function of the density of states. Even the sign of the magnetic moment remains ambiguous. Any positive component of the magnetoresistance in these high heat treatment temperature glassy carbons is small and not easily separable, and was ignored.

Consider that negative magnetoresistance is due to the interaction of localized and extended states as influenced by a magnetic field and that the positive magnetoresistance observed is due to interaction between only localized states. It appears then that the interaction of localized states decreases with heat treatment temperature, most likely due to the annealing out of localized states. At high heat treatment temperature, the interaction increases as the heat treatment temperature is raised.

This view is supported by the electron spin resonance data shown in Figure IV.10 except in the transition range where the Hall effect changes signs. Apparently, negative magnetoresistance is inversely proportional in some way to the density of states, even though the moment model predicts that it should also be proportional to the square of the number of spins.

Thus the negative magnetoresistance for high heat treatment temperature glassy carbon is well behaved, unlike that for a great many

other carbons, in that it is a monotonically increasing function of magnetic field, saturating with inverse temperature. Theory predicts that this negative magnetoresistance is proportional to the square of the magnetic moment; several models for the literature have been examined as possible candidates. The magnetoresistance for low temperature heat treated glassy carbon which is positive at low measurement temperatures remains unexplained.

#### B. Electrical Conductivity

The most recent comprehensive study of the electrical conductivity of glassy carbon in the high heat treatment temperature (greater than 1000°C) regime was done by R. Saxena and R. H. Bragg.<sup>98</sup> They found that the conductivity  $\sigma$  could be empirically written as

$$\sigma = A + B \exp(-CT^{-1/4}) + \delta(T) \quad (6)$$

where A, B, and C are constants and  $\delta(T)$  is a term appearing only at low temperatures for low temperature (less than 2000°C) heat treated material. The first and largest term A was attributed to metallic conduction and was thought to be influenced by scattering from "crystal-lite" boundaries. The second term was in the form for Mott scattering or variable range hopping of carriers between localized states. Since this work is basically in agreement with Saxena and Bragg on these points, elucidation of these components is left to Appendix B. Thus the new contribution to the body of knowledge concerning the electrical conductivity of glassy carbon is the third term of Saxena and Bragg, which was a negative correction term of the Kondo logarithmic form. Because of the extended temperature range in this work, it was found

that instead this negative component has a square root inverse temperature dependence, compatible with the recent theory for the low temperature correction for one-dimensional metallic filaments. No explanation is given for the very low temperature conduction behavior of high temperature heat treated glassy carbon, though it may be related to increasing apparent crystallite size and dimensionality.

Kaveh and Mott<sup>141</sup> have reviewed two approaches to a correction of the metallic conductivity. They are the localization approach by Abrahams, Anderson, Licciardello and Ramakrishnan<sup>142</sup> and the electron interaction approach by Altshuler, Aronov, and Lee.<sup>143</sup> In the localization approach, the carrier is allowed to diffuse until an inelastic scattering even takes place (trapping by a localized state) and thus diffusion of the carriers is limited by the inelastic scattering time. In the electron interaction approach, the effective number of carriers is affected by the correlation between the shift of potential energy and the broadening of the momentum distribution of the carriers themselves as scaled by the physical dimensions. Both mechanisms may be operating simultaneously. They give identical results for conduction in two dimensions:

$$\delta\sigma = -\frac{e^2}{2\pi^2\hbar} \ln \frac{kT\tau}{\hbar} \quad (7)$$

where  $\tau$  is the effective scattering time. The difference between the two approaches is seen in the Hall effect: The localization approach

predicts that there will be no correction in the Hall effect but the interaction approach predicts that the relative change in the Hall coefficient will be twice that for the conduction. The interaction approach has been used to predict corrections in three dimensions

$$\frac{\delta\sigma}{\sigma} = \left( \frac{kT}{hD} \right)^{1/2} \frac{1}{N(E_F)} \quad (8)$$

and in one dimension

$$\delta\sigma = - \frac{e^2}{h} \left( \frac{2}{\pi} \right)^2 \frac{1}{A} \left( \frac{hD}{kT} \right)^{1/2} \quad (9)$$

where  $D$  is a diffusion coefficient related to the near free path and  $A$  is the cross sectional area. Such a  $-T^{-1/2}$  dependence was found in this work for a component of the electrical conducting inducing the possibility of one-dimensional transport.

The correction term parameter  $D$  becomes progressively smaller as the heat treatment temperature is increased (Figure IV.21) until the term disappears for heat treatment temperatures greater than 2200°C. Several possible causes are that the diameter of the one-dimensional wires becomes greater or their length becomes shorter, or that there are fewer conducting paths. Because individual filaments are not measured, but rather the resistivity of a highly interconnected network, individual filament parameters cannot be evaluated.

As discussed in Appendix B.1, the strongly scattering metallic term of the conductivity is independent of temperature. Figure IV.22 shows that it also appears to be independent of heat treatment temperature and thus apparent "crystallite" size as measured by x-ray diffraction. Using the well worked out three dimensional formula thought to be applicable for high heat treatment temperatures, the mean scattering length is estimated to be about 13 Å.

In Appendix B.2, the variable range hopping term is discussed. Figure IV.23 shows that the linear term B is independent of heat treatment temperature. The exponential constant  $C_0$  ( $\approx 14.5 \text{ }^\circ\text{K}^{1/4}$ ) is also independent of this parameter; thus, the variable range hopping term is approximately the same for all heat treatment temperatures. The localization range, the inverse of the decay parameter of an exponential localized wavefunction, is approximately 15 Å.

Thus the new part to the basic description of the electrical conductivity as advanced by Saxena and Bragg is a one dimensional correction term to the strongly scattering metallic conductivity term, applicable only for glassy carbon heat treated below about 2200°C.

### C. Hall Effect

In glassy carbon, the Hall effect is temperature insensitive (Figures III.21 and III.22), dependent on heat treatment temperature (Figure III.23) and independent of magnetic field, unlike many other carbons. If the metallic scattering component is considered to be the dominant component to the Hall coefficient, an assumption most likely to be valid at high heat treatment temperatures, then the carrier concentration is estimated to be  $7 \times 10^{19}$  holes/cm<sup>3</sup> for 2700°C

material. A fuller discussion of the Hall effect, and the uncertainty introduced by theory (or lack thereof) as to the calculation of fundamental parameters from the Hall effect in disordered materials is given in Appendix C.

#### D. Correlation to Microstructure

The microstructure of glassy carbon is essentially the skeleton of its polymer precursors at low heat treatment temperatures. This material does not readily give lattice images in the transmission electron microscope; also, small angle x-ray scattering shows that at least some of the pore surfaces are diffuse.<sup>30,31</sup> As the heat treatment temperature is increased to about 2000°C, ribbons or laths are imaged in the transmission electron microscope, and the diffuseness of the pore surfaces is no longer apparent in small angle x-ray scattering. In wide angle x-ray diffraction, the interplanar spacing associated with the first diffraction maximum remains constant at 3.44 Å characteristically the spacing associated with the (002) plane in turbostratic carbons, up to a heat treatment temperature of about 2200°C.<sup>27,144</sup> The interplanar spacing slowly decreases with higher heat treatment temperature. The weight loss during heat treatment also saturates at about this temperature.<sup>145</sup> The Hall effect becomes positive at about 1700°C, also about the lower limit for the negative magnetoresistance models. While the magnitude of the conductivity does not change greatly, the form is slightly altered in that a low temperature correction term characteristic of a one dimensional filamentary skeleton network appears for heat treatment temperatures less than about

2200°C. The two linear conductivity parameters appear to be independent of heat treatment temperature. The range of localization appears to be about 15 Å and the mean free path perhaps 13 Å; they cannot be correlated to either an apparent crystallite size or a pore size which increases monotonically with heat treatment temperature. There does appear to be some inhomogeneities in the material which may be responsible for some of the scatter in the parameters.

The idea of two-phase graphitization of hard carbons is not new. Franklin<sup>146</sup> advanced the idea of two- and three-phase graphitization from detailed x-ray diffraction measurements. Loebner<sup>147</sup> also cited a two phase graphitization scheme, using not only x-ray diffraction data, but electrical resistivity and thermoelectric power data also. Recently, Hishiyama et al.<sup>148</sup> made the observation that negative magnetoresistance is characteristic of turbostratic carbons as opposed to positive magnetoresistance in graphitic carbons, and that this negative magnetoresistance is proportional to apparent crystallite size along the c-axis or [002] direction, an idea used earlier by Kawamura and Tsuzuku<sup>149</sup> in their study of porosity and graphitization of glassy carbon. This analysis is only valid for heat treatment temperatures greater than about 1700°C, and is not an explanation for the low heat treatment temperature, low temperature positive magnetoresistance.

The most important implication that the electrical measurements have on the general view of the microstructure of glassy carbon is that glassy carbon heated at temperatures less than 2200°C has a one dimensional metallic component, as shown by the inverse square root dependence of the low temperature correction term. This view is also

supported by evidence from transmission electron microscopy, small angle x-ray scattering, and a saturation of the weight loss during heat treatment. The disappearance of this one-dimensional component of the microstructure is also demonstrated by the sharp change in the Hall effect and the less marked change in the magnetoresistance.

### CONCLUSIONS AND RECOMMENDATIONS

The following conclusions have been made:

1. Negative magnetoresistance in high temperature heat treated glassy carbon saturates with reciprocal temperature but not with magnetic field for fields less than five tesla. Several models were considered as plausible explanations for this behavior but none could be confirmed as correct. Positive magnetoresistance found at low observation temperature in low temperature heat treated glassy carbon remains unexplained.

2. The Hall effect is temperature insensitive. The results are comparable to other literature values. The Hall coefficient changes signs from negative to positive with increasing heat treatment temperature at about 1700°C and shows a negative maximum at about 1200°C.

3. The electrical conductivity of glassy carbon in the heat treatment temperature range 1000 to 2700°C was found to have three empirical components:

a temperature independent component attributed to the conductivity or transport between extended states and fitting the description for a metal with strong scattering.

a variable range hopping component, for which the exponential term  $\exp(-(T_0/T)^{-1/4})$  is constant for all heat treatment temperatures. The power of the temperature in this exponential argument indicates transport in three dimensions.

a low temperature term that for heat treatment temperatures less than about 2200°C is the same as for the one-dimensional

conduction correction for metallic thin wires or filaments. For higher temperatures, the conductivity decreases to a shallow minimum as the temperature decreases. The nature of the conductivity for temperatures below the minimum remains to be explored.

4. The microstructure of glassy carbon has a one dimensional component at low heat treatment temperatures as supported by evidence from the electrical conductivity and also from the transmission electron microscope and small angle x-ray scattering. The transition from one dimensional behavior is marked by a change in the sign of the Hall coefficient, and the disappearance of the one dimensional metallic conductivity correction term. The nature of the transition remains unknown as to whether it is simply a coarsening of the filaments or whether a true phase transformation takes place. At higher heat treatments, the "apparent" crystallite size of the turbostratic laths increases, and the increase in negative magnetoresistance is thought to be due to this. This view of the microstructure of glassy carbon as a function of heat treatment temperature is consistent with the consensus literature model.

The parameters of the present experiment are simply heat treatment temperature, observation temperature, and magnetic field. The heat treatment time and electrical field and current are held constant. In extending the scope of the present experiment, the most interesting results would seem to be obtained by lowering the measurement temperature and varying the heat treatment time. The magnetic susceptibility should also be measured.

At lower measurement temperatures, the conductivity for low heat treatment temperatures should asymptotically approach zero with decreasing temperature as for both hopping conductivity and one-dimensional filamentary metallic conductivity theoretically go to zero at zero temperature. No new behaviour is expected regarding negative magnetoresistance as the present data shows that the negative magnetoresistance saturates with inverse temperature. The nature of the positive magnetoresistance found at low temperature should reveal more about that phenomenon, such as whether positive magnetoresistance exists in glassy carbon heat treated in the range between 1600°C and 2200°C for low enough temperatures and thus determine whether the positive magnetoresistance is associated with the negative Hall effect and/or the one dimensional carbon filaments. The present cryogenic system is not capable of achieving temperatures in the range 0.1 - 4.2°K which would be a reasonable and desirable range for such an experiment.

A systematic set of heat treatment times for a representative set of heat treatment temperatures should help answer the question of whether there is a separate transformation of carbon filaments to turbostratic laths or whether there is a single coarsening process. R. Saxena and R. H. Bragg<sup>27</sup> have done such a study and measured an activation energy of  $215 \pm 40$  kcal/mole for the coarsening of the turbostratic laths which is comparable to the energy for graphitization in other carbons. The present model predicts that low temperature electrical conductivity and the Hall effect should be affected most. If Hishiyama et al.<sup>141</sup> are correct in their contention that the negative

magnetoresistance is proportional to the size of the turbostratic lath, then an activation energy close to that that Saxena and Bragg measured should be derived from magnetoresistance observations on glassy carbon heat treated for a systematic set of times, at least for temperatures greater than 2200°C.

In the discussion section concerning the magnetoresistance, several models were mentioned as possibilities for satisfying the condition that the negative magnetoresistance is proportional to the square of the magnetic moment. Thus, it would be desirable to measure the magnetic susceptibility to determine which of the magnetic moment models, if indeed any, is correct.

REFERENCES

1. G. M. Jenkins, K. Kawamura, "Polymeric Carbons--Carbon Fibre, Glass and Char," Cambridge University Press, Cambridge (1976).
2. P. L. Walker, Jr., L. G. Austin, S. P. Nandi, "Activated Diffusion of Gases in Molecular-Sieve Materials," Chemistry and Physics of Carbon, Philip L. Walker, Jr., ed., Marcel Dekker, New York, Vol. 2, pp. 257-371 (1966).
3. H. M. Hawthorne, "The Microindentation Hardness Behaviour of Carbon Filaments, Glassy Carbons and Pyrolytic Graphites," Carbon 13 215-23 (1975).
4. W. V. Kottlensky, H. E. Martens, "Tensile Properties of Glassy Carbon to 2900°C," Nature 206 1246 (1965).
5. J. J. Melcholsky, R. W. Rice, S. W. Freiman, "Prediction of Fracture Energy and Flaw Size in Glasses from Measurements of Mirror Size," J. Amer. Cer. Soc. 57 440 (1974).
6. Gwyn M. Jenkins, "Deformation Mechanisms in Carbons," Chemistry and Physics of Carbon, Philip L. Walker, Jr., Peter A. Thrower, eds., Marcel Dekker, New York, Vol. 11, pp. 169-242 (1975).
7. J. S. Nadeau, "Hertzian Fracture of Vitreous Carbon," J. Amer. Cer. Soc. 56 467 (1973).
8. J. S. Nadeau, "Subcritical Crack Growth in Vitreous Carbon at Room Temperature," J. Amer. Cer. Soc. 57 303-6 (1974).
9. W. P. Minnear, T. M. Hollenbeck, R. C. Bradt, P. L. Walker, Jr., "Subcritical Crack Growth of Glassy Carbon in Water," J. Non-Cryst. Sol. 21 107-15 (1976).

10. E. Fitzer, W. Schaeffer, S. Yamada, "The Formation of Glasslike Carbon by Pyrolysis of Polyfurfuryl Alcohol and Phenolic Resin," Carbon 7 643-8 (1969).
11. S. Yamada, H. Sato, "Some Physical Properties of Glassy Carbon," Nature (London) 193 261 (1962).
12. F. C. Cowland, J. C. Lewis, "Vitreous Carbon - A New Form of Carbon," J. Mat. Sci. 2 507-12 (1967).
13. F. Rodriguez-Reinso, P. L. Walker, Jr., "Reaction of Glassy Carbon with Oxygen," Carbon 13 7-10 (1975).
14. T. C. Peng, "Oxidation Effects on the Tensile Strength of ATJS Graphite and Vitreous Carbon, Carbon 17 157-74 (1979).
15. G. L. Tingey, "Chemical Reactivity of Glass-like Carbons," 12th Biennial Conf. Carbon, Pittsburgh, PA, July 28 - Aug. 1 (1975), ext. abstracts p. 181.
16. Tylan Corporation, 19220 S. Normandie Ave., Torrance, CA 90502.
17. A. Kellomaki, "Electrolytic Durability of Glassy Carbon," J. Mat. Sci. 15 1316-7 (1980).
18. S. Hosoki, S. Yamamoto, M. Futamoto, S. Fukuhara, "Field Emission Characteristics of Carbon Tips, Surface Science 86 723-33 (1979).
19. R. W. Hendricks, L. B. Shaffer, A. Bonfiglioli, F. A. Rojas, V. Gerold, H. Dunkeloh, J. E. Epperson, B. T. Jensen, A. M. Levelut, E. Dartyge, R. Perret, R. E. Burge, H. H. M. Balyuzi, M. Woodcock, P. W. Schmidt, J. S. Lin, R. L. Wershaw, "Final Report of the International Project for the Calibration of Absolute Intensities in Small-Angle X-ray Scattering," Commission on Crystallographic

- Apparatus, International Union of Crystallography, J. Appl. Cryst, 11, 196-205 (1978).
20. R. Perret, W. Ruland, "Glassy Carbon as Standard for the Normalization of Small-Angle Scattering Intensities," J. Appl. Cryst. 5 116-119 (1972).
  21. R. H. Bragg, M. L. Hammond, "X-Ray Study of Pyrolytic Graphites and Glassy Carbon," 7th Conf. Carbon, Cleveland, Ohio, June 21-25, 1965, paper #57.
  22. Sabri Ergun, Richard R. Schehl, "Analysis of the Structure of a Glassy Carbon Using the Fourier Transform Technique," Carbon 11 127-38 (1973).
  23. G. M. Jenkins, K. Kawamura, L. L. Ban, "Formation and Structure of Polymeric Carbons," Proc. Roy. Soc. Lond. A327 501-17 (1972).
  24. K. Kabayash, S. Sugawara, S. Toyoda, H. Honda, "An X-Ray Diffraction Study of Phenol-Formaldehyde Resin Carbons," Carbon 6 359-63 (1968).
  25. F. Rousseaux, D. Tchoubar, "Structural Evolution of a Glassy Carbon as a Result of Thermal Treatment Between 1000 and 2700°C--I. Evolution of the Layers," Carbon 15 55-61 (1977).
  26. R. Rousseaux, D. Tchoubar, "Structural Evolution of a Glassy Carbon as a Result of Thermal Treatment Between 1000 and 2700°C--II. Tridimensional Configuration of a Glassy Carbon," Carbon 15 63-68 (1977).
  27. Ram R. Saxena, Robert H. Bragg, "Kinetics of Graphitization in Glassy Carbon," Carbon 16 373-6 (1978).

28. G. D. Wignall, C. J. Pings, "The Structure of Vitreous Carbon from Wide Angle and Low Angle X-Ray Diffraction," *Carbon* 12 51-55 (1974).
29. S. Yamada, M. Yamamoto, "Structural Isotropy in Glassy Carbon Monofilament," *Carbon* 6 741-2 (1968).
30. R. G. Jenkins, P. L. Walker, Jr., "Small Angle X-Ray Scattering Studies on Carbons Derived from Polyfurfuryl Alcohol and Polyfurfuryl Alcohol-Ferrocene Copolymers," *Carbon* 14 7-11 (1976).
31. R. Perret, W. Ruland, "X-Ray Small-Angle Scattering of Glassy Carbon," *J. Appl. Cryst.* 5 183-7 (1972).
32. W. S. Rothwell, "Small Angle X-Ray Scattering from Glassy Carbon," *J. Appl. Phys.* 39 1840-5 (1972).
33. S. Bose, R. H. Bragg, "Kinetics of Pore Coarsening in Glassy Carbon," *Carbon* 19 289-95 (1981).
34. Madan Biswal, Robert H. Bragg, "Void Growth in Glassy Carbon," *Proc. 12th Biennial Conf. Carbon, Pittsburgh, PA., July 28 - Aug. 1, 1975.* p. 151.
35. L. R. Bunnell, "Structural Development in Vitreous Carbon as Observed by Scanning Electron Microscopy," *Carbon* 12 693-6 (1974.)
36. Edward E. Hucke, "Glassy Carbons," Final Report, June 1975, Advanced Research Projects Agency (ARPA) Order #1824, U. Mich. Dept. Mat. & Met. Eng.
37. S. Bose, U. Dahmen, R. H. Bragg, G. Thomas, "Lattice Image of LMSC Glassy Carbon," *J. Amer. Cer. Soc.* 61 174 (1978).
38. J. L. Kaae, "Microstructural Observations on a Commercial Glassy Carbon," *Carbon* 13 246-8 (1975).

39. Victor A. Phillips, "Lattice Structure in 1800°C Processed Vitreous Carbon," *Metallography* 6 361-4 (1973).
40. A. G. Whittaker, B. Tooper, "Single-Crystal Diffraction Patterns from Vitreous Carbon," *J. Amer. Cer. Soc.* 57 443-6 (1974).
41. Ram R. Saxena, "The Structure and Electrical Properties of Glassy Carbon," Ph.D. thesis, University of California, Berkeley, June 1976, LBL-5129.
42. L. L. Ban, D. Crawford, H. Marsh, "Lattice-Resolution Electron Microscopy in Structural Studies of Non-graphitizing Carbons from Polyvinylidene Chloride (PVDC)," *J. Appl. Cryst.* 8 415 (1975).
43. T. Noda, M. Inagaki, "The Structure of Glassy Carbon," *Bull. Chem. Soc. Japan* 37 1534-8 (1964).
44. R. W. Lindberg, "Radial Distribution Analysis of Glassy Carbon," M. S. thesis, Stanford University, Palo Alto, Calif., Oct. 1969.
45. J. P. Urban, D. Weick, "Comparison of the Momentum of Glassy Carbon and Graphite," *J. Appl. Phys.* 50 5947-9 (1979).
46. R. R. Saxena, R. H. Bragg, "K-Emission from Glassy Carbon," *Carbon* 12 210-2 (1974).
47. M. Nakamizo, R. Kammereck, P. L. Walker, Jr., "Laser Raman Studies on Carbons," *Carbon* 12 259 (1974).
48. Ian L. Spain, "Electronic Transport Properties of Graphite, Carbons, and Related Materials," *Chemistry and Physics of Carbon*, Philip L. Walker, Jr., Peter A. Thrower, eds., Marcel Dekker, New York, Vol. 16, pp. 119-304 (1981).
49. J. C. Slonczewski, P. R. Weiss, "Band Structure of Graphite," *Phys. Rev.* 109 272 (1958).

50. A. W. Moore, "Highly Oriented Pyrolytic Graphite," Chemistry and Physics of Carbon, Philip L. Walker, Jr., Peter A. Thrower, eds., Marcel Dekker, New York, Vol. 17, pp. 233-86 (1981).
51. Ian L. Spain, "Electronic Properties of Graphite," Chemistry and Physics of Carbon, Philip L. Walker, Jr., ed., Marcel Dekker, New York, Vol. 8, pp. 1-150 (1973).
52. P. Delhaes, "Positive and Negative Magnetoresistance in Carbons," Chemistry and Physics of Carbon, Philip L. Walker, Jr., ed., Marcel Dekker, New York, Vol. 7, pp. 193-235 (1971).
53. P. Delhaes, P. De Kepper, M. Ulrich, "A Study of the Negative Magnetoresistance in Pyrocarbons," Phil. Mag. 29 1301-1330 (1974).
54. A. A. Bright, L. S. Singer, "The Electronic and Structural Characteristics of Carbon Fibers from Mesophase Pitch," Carbon 17 59-69 (1979).
55. Y. Hishiyama, Y. Kaburagi, A. Ono, "Variable-Range Hopping Conduction and Negative Magnetoresistance of Disordered Carbons at Low Temperature," Carbon 17 265-76 (1979).
56. Y. Hishiyama, "Negative Magnetoresistance in Soft Carbons and Graphite," Carbon 8 259-69 (1970).
57. M. Inagaki, Y. Komatsu, J. V. Zanchetta, "Hall Coefficient and Magnetoresistance of Carbons and Polycrystalline Graphite in the Temperature Range 1.5-300°K," Carbon 7 163-75 (1969).
58. S. Mrozowski, A. Chaberski, "Hall Effect and Magnetoresistivity in Carbons and Polycrystalline Graphite," Phys. Rev. 104 74 (1956).
59. K. Yazawa, "Negative Magnetoresistance in Pyrolytic Carbons," J. Phys. Soc. Japan 26 1407 (1969).

60. K. Yazawa, "Origin of the Negative Magnetoresistance in Carbons and Its Relation with the Degree of Graphitization," *J. de Chimie Physique* 64 Numero Special p. 961 (1969).
61. S. Yugo, "Negative Magnetoresistance in Carbons," *J. Phys. Soc. Japan* 34 1421 (1973).
62. G. A. Saunders, "Electron Transport in Graphites and Carbons," Modern Aspects of Graphite Technology, L. C. F. Blackman, ed., Academic Press, New York, Ch. 3 pp. 79-127 (1970).
63. Ted G. Berlincourt, M. C. Steele, "Oscillatory Hall Effect, Magnetoresistance, and Magnetic Susceptibility of a Graphite Single Crystal," *Phys. Rev.* 98 956 (1955).
64. R. O. Dillon, I. L. Spain, J. W. McClure, "Electronic Energy Band Parameters of Graphite and Their Dependence on Pressure, Temperature and Acceptor Concentration," *J. Phys. Chem. Solids* 38 635 (1977).
65. G. H. Kinchin, "The Electrical Properties of Graphite," *Proc. Roy. Soc.* A217 (1953)
66. Claude A. Klein, "STB Model and Transport Properties of Pyrolytic Graphites," *J. Appl. Phys.* 35 2947 (1964).
67. Claude A. Klein, "Electrical Properties of Pyrolytic Graphites," *Revs. Modern Phys.* 34 56-79 (1962).
68. Claude A. Klein, "Pyrolytic Graphites: Their Description as Semimetallic Molecular Solids," *J. Appl. Phys.* 33 3338-57 (1962).
69. Claude A. Klein, W. Deter Straub, "Carrier Densities and Mobilities in Pyrolytic Graphite," *Phys. Rev.* 123 1581-3 (1961).

70. Y. Komatsu, "Hall Coefficient and Magnetoresistance of Soft Carbons Doped with Acceptors," Carbon 7 177-83 (1969).
71. S. Mrozowski, "Electronic Properties and Band Model of Carbons," Carbon 9 97-109 (1971).
72. S. Mrozowski, A. Chaberski, "Hall Effect and Magnetoresistivity in Carbons," Phys. Rev. 94 1427-8 (1954).
73. S. Toyoda, S. Mrozowski, "Studies of the Hall Coefficient and of the Magneto-Resistance of a Donor Doped Soft Carbon in the Temperature Range 1.5°-300°K," Carbon 7 239-59 (1969).
74. D. E. Soule, "Magnetic Field Dependence of the Hall Effect and Magnetoresistance in Graphite Single Crystals," Phys. Rev. 112 698-707 (1958).
75. Ian L. Spain, "Galvanomagnetic Effects in Graphite," Carbon 17 209-22 (1979).
76. R. O. Dillon, I. L. Spain, "Effects of Warped Energy Surfaces on the Low Field Hall Coefficient of Graphite," Sol. St. Comm. 26 333 (1978).
77. H. Oshima, K. Kawamura, T. Tsuzuku, K. Sugihara, "Hall Effect in Graphite and Its Relation to the Trigonal Warping of Energy Bands. I. Experimental," J. Phys. Soc. Japan 51 1476-81 (1982).
78. K. Sugihara, S. Ono, H. Oshima, K. Kawamura, T. Tsuzuku, "Hall Effect in Graphite and Its Relation to the Trigonal Warping of Energy Bands. II. Theoretical," J. Phys. Soc. Japan 51 1900-3 (1982).

79. C. S. Anithkumar, N. Umakantha, "Electrical Conduction in Molecular Organic Polycrystalline Substances, *Phil. Mag.* B44 615-21 (1981).
80. G. Pfister, C. H. Griffiths, "Temperature Dependence of Transient Hole Hopping Transport in Disordered Organic Solids: Carbazole Polymers," *Phys. Rev. Lett.* 40 659-62 (1978).
81. H. A. Pohl, J. R. Wyhof, "Effects of High Pressure on the Conductivity and Dielectric Constant of Conductive Organic Polymers," *J. Polymer Sci. Pt. A-1* 10 387-98 (1972).
82. K. Saha, S. C. Abbi, H. A. Pohl, "Temperature Dependence of Hopping Transport in Polymeric Semiconductors," *J. Non-Cryst. Sol.* 21 117-24 (1976).
83. C. J. Adkins, S. M. Freake, E. M. Hamilton, "Electrical Conduction in Amorphous Carbon," *Phil. Mag.* 22 183-8 (1970).
84. H. Morisaki, K. Yazawa, "Electrical Transport in Amorphous Carbon Films," *Elect. Eng. Japan* 96 #4 8-14 (1976).
85. M. Morgan, "Electrical Conduction in Amorphous Carbon Films," *Thin Solid Films* 7 313-23 (1971).
86. F. Carmona, P. Delhaes, G. Keryer, M. P. Manceau, "Non-Metal-Metal Transition in a Non-Crystalline Carbon," *Sol. St. Comm.* 14 1183-7 (1974).
87. F. Carmona, P. Delhaes, "Effect of Density Fluctuations on the Physical Properties of a Disordered Carbon," *J. Appl. Phys.* 49 618-28 (1978).

88. J. C. Giuntini, J. V. Zanchetta, "Use of Conduction Models in the Study of "Low Temperature" Carbons," J. Non-Cryst. Sol. 34 419-24 (1979).
89. J. C. Giuntini, D. Jullien, J. V. Zanchetta, F. Carmona, P. Delhaes, "Electrical Conductivity of Low-Temperature Carbons as a Function of Frequency," J. Non-Cryst. Sol. 30 87-98 (1978).
90. W. Bucker, "Preparation of and DC Conductivity of an Amorphous Organic Semiconducting System," J. Non-Cryst. Sol. 12 115-28 (1973).
91. K. Rozwadowska, "Preparation and DC Conductivity of the Low-Temperature Glassy Carbon," Phys. Stat. Sol. A54 93 (1979).
92. W. Bucker, "ESR, Seebeck and Hall Measurements on an Amorphous System with Hopping Conduction," J. Non-Cryst. Sol. 18 11-19 (1975)
93. K. Antonowicz, L. Cacha, J. Turlo, "Switching Phenomena in Glassy Carbon," Carbon 11 1 (1973).
94. K. Antonowicz, A. Jesmanowicz, J. Wieczerek, "Switching Phenomenon in Amorphous Carbon," Carbon 10 81 (1972).
95. T. Yamaguchi, "Galvanomagnetic Properties of Glassy Carbon," Carbon 1 47-50 (1963).
96. T. Tsuzuku, K. Saito, "Electric Conduction in Glassy Carbons," Japan. J. Appl. Phys. 5 738-9 (1966).
97. Ram R. Saxena, Robert H. Bragg, "Electrical Conduction in Glassy Carbon," J. Non-Cryst. Sol. 28 45-60 (1978).
98. Ram R. Saxena, Robert H. Bragg, "Negative Magnetoresistance in Glassy Carbon," Phil. Mag. 36 1445-56 (1977).

99. Y. Toyozawa, "Theory of Localized Spins and Negative Magnetoresistance in the Metallic Impurity Conduction," J. Phys. Soc. Japan 17 986 (1962).
100. Numerical Algorithm Group, University of Oxford, England.
101. Philip E. Gill, Walter Murray, "Algorithms for the Solution of the Nonlinear Least-Squares Problem," SIAM J. Numerical Analysis 15 977-992 (1978).
102. J. R. Wolberg, "Prediction Analysis," D. Van Nostrand, Princeton, Ch. 3-4 (1967).
103. A. Hald, "Statistical Theory with Engineering Applications," J. Wiley & Sons, New York, Ch. 10, 11, 23 (1952).
104. N. F. Mott, E. A. Davis, "Electronic Processes in Non-Crystalline Materials," 2nd ed., Clarendon Press, Oxford (1979).
105. F. T. Hedgecock, "Localized Magnetic Moments in Impurity-Banded Semiconductors," Can. J. Phys. 45 1473-80 (1967).
106. D. Shaltiel, J. H. Wernich, H. J. Williams, M. Peter, "Paramagnetic Resonance of s-State Ions in Metals of High Paramagnetic Susceptibility," Phys. Rev. 135 A1346 (1964).
107. G. G. Low, T. M. Holden, "Distribution of the Ferromagnetic Polarization Induced by Iron and Cobalt Atoms in Palladium," Proc. Phys. Soc. 89 119 (1966).
108. N. Ganguli, K. S. Krishnan, "The Magnetic and Other Properties of the Free Electrons in Graphite," Proc. Roy. Soc. A177 168 (1941).
109. A. Pacault, "Along the Carbon Way," Carbon 12 1-25 (1974).

110. A. Pacault, A. Marchand, "A Study of the Magnetism and Structure of Carbon Blacks," Proc. 3rd Conf. Carbon, Pergamon Press, New York, p. 37-41, (1957).
111. D. B. Fischbach, "The Magnetic Susceptibility of Pyrolytic Carbon," Proc. 5th Conf. Carbon, Pergamon Press, New York, Vol. 2, p. 27 (1961).
112. J. W. McClure, "Theory of Diamagnetism of Graphite," Phys. Rev. 119 606 (1960).
113. J. W. McClure, "Diamagnetism of Graphite," Phys. Rev. 104 666 (1956).
114. G. Volpilhac, J. Hoarau, "Effect of the Interlayer Interactions on the Diamagnetism of Graphitic Ribbons," Phys. Rev. B17 1445 (1978).
115. J. Hoarau, G. Volpilhac, "Theory of the Diamagnetic Susceptibility of Condensed Ring Systems: Reinterpretation of Diamagnetism of Pregraphitic Carbons," Phys. Rev. B14 4045 (1976).
116. J. W. McClure, B. B. Hickam, "Analysis of Magnetic Susceptibility of Carbon Fibers," Carbon 20 373-8 (1982).
117. D. B. Fischbach, "Magnetic Susceptibility of Glassy Carbon," Carbon 5 565-70 (1967).
118. M. Omori, S. Yajima, "Identification and Properties of Ultra-Fine Iron Particles Dispersed in a Glass-Like Carbon Matrix," J. Mat. Sci. 14 2537-42 (1979).
119. F. W. Smith, M. P. Sarachik, "Thermally Activated Paramagnetism in Carbon Chars," Sol. St. Comm. 34 503-6 (1980).

120. M. P. Sarachik, F. W. Smith, "Magnetic Interactions Between Carbon Localized Spins in an Amorphous Carbon," J. Appl. Phys. 50 7627 (1979).
121. F. Carmona, P. Delhaes, J. L. Thallence, J. C. Lasjanias, "Anomalous Low Temperature Magnetic and Thermal Properties of an Amorphous Carbon," Sol. St. Comm. 24 511-4 (1977).
122. T. Szczurek, "Magnetic Susceptibility of Evaporated Carbon," Acta Phys. Pol. A51 239-48 (1977).
123. A. F. Adamson, H. E. Blayden, "Magnetic Studies of Graphites and Mesomorphous Carbons," Proc. 3rd Conf. Carbon, Pergamon Press, New York, p. 147 (1959).
124. K. Antonowicz, "Formation of Spin Centers in Carbons by Oxidation and Their Thermal Anneal," Proc. Fifth Carbon Conf., Pergamon Press, New York, Vol. I, p. 46 (1962).
125. C. Jackson, W. F. K. Wynne-Jones, "Electron Spin Resonance in Carbonized Organic Polymers - I," Carbon 2 227-37 (1964).
126. J. W. Armstrong, C. Jackson, H. Marsh, "Electron Spin Resonance in Carbonized Organic Polymers - II Effects of Adsorbed Oxygen," Carbon 2 239-52 (1964).
127. D. Campbell, C. Jackson, H. Marsh, W. F. K. Wynne-Jones, "Electron Spin Resonance in Carbonized Organic Polymers - III Temperature Dependence of Susceptibility of Non-Oxidized and Oxidized Carbons," Carbon 4 159-66 (1966).

128. H. E. Blayden, D. T. Westcott, "A Magnetic Study of the Carbonization and Graphitization of Some Representative Polymers," Proc. Fifth Carbon Conf., Pergamon Press, New York, Vol. II, p. 97 (1963).
129. S. Toyoda, S. Sugawara, T. Furuta, H. Honda, "Electron Spin Resonance of Heattreated Phenol-Formaldehyde Resins," Carbon 8 473-7 (1970).
130. S. Orzeszko, K. T. Yang, "Electron Spin Resonance in Glassy Carbon," Carbon 12 493-8 (1974).
131. S. Mrozowski, "Electron Spin Resonance in Neutron Irradiated and in Doped Polycrystalline Graphite, Part I," Carbon 3 305-20 (1965).
132. S. Kobayashi, Y. Fukagawa, S. Ikehata, W. Sasaki, "NMR Study on Electronic States in Phosphorous Doped Silicon," J. Phys. Soc. Japan 45 1276-81 (1978).
133. A. A. Bright, "Negative Magnetoresistance of Pregraphitic Carbons," Phys. Rev. B20 5142-9 (1979).
134. B. Movaghar, L. Schweitzer, "A Model for thr Anomalous Magnetoresistance in Amorphous Semiconductors," J. Phys. C 11 125-35 (1977).
135. B. Giovannini, F. T. Hedgcock, "Influence of Temperature on the Two Band Model for Negative Magnetoresistance in Heavily Doped Semiconductors," Sol. St. Comm. 11 367 (1972).
136. H. Fukuyama, K. Yosida, "Negative Magnetoresistance in the Anderson Localized States," J. Phys. Soc. Japan 46 102 (1979).

137. H. Fukuyama, K. Yosida, "Negative Magnetoresistance in the Anderson Localized States, II. Effect of Electron Correlations," J. Phys. Soc. Japan 46 1522 (1979).
138. A. Kawabata, "Theory of Negative Magnetoresistance, I. Application to Heavily Doped Semiconductors," J. Phys. Soc. Japan 49 628-37 (1980).
139. A. H. Wilson, "Theory of Metals," Cambridge University Press, 2nd ed., London (1953).
140. B. I. Shklovskii, N. V. Lien, "Hopping Magnetoresistance of n-Type Germanium," Sov. Phys. Semicond. 12 796 (1978).
141. M. Kaveh, N. F. Mott, "Electron Correlations and Logarithmic Singularities in Density of States and Conductivity of Disordered Two-Dimensional Systems," J. Phys. C 14 L183-90 (1981).
142. E. Abrahams, P. W. Anderson, D. C. Licciardello, T. V. Ramakrishnan, "Scaling Theory of Localization: Absence of Quantum Diffusion in Two Dimensions," Phys. Rev. Lett. 42 673 (1979).
143. B. L. Altshuler, A. G. Aronov, P. A. Lee, "Interaction Effects in Disordered Fermi Systems in Two Dimensions," Phys. Rev. Lett. 44 1288 (1980).
144. Leo G. Henry, Robert H. Bragg, "Anomalous Large Layer Spacings in Glassy Carbon," LBL Report # 13544, 1978; Extended Abstracts 14th Biennial Conf. Carbon, Penn State, University Park, Pa., June 25-29 (1979), p. 129.

145. Bholá N. Mehrotra, R. H. Bragg, A. S. Rao, "Effect of Heat Treatment Temperature (HTT) on Density, Weight and Volume of Glass-Like Carbon (GC), LBL Report #15072, To be published in J. Mat. Sci.
146. R. E. Franklin, "Crystallite Growth in Graphitizing and Non-Graphitizing Carbons," Proc. Roy. Soc. 209 196 (1951).
147. E. E. Loebner, "Thermoelectric Power, Electrical Resistance, and Crystalline Structure of Carbons," Phys. Rev. 102 46-57 (1956).
148. Y. Hishiyama, Y. Kaburagi, A. Ono, M. Inagaki, K. Kamiya, "Magnetoresistance of Two-Phase Carbons," Carbon 18 427-32 (1980).
149. K. Kawamura, T. Tsuzuku, "Partial Graphitization in Relation to the Porosity of Glassy Carbons," Carbon 12 352-55 (1974).

FIGURE CAPTIONS

- |  |  |                |
|--|--|----------------|
| I.1  | Sketch of Glassy Carbon Structure  | XBL 766-8079   |
| I.2-5.   | Lattice Images of Glassy Carbon  | XBB 8010-12199 |
|  | Heat Treated at 2700°C, 2550°C, 2250°C,                                    | XBB 8010-12198 |
|  | and 1800°C respectively  | XBB 8010-12197 |
|  |  | XBB 8010-12196 |
| <p>The subfigures a, b, and c, are underfocused, in focus, and overfocused with the change of focus about 200 Å. The "in focus" condition is optimally theoretically about 600 Å underfocused. The series of subfigures for each heat treatment temperature gives a depth distribution of the fringes in the thin specimen. The fringes are 3.4 Å thick.</p> <p>Microscopy courtesy of Dr. RonGronsky.</p> |  |                |
| I.6  | Mrozowski Model Band Diagram for Soft Carbons (Ref. 71)                    | XBL 842-5494   |
| I.7  | Bucher Low Heat Treatment Temperature Glassy Carbon Conductivity (Reg. 90) | XBL 828-11094  |

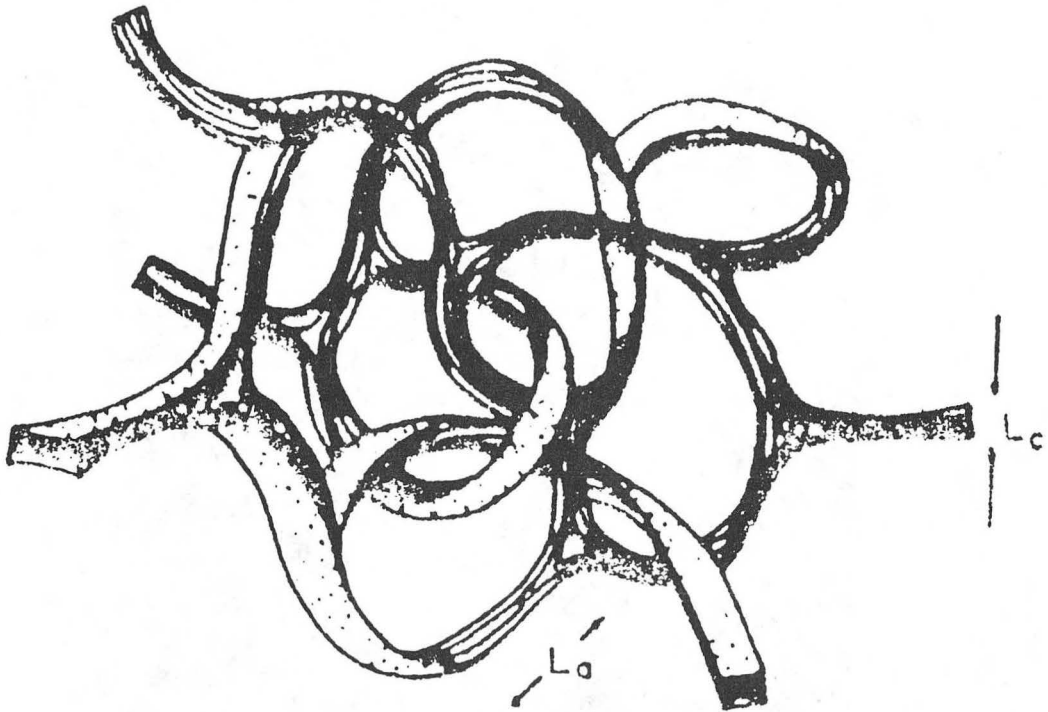
III.1-10	Magnetoresistance as a function of the	LBL 829-11524
	magnetic field squared plotted as isotherms	LBL 829-11525
	for heat treatment temperatures of 1000,	LBL 829-11526
	1200, 1400, 1600, 1800, 2000, 2250, 2350,	LBL 829-11527
	2550, and 2700 °C respectively.	LBL 829-11528
		LBL 829-11529
		LBL 829-11530
		LBL 829-11531
		LBL 829-11532
		LBL 829-11533
III.11-20	Electrical conductivity as a function of	LBL 829-11534
	temperature for glassy carbon heat treated	LBL 829-11535
	at 1000, 1200, 1400, 160, 1800, 2000, 2250,	LBL 829-11536
	and 2700 °C respectively. The solid lines	LBL 829-11537
	have been fitted according to the empirical	LBL 829-11538
	equation $\sigma = A + B \exp(-C_0 T^{-1/4}) - DT^{-1/2}$ .	LBL 829-11539
		LBL 829-11540
		LBL 829-11541
		LBL 829-11542
		LBL 829-11543

- III.21 The Hall Coefficient plotted as a function of the inverse fourth root of temperature. LBL 828-6431
- III.22 The Hall mobility plotted as a function of the inverse fourth root of temperature. LBL 828-6432
- III.23 The Hall coefficient as a function of heat treatment temperature. LBL 816-5907A
- III.24 Literature values of the Hall coefficient as a function of heat treatment temperature. LBL 828-6433

- IV.1. Curie-Pauli parameter  $\chi$  vs. heat treatment temperature. LBL 828-6437
- IV.2. Curie-Pauli parameter  $\Gamma$  vs. heat treatment temperature. LBL 828-6438
- IV.3-9. Fit of Curie-Pauli model plotting isomagnetic field lines for glassy carbon heated at 2700, 2550, 2350, 2250, 2000, 1800, and 1600 °C. LBL 829-11517  
LBL 829-11518  
LBL 829-11519  
LBL 829-11520  
LBL 829-11521  
LBL 829-11522  
LBL 829-11523
- IV.10. Spin Concentration (Electron Spin Resonance; Ref. 130) as a function of heat treatment for localized and conduction or extended electron states. LBL 765-6929
- IV.11. Kobayashi moment (Ref. 132) model parameter Q as a function of heat treatment temperature. LBL 828-6439

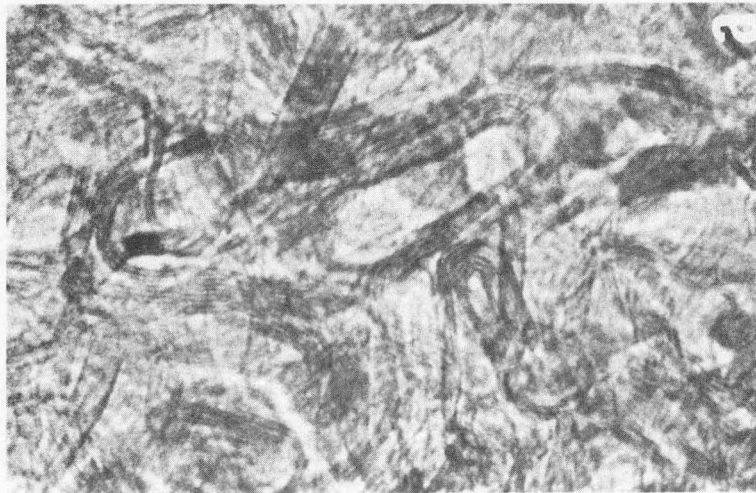
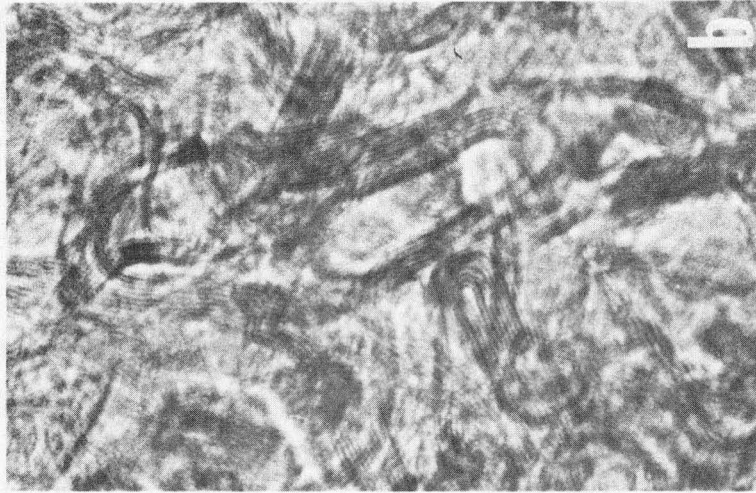
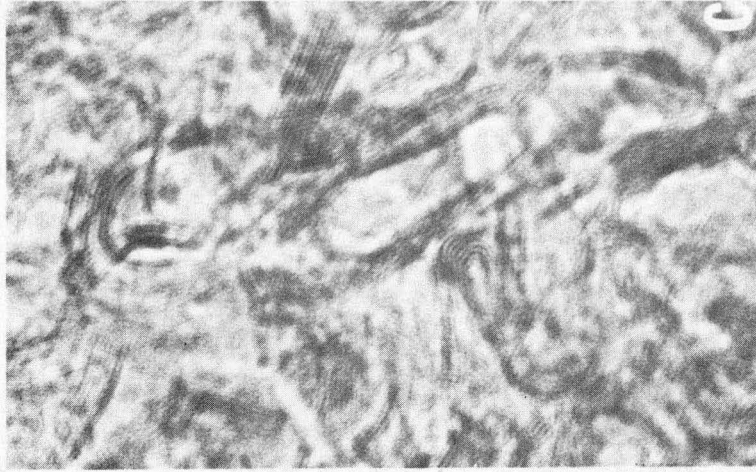
- IV.12. Kobayashi moment (Ref. 132) model interaction energy  $U$  vs. heat treatment temperature. LBL 828-6440
- IV.13. Bright model proportionality parameter as a function of heat treatment temperature. LBL 825-11510
- IV.14-20. Bright (Ref. 133) model plots of the square root of the absolute value of the magneto-resistance against the magnetic field divided by the square root of temperature  $H/T^{1/2}$  for glassy carbon heat treated at 2700, 2550, 2350, 2250, 2000, 1800, and 1600 °C. LBL 829-11510  
LBL 829-11511  
LBL 829-11512  
LBL 829-11513  
LBL 829-11514  
LBL 829-11515  
LBL 829-11516
- IV. 21. The one-dimensionality parameter  $D$  of the electrical conductivity of glassy carbon as a function of heat treatment temperature. LBL 828-6436
- IV. 22. The strongly scattering metallic component  $A$  of the electrical conductivity plotted as a function of heat treatment temperature. LBL 828-6434

IV.23. The prefactor constant B of the variable range LBL 828-6535 hopping component of the electrical conductivity plotted as a function of heat treatment temperature.



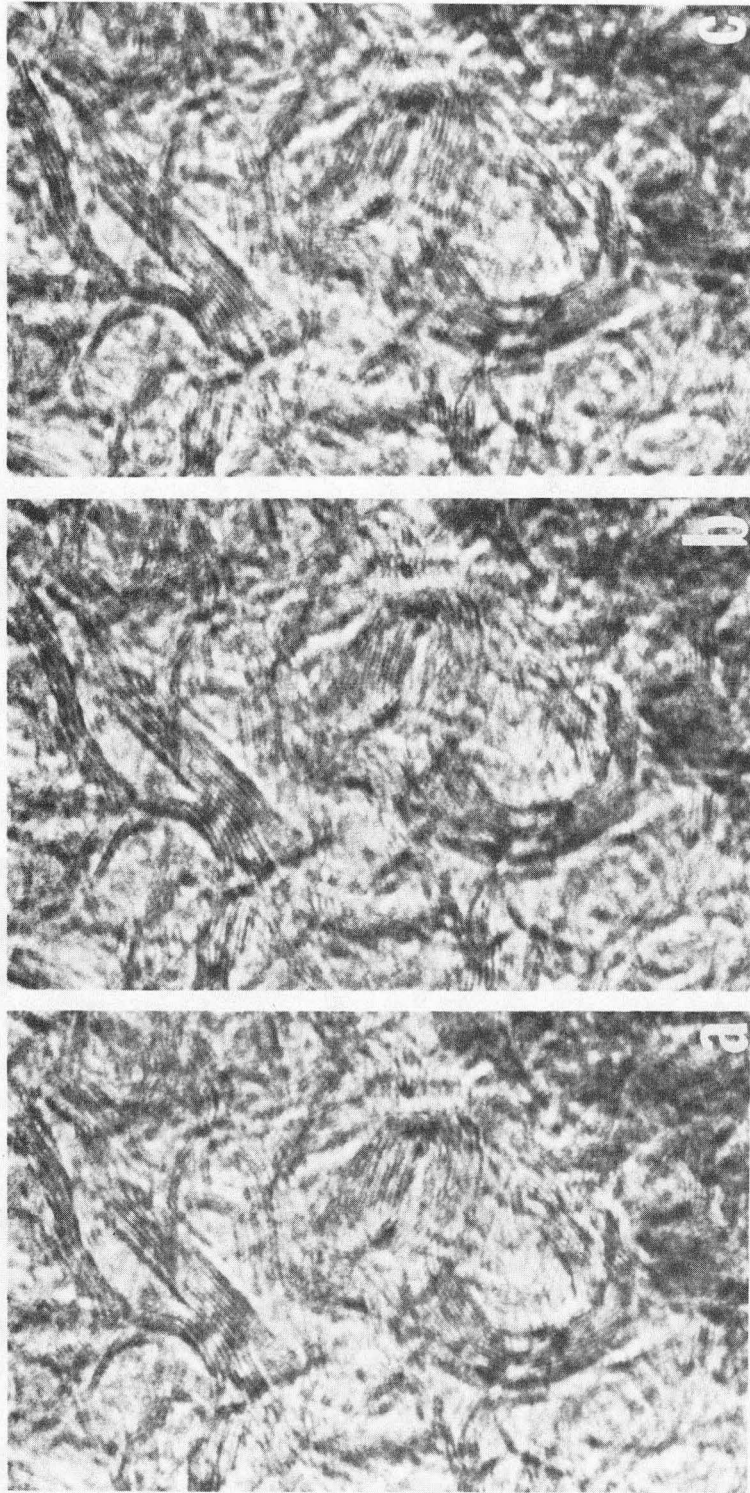
XBL 766-8079

Figure I.1



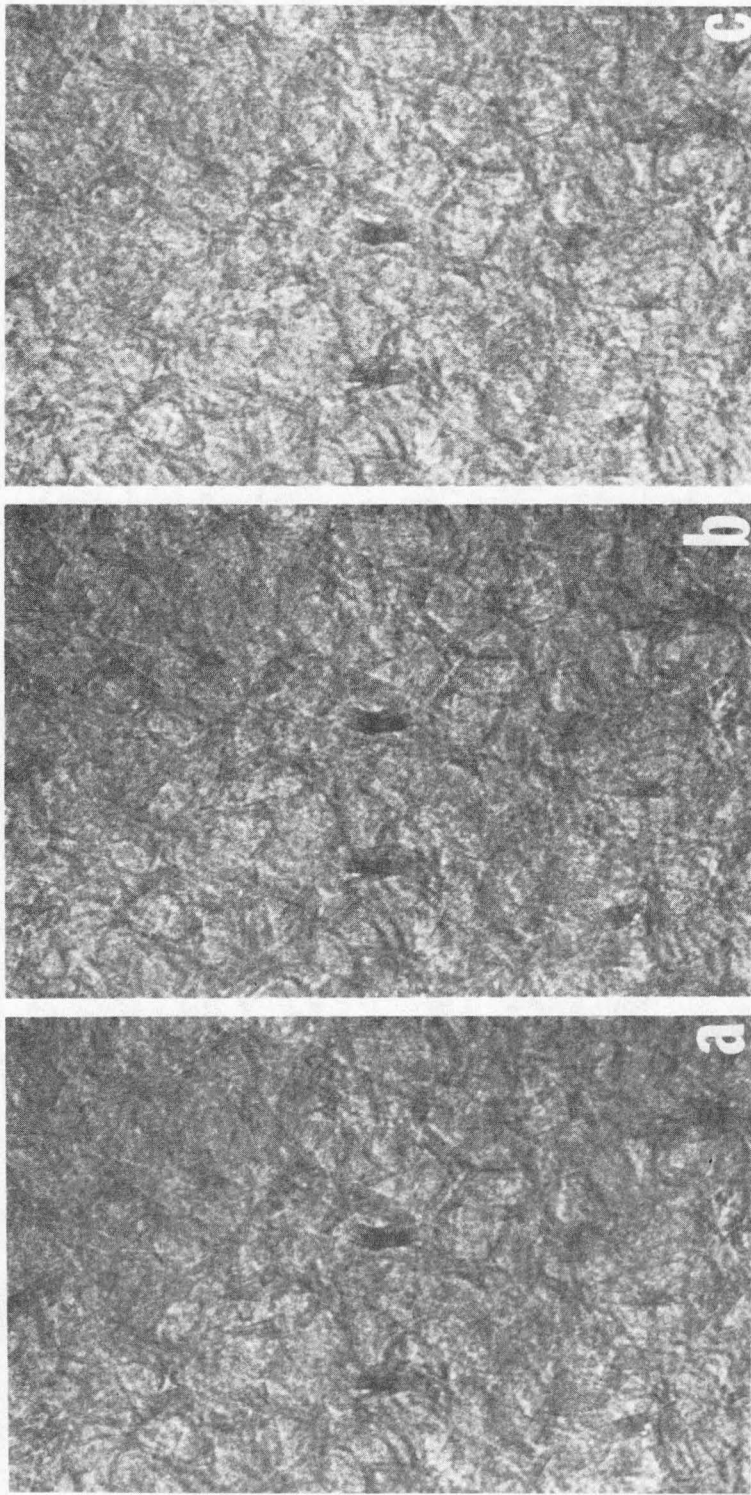
XBB 800-12199

Figure I.2



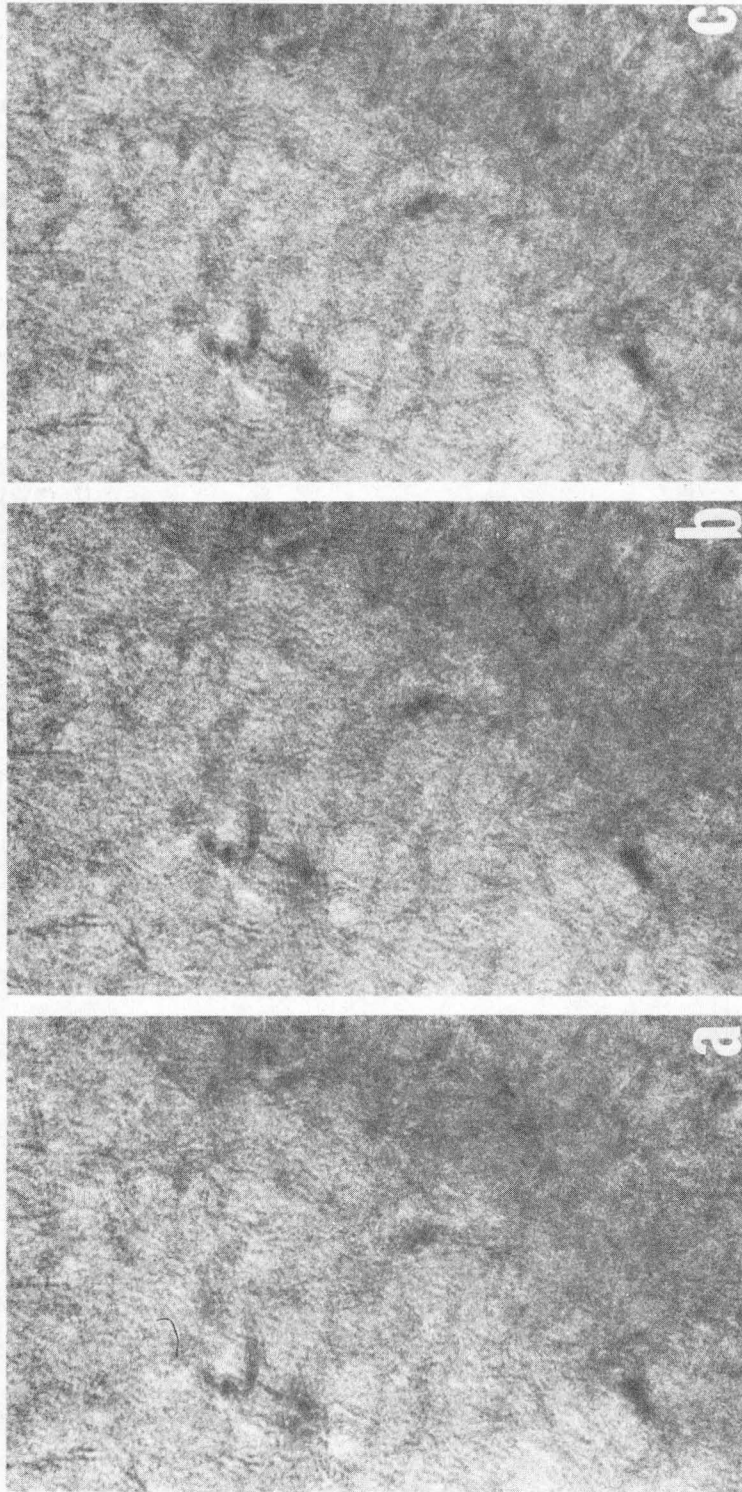
XBB 800-12198

Figure I.3



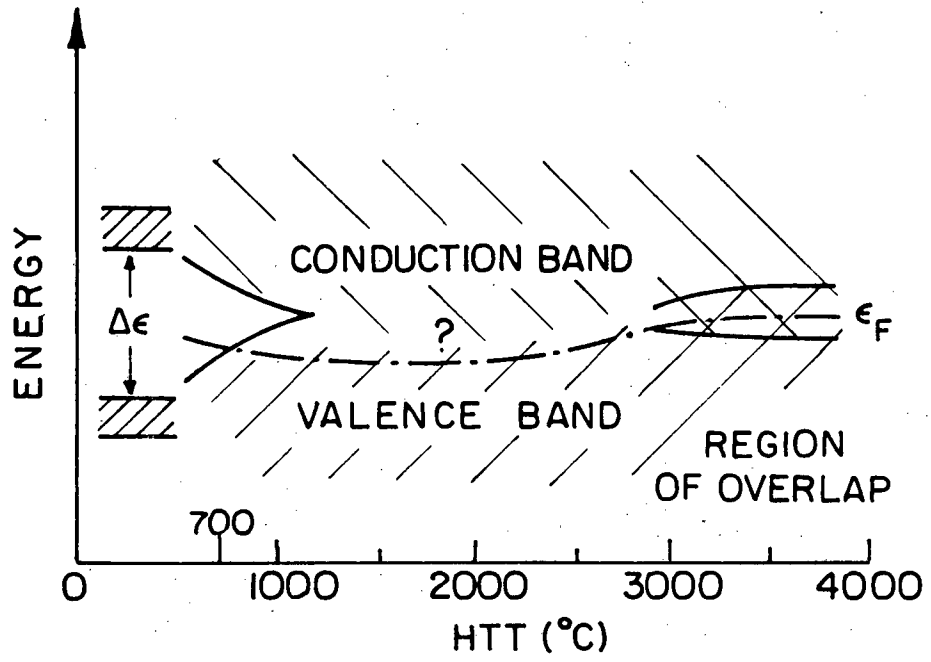
XBB 800-12197

Figure I.4



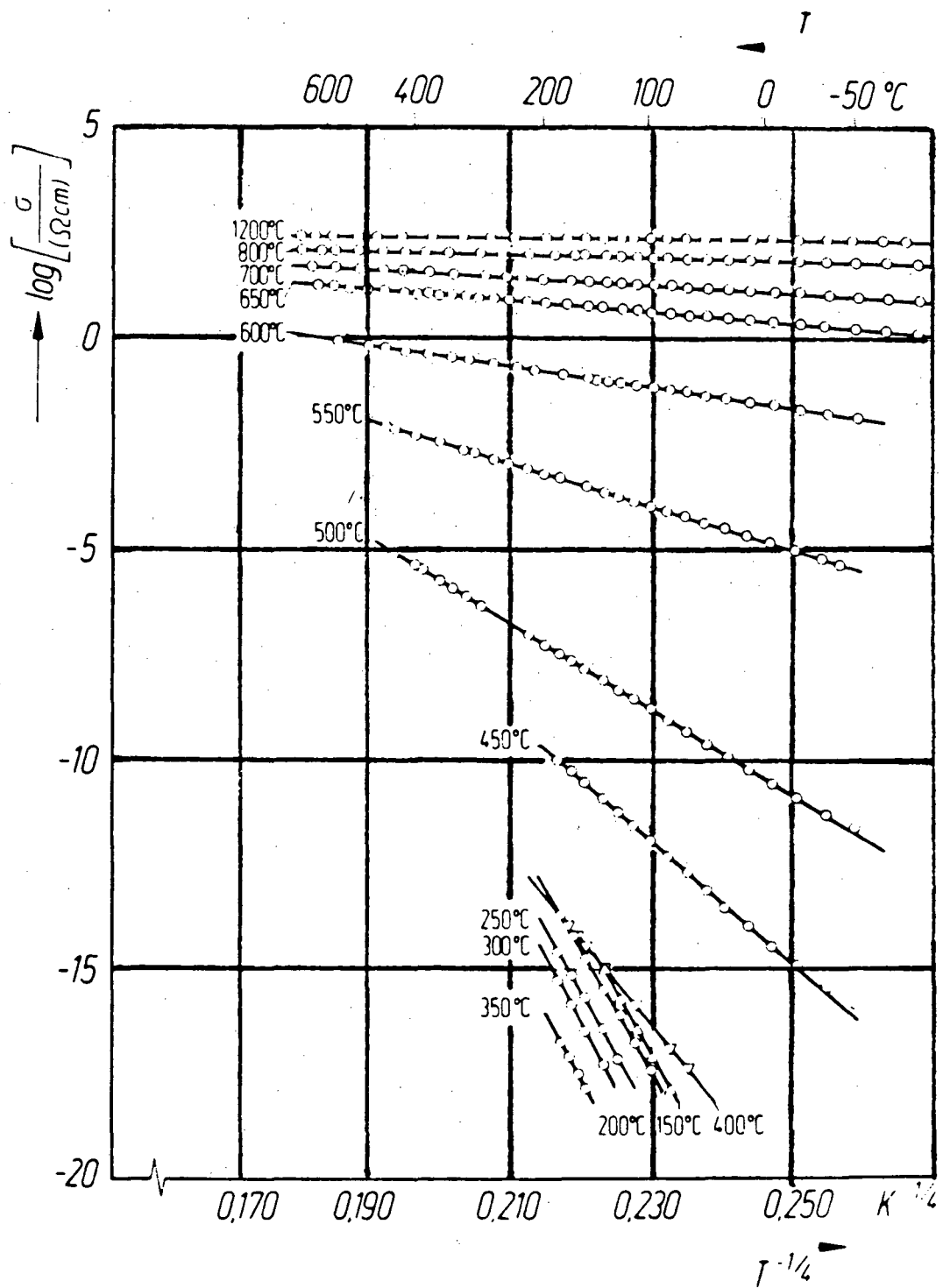
XBB 800-12196

Figure I.5



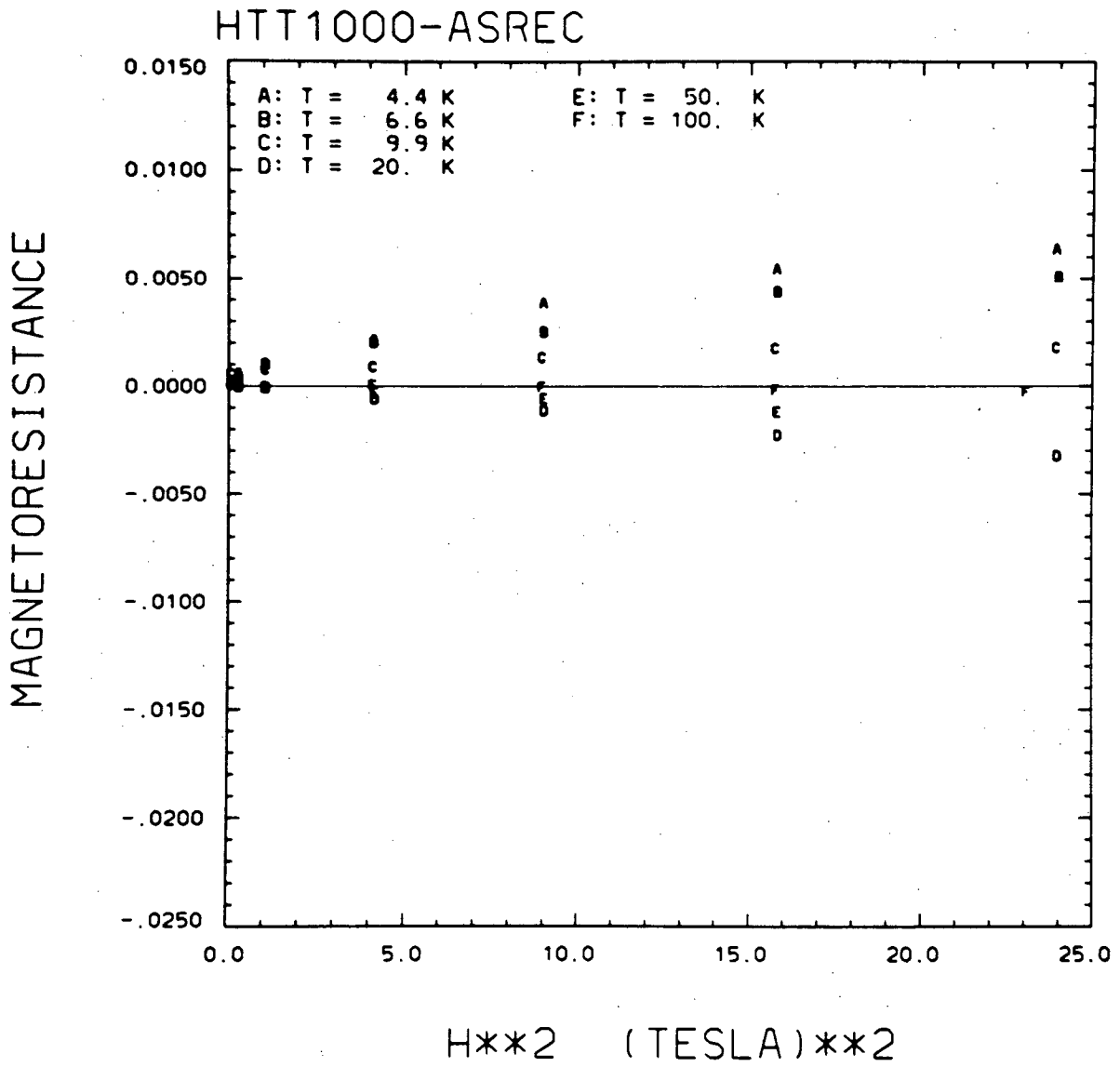
XBL824-5494

Figure I.6



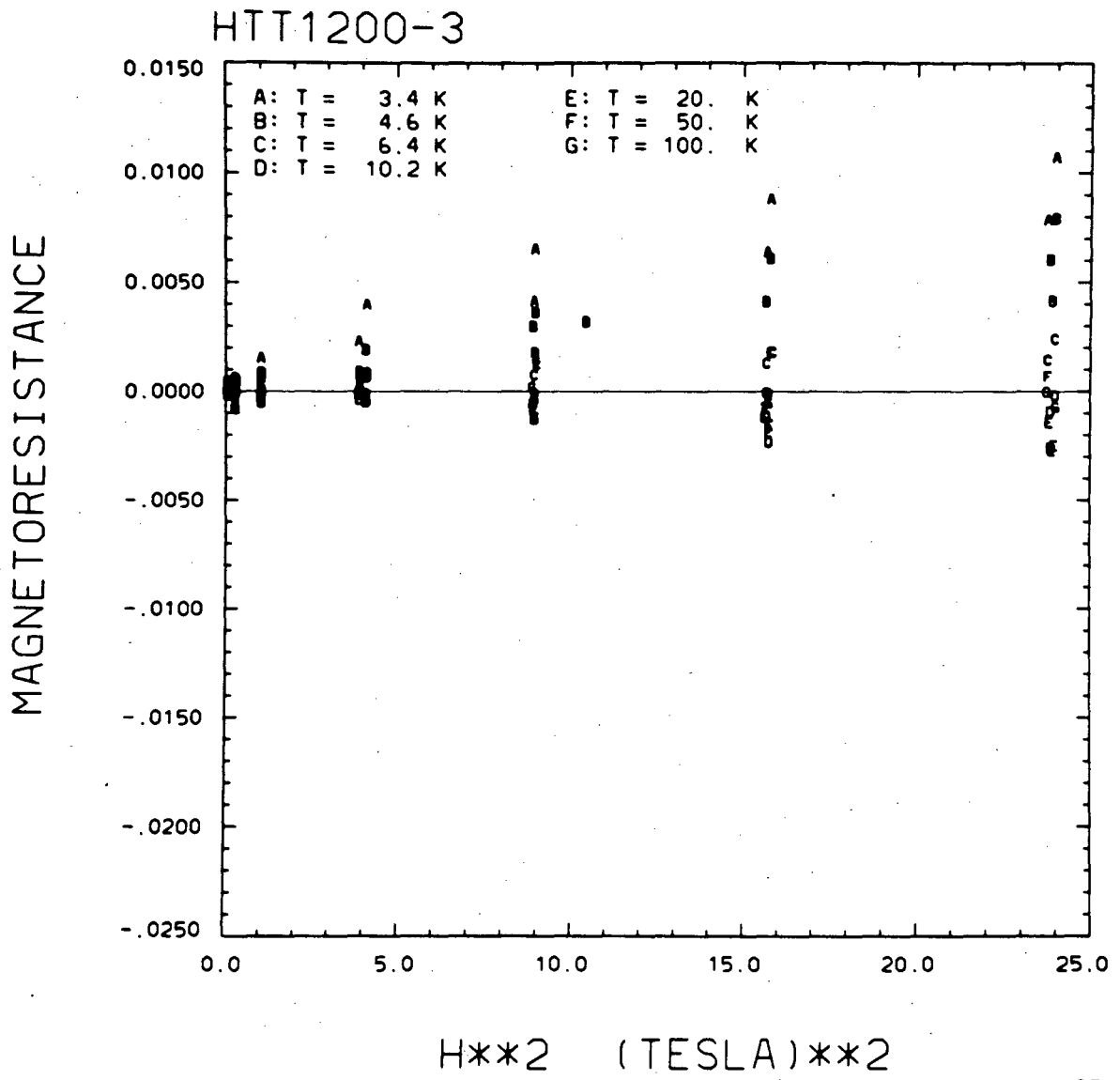
XBL 828-11094

Figure I.7



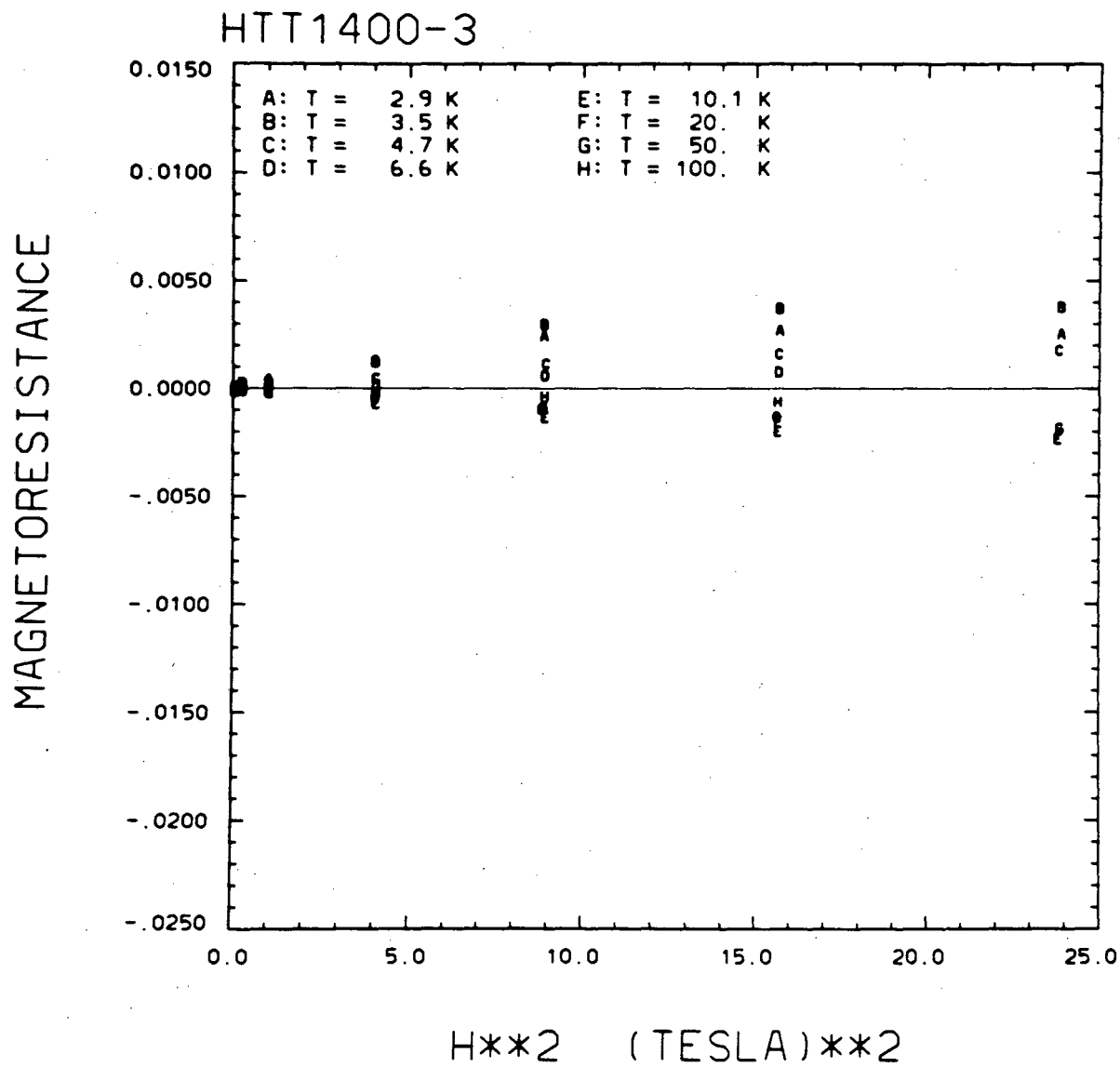
XBL 829-11524

Figure III.1



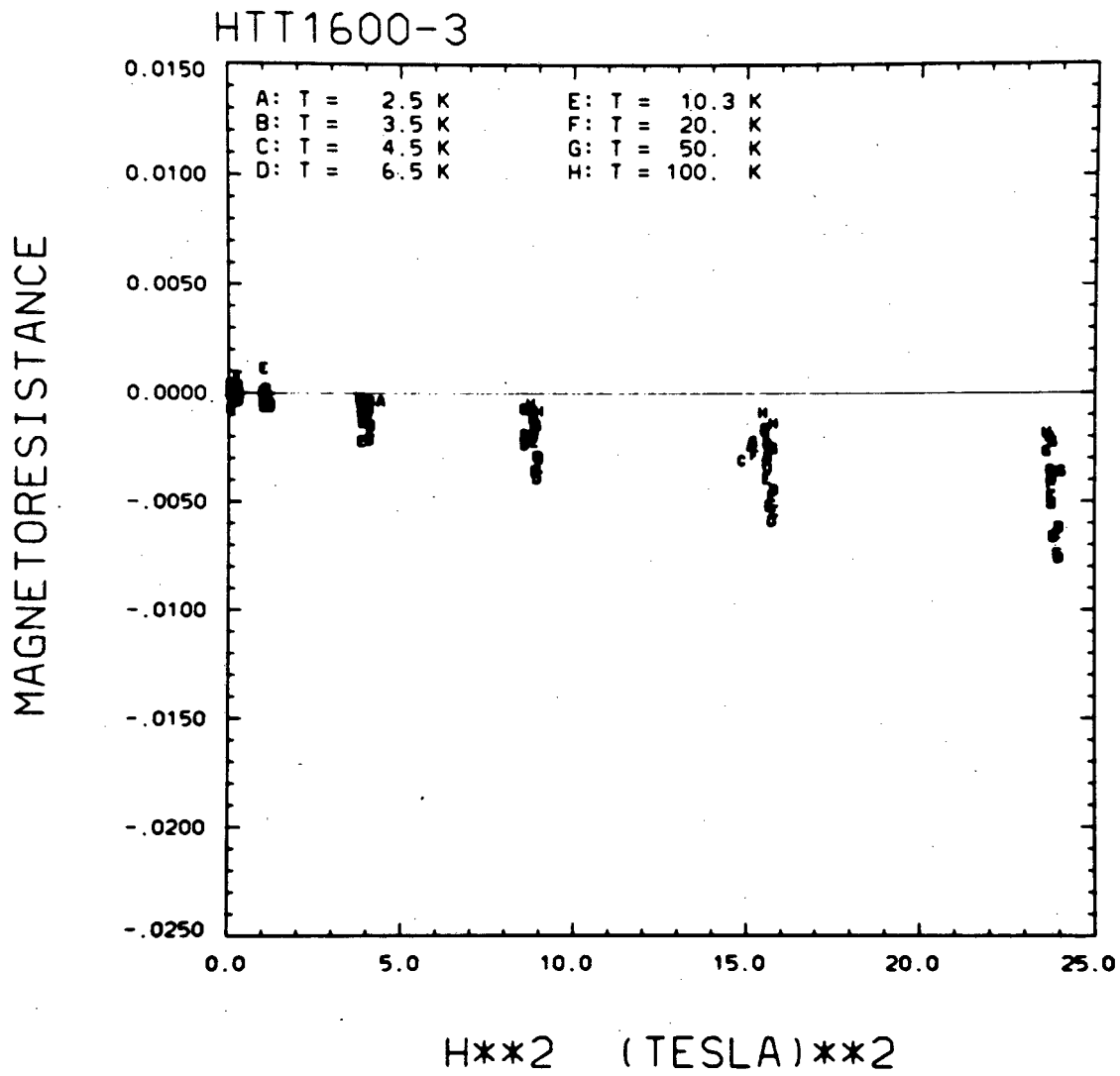
XBL 829-11525

Figure III.2



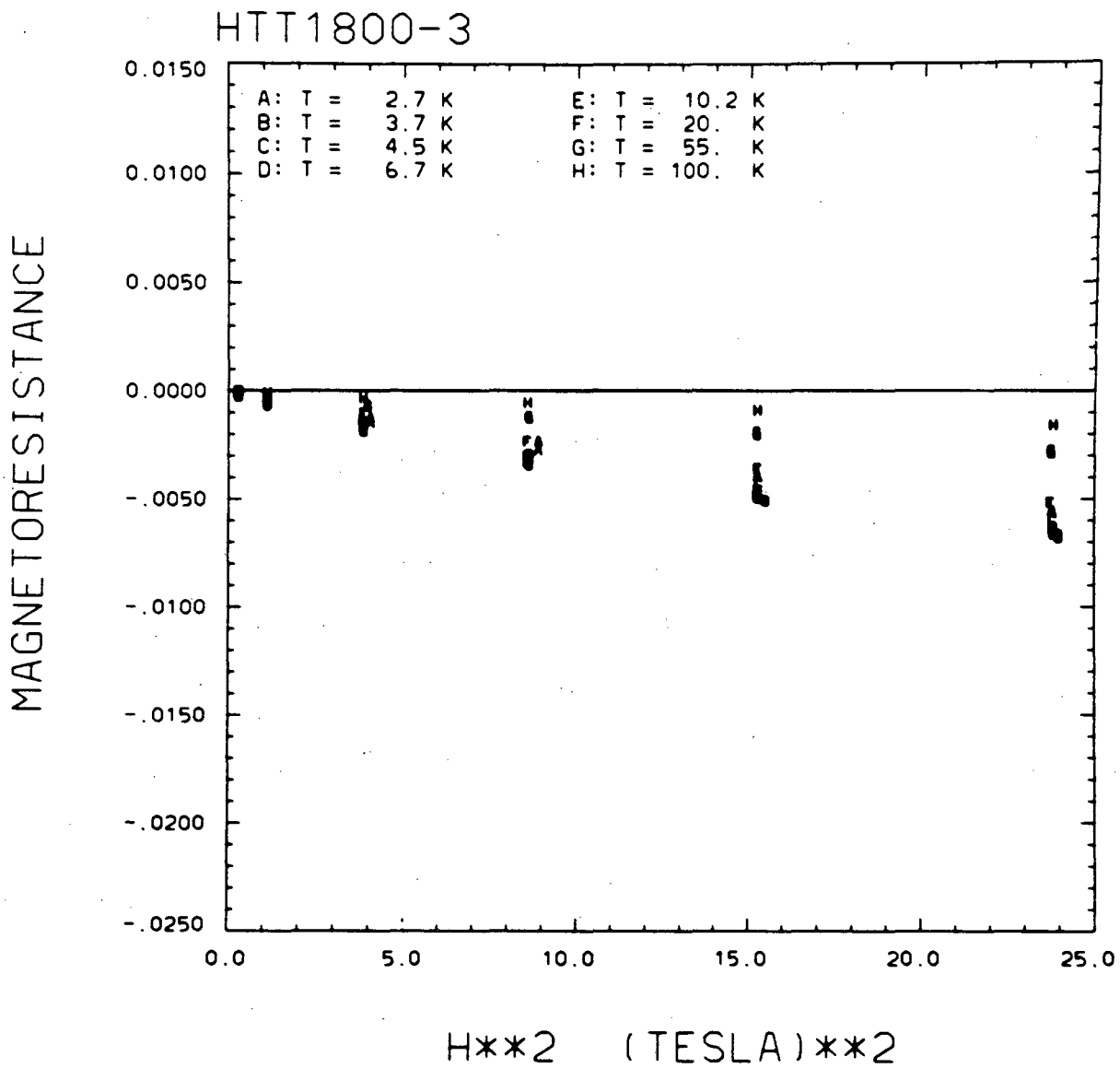
XBL 829-11526

Figure III.3



XBL 829-11527

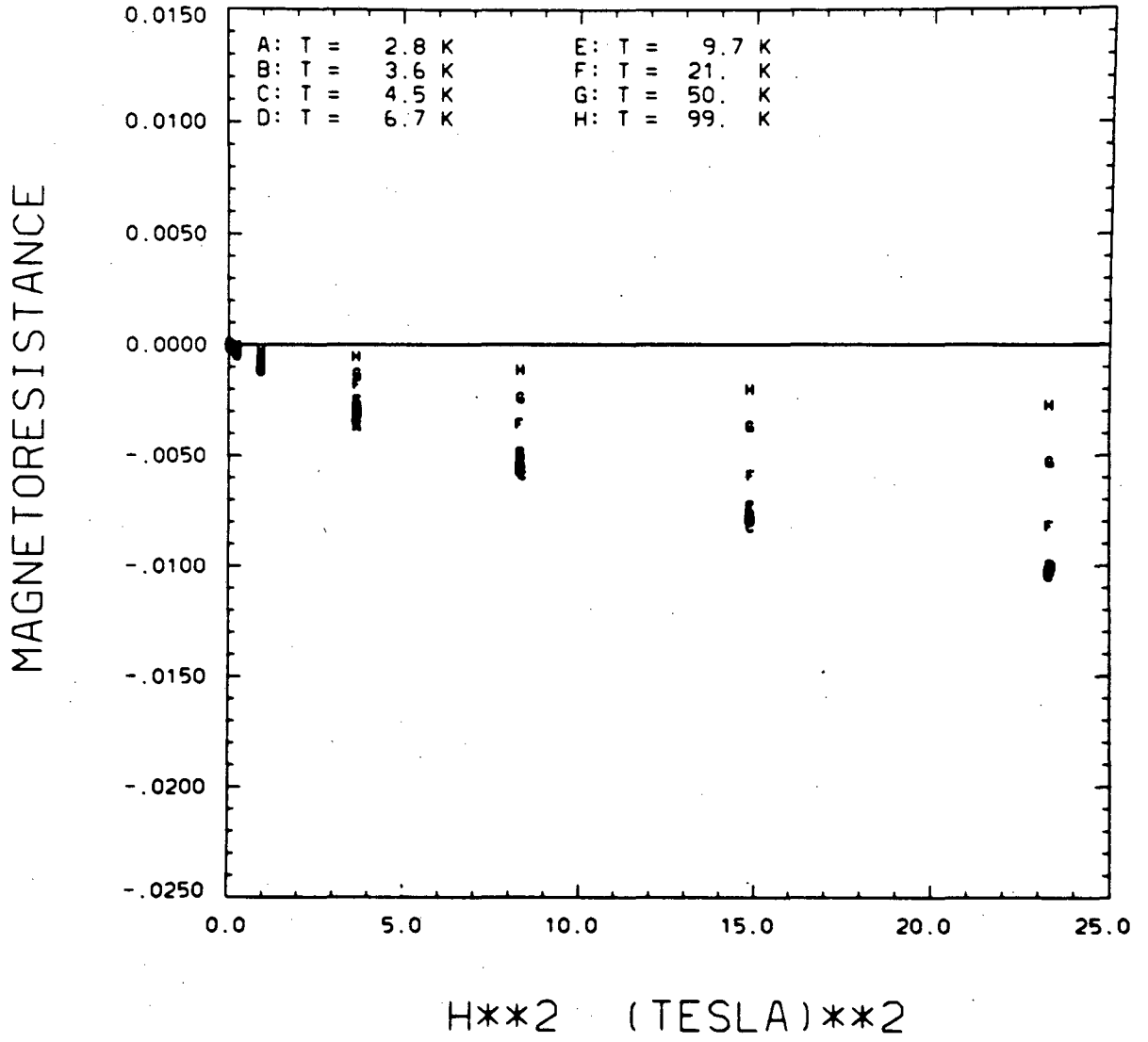
Figure III.4



XBL 829-11528

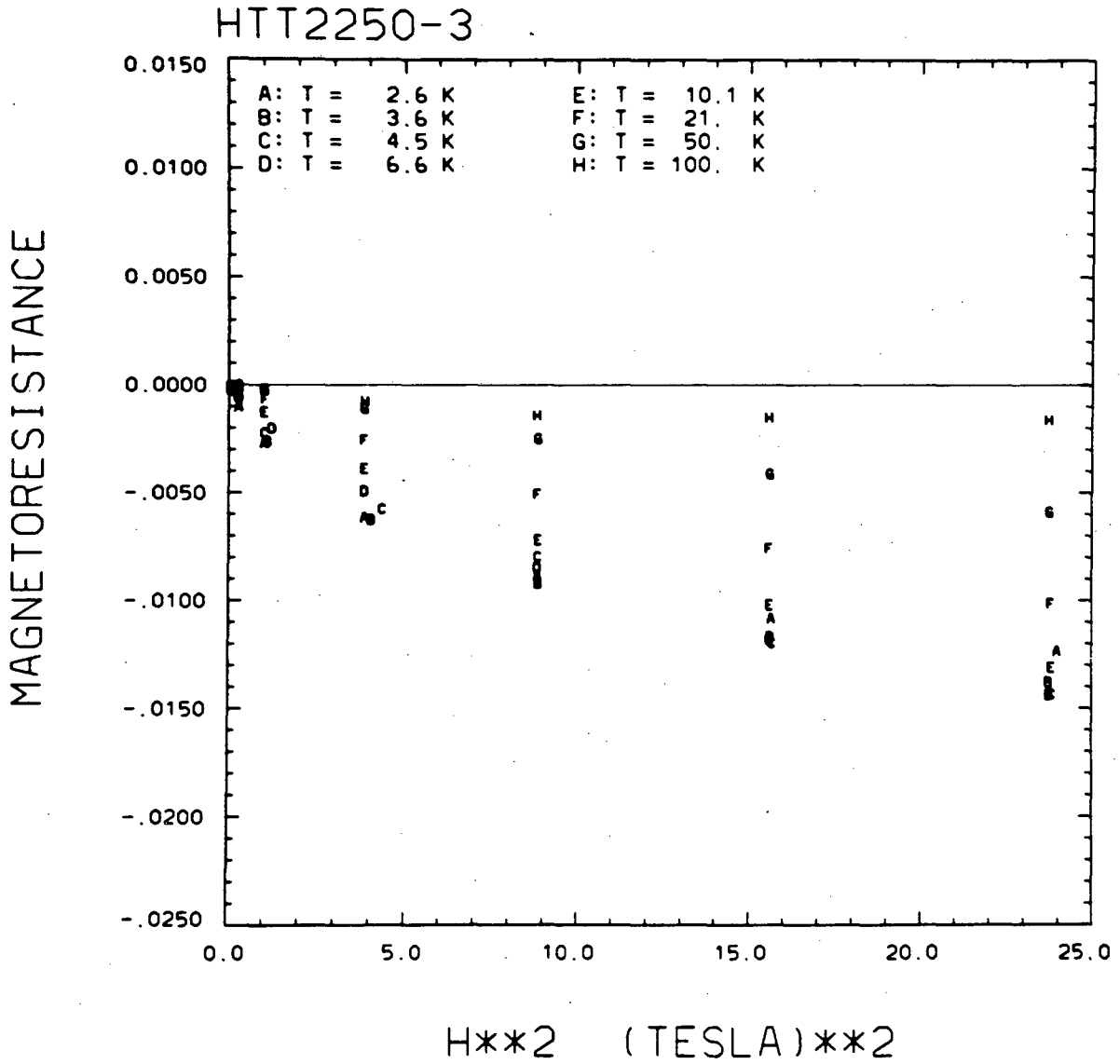
Figure III.5

HTT2000-3



XBL 829-11529

Figure III.6

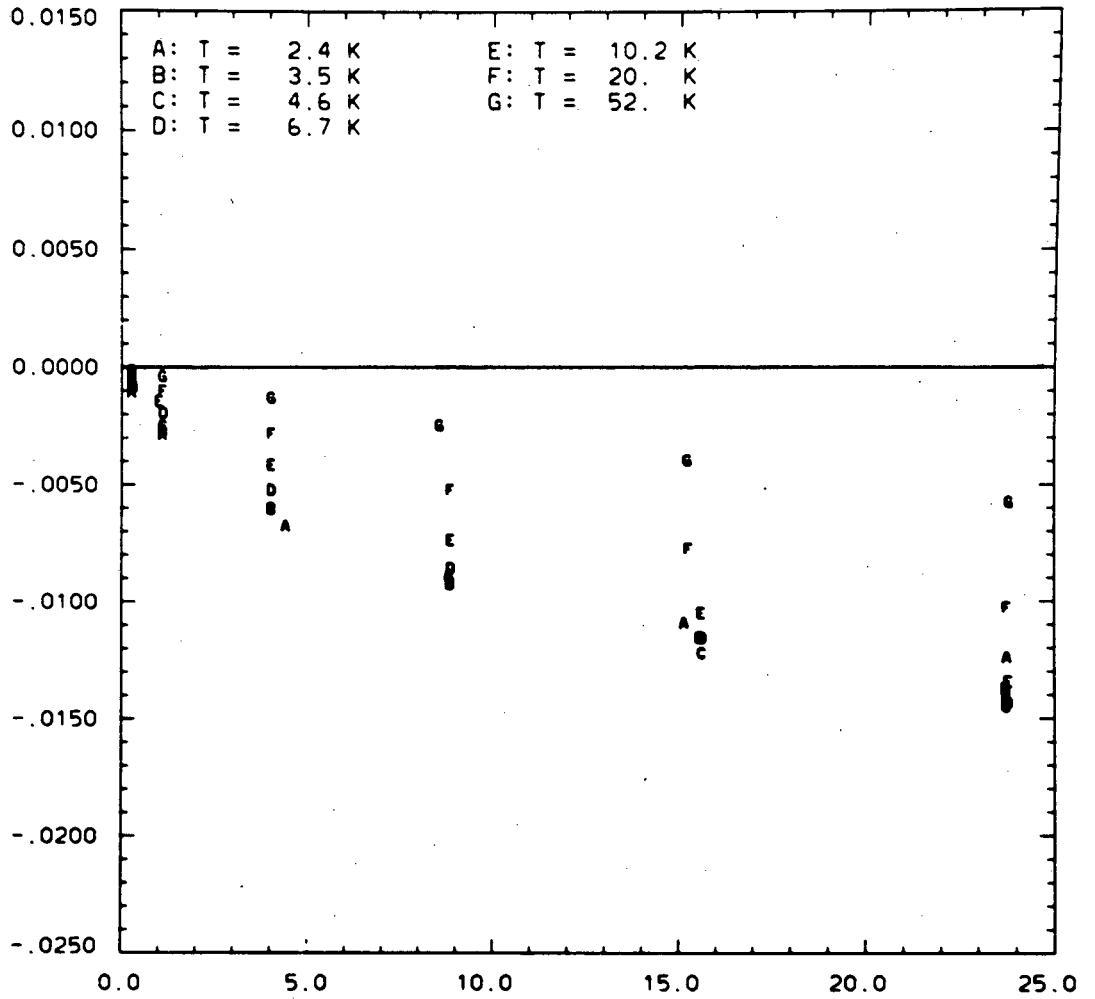


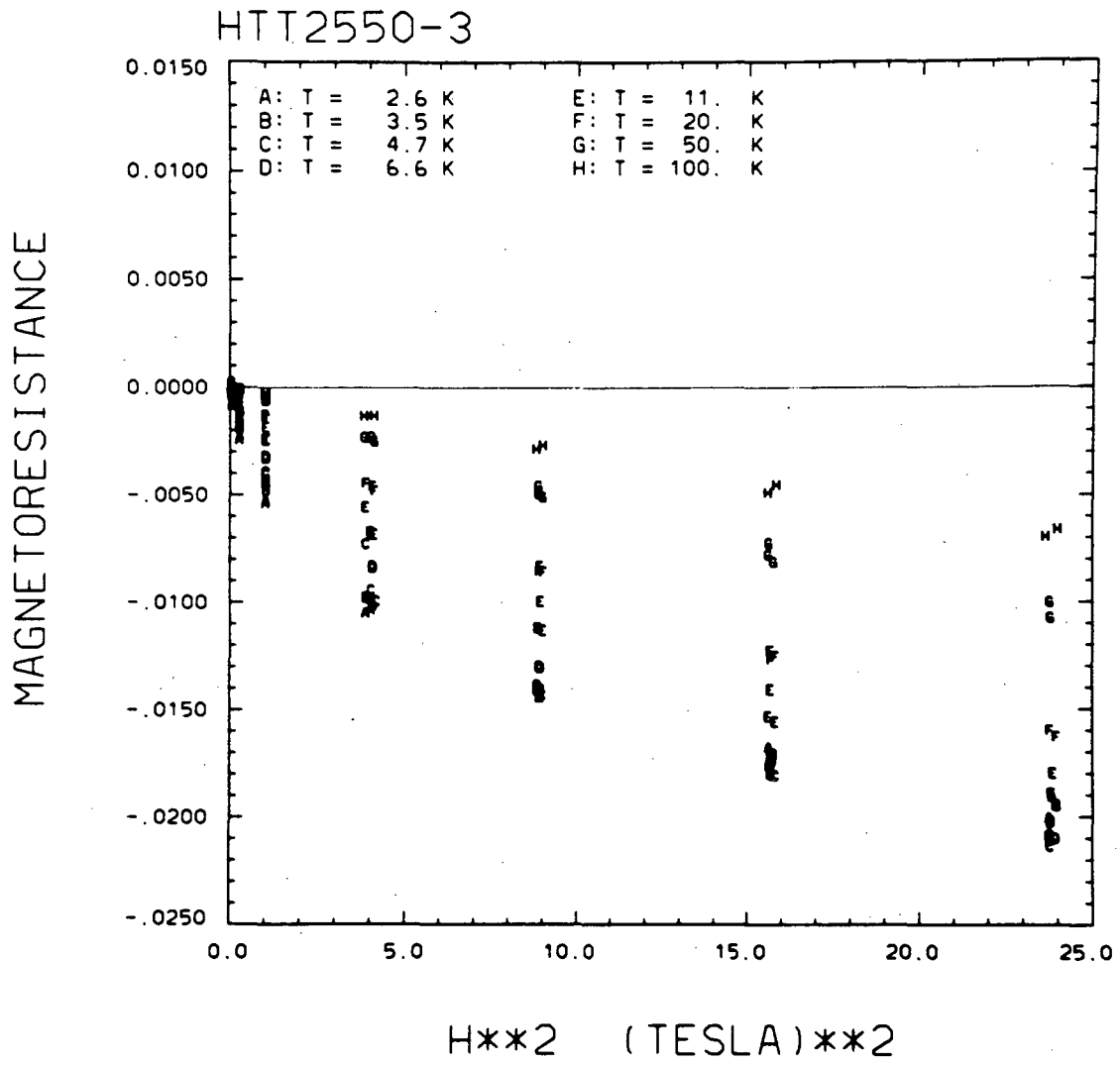
XBL 829-11530

Figure III.7

HTT2350-3

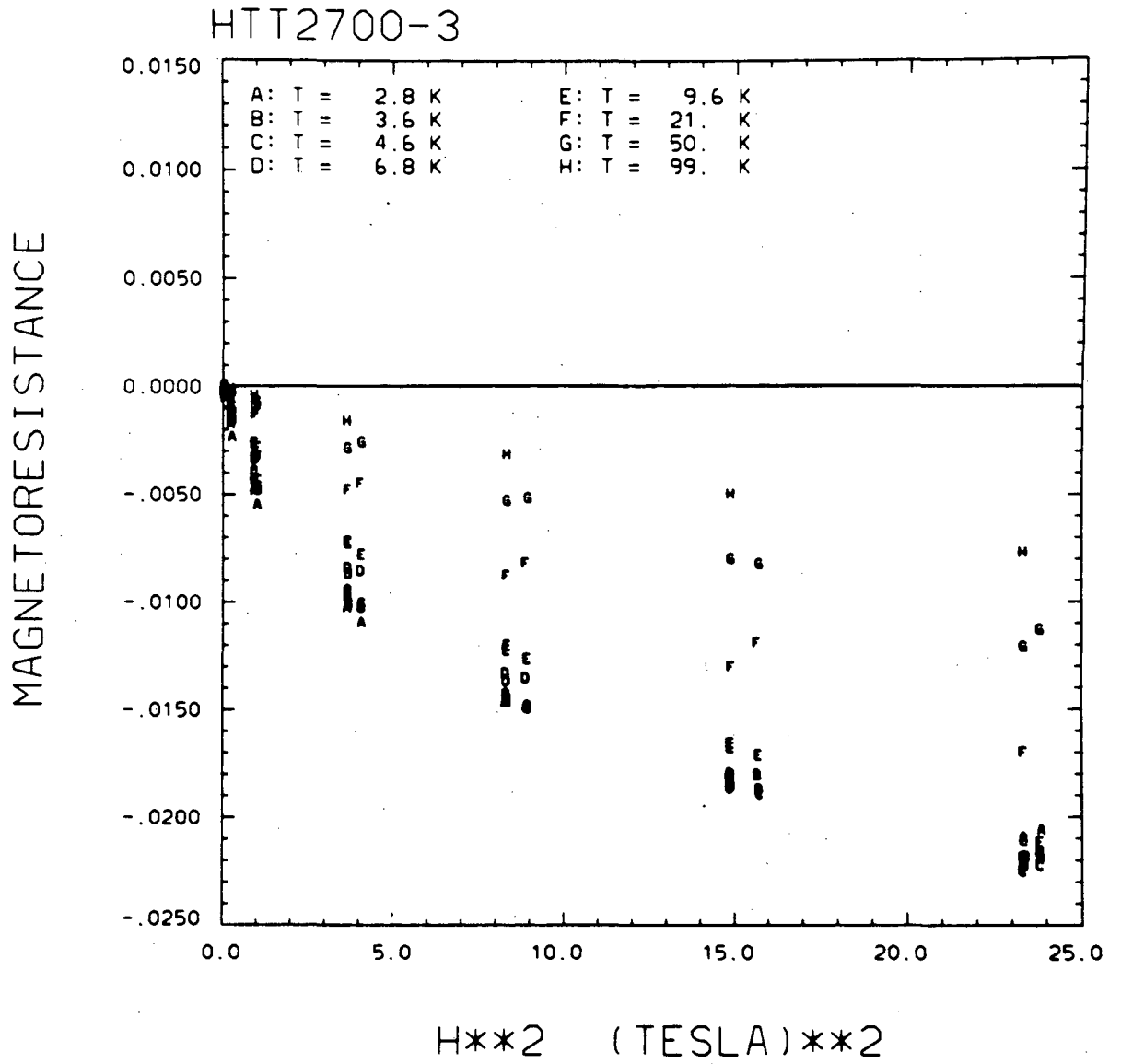
MAGNETORESISTANCE





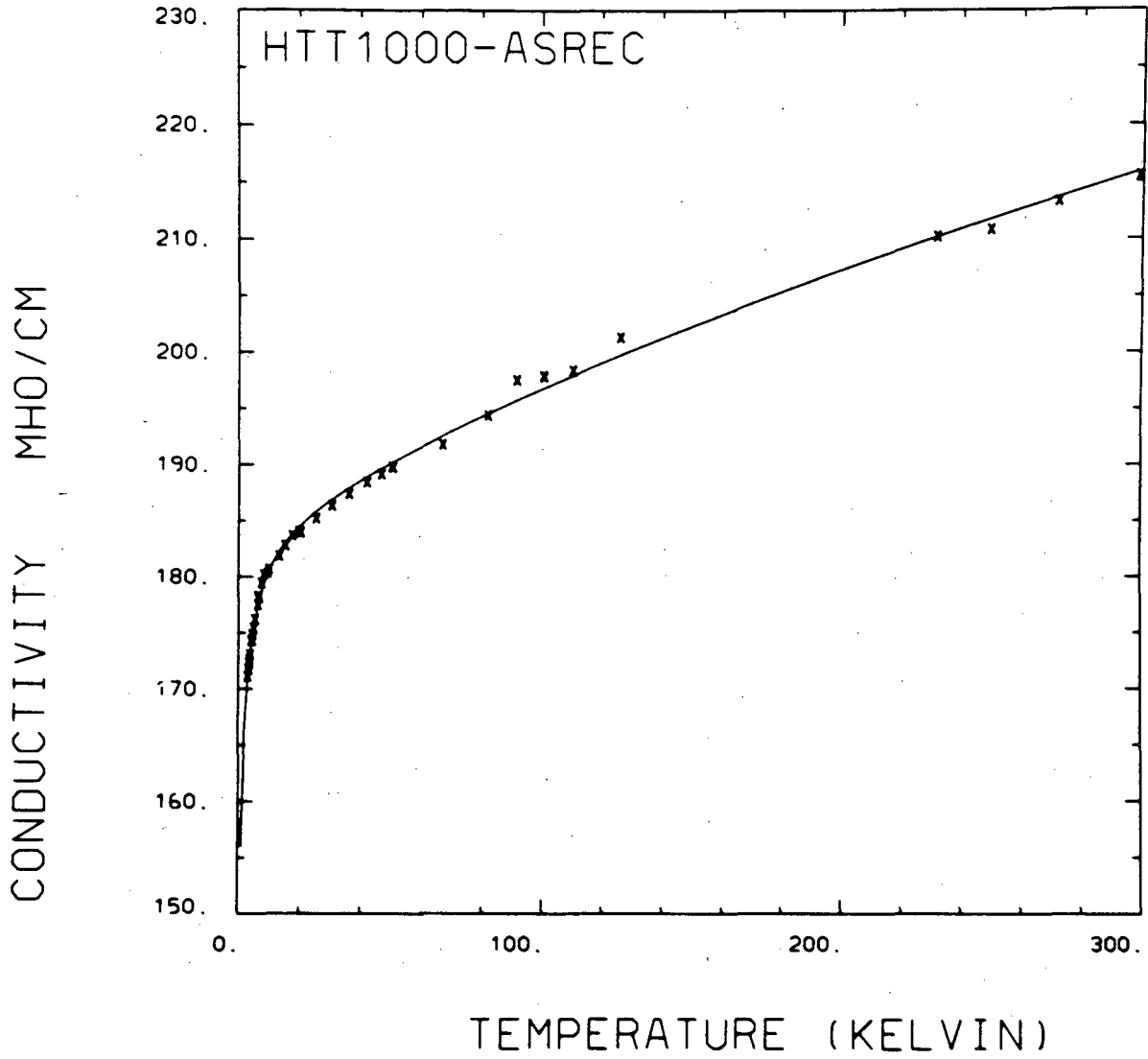
XBL 829-11532

Figure III.9



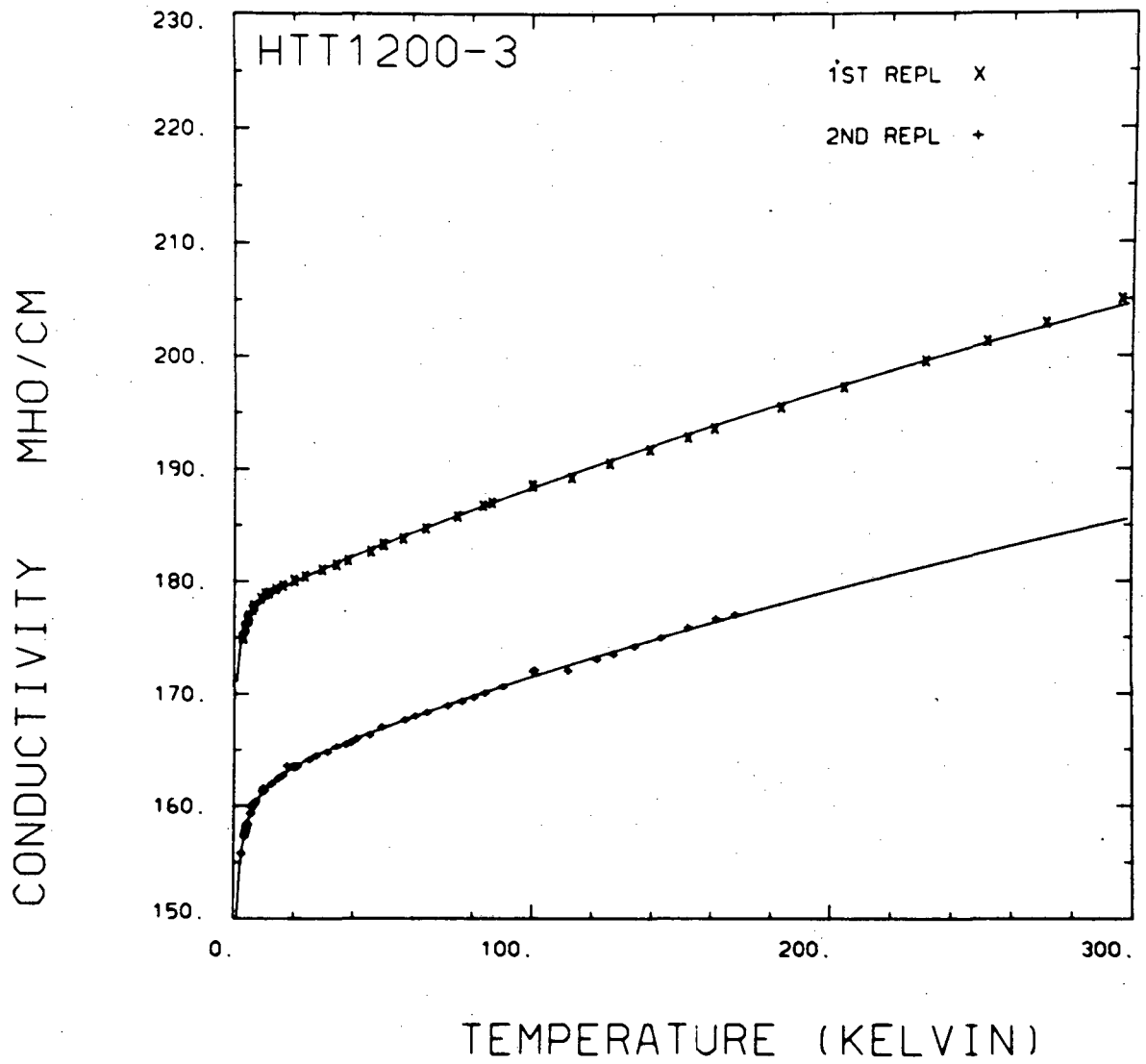
XBL 829-11533

Figure III.10



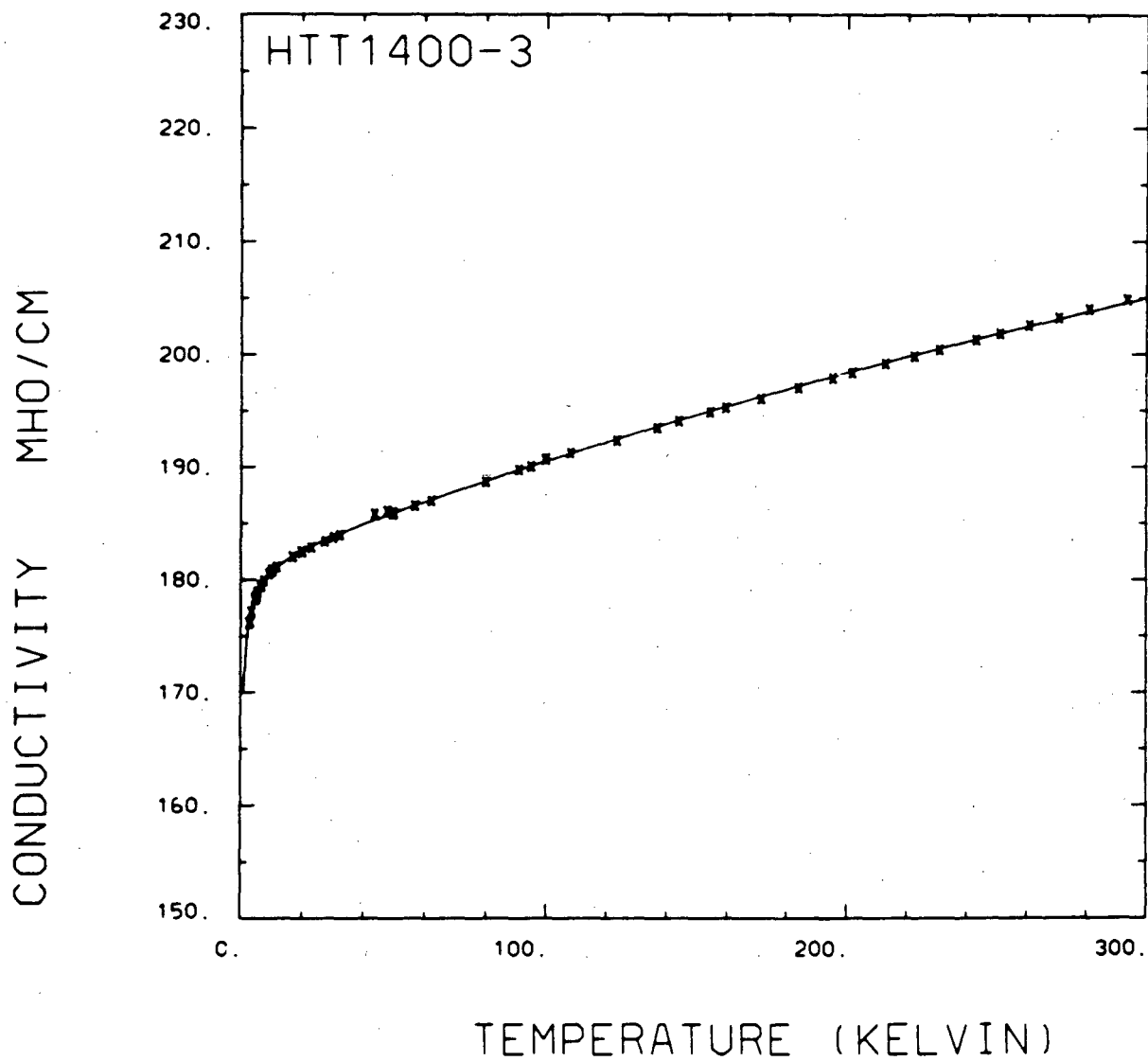
XBL 829-11534

Figure III.11



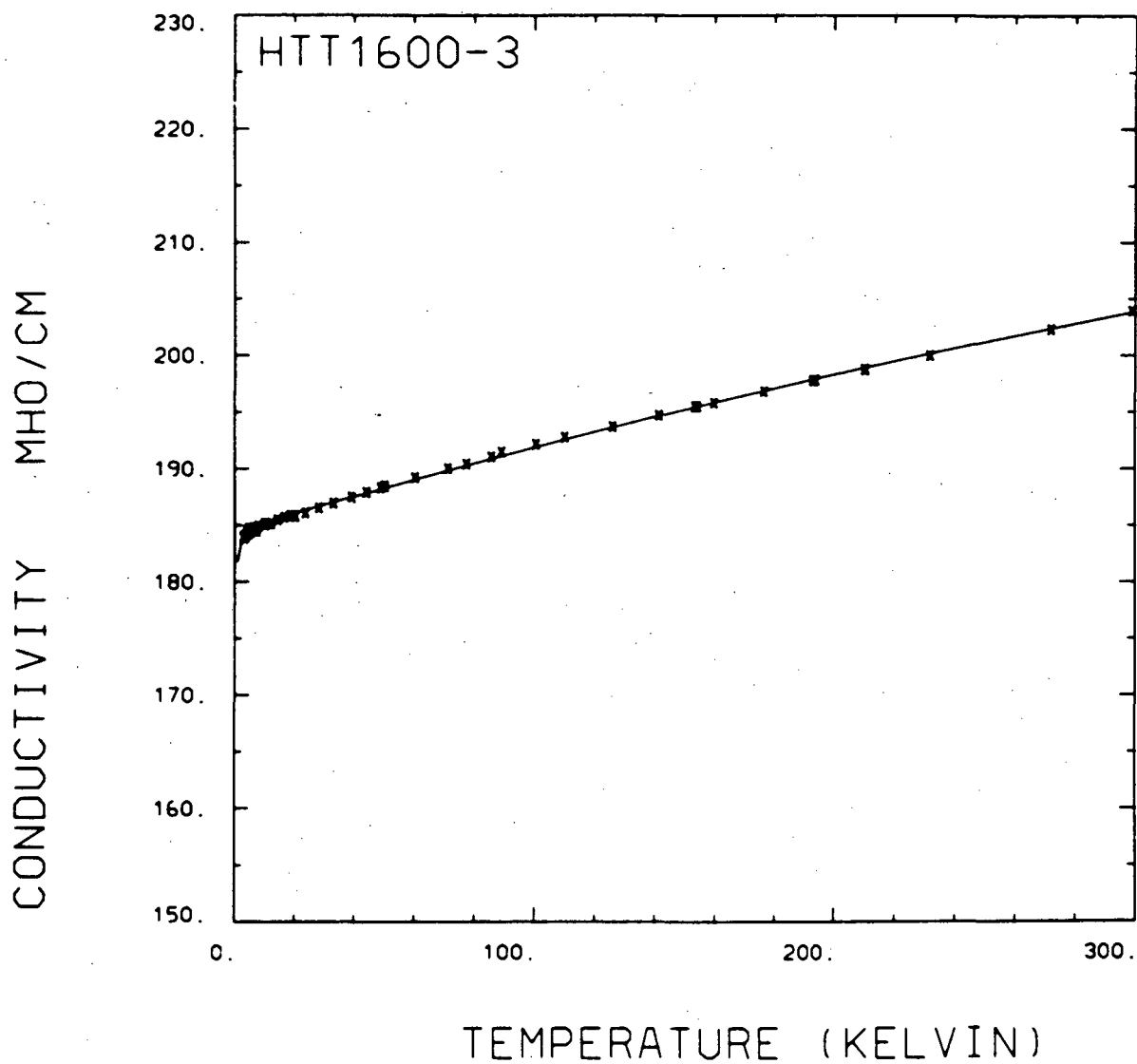
XBL 829-11535

Figure III.12



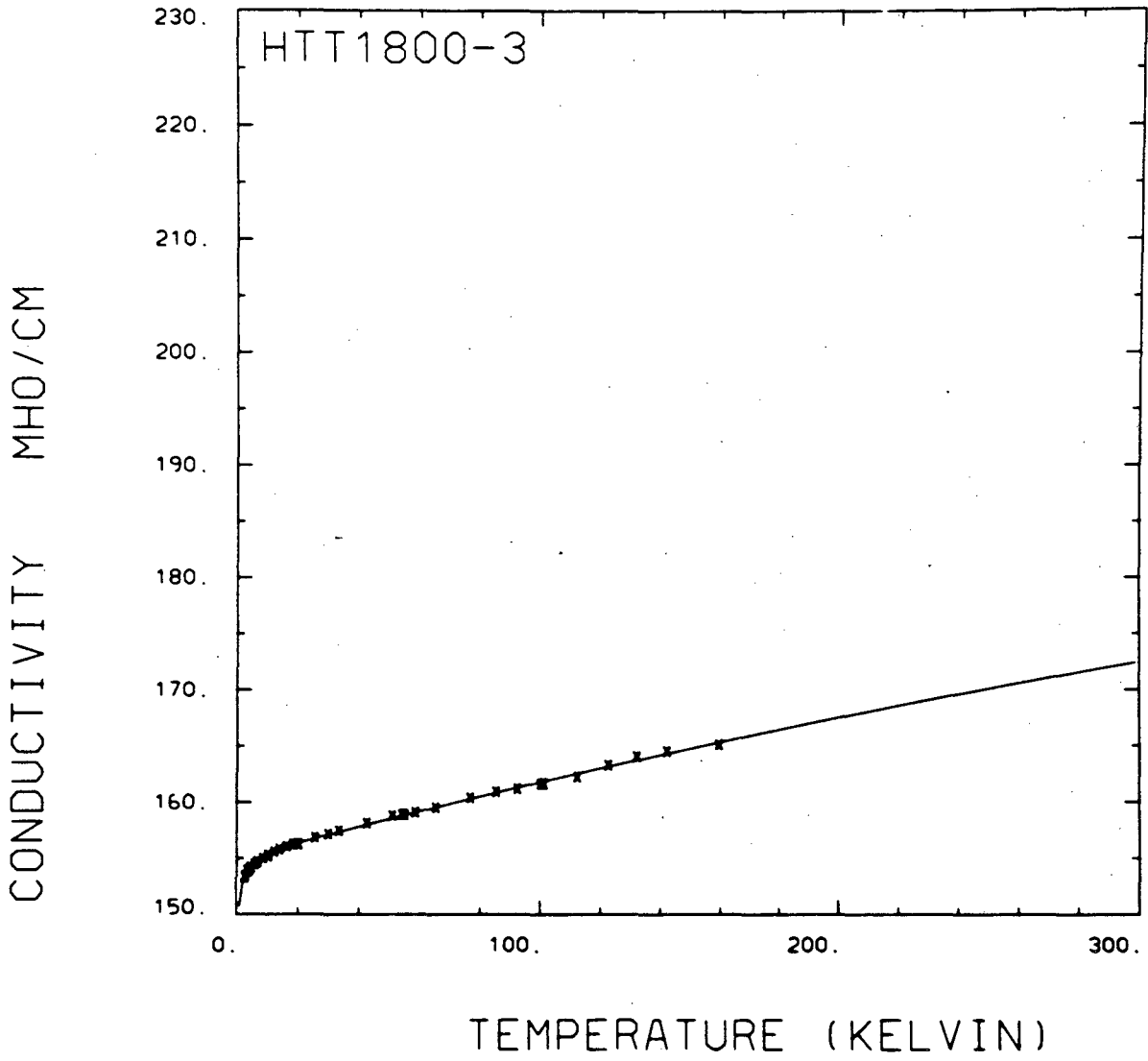
XBL 829-11536

Figure III.13



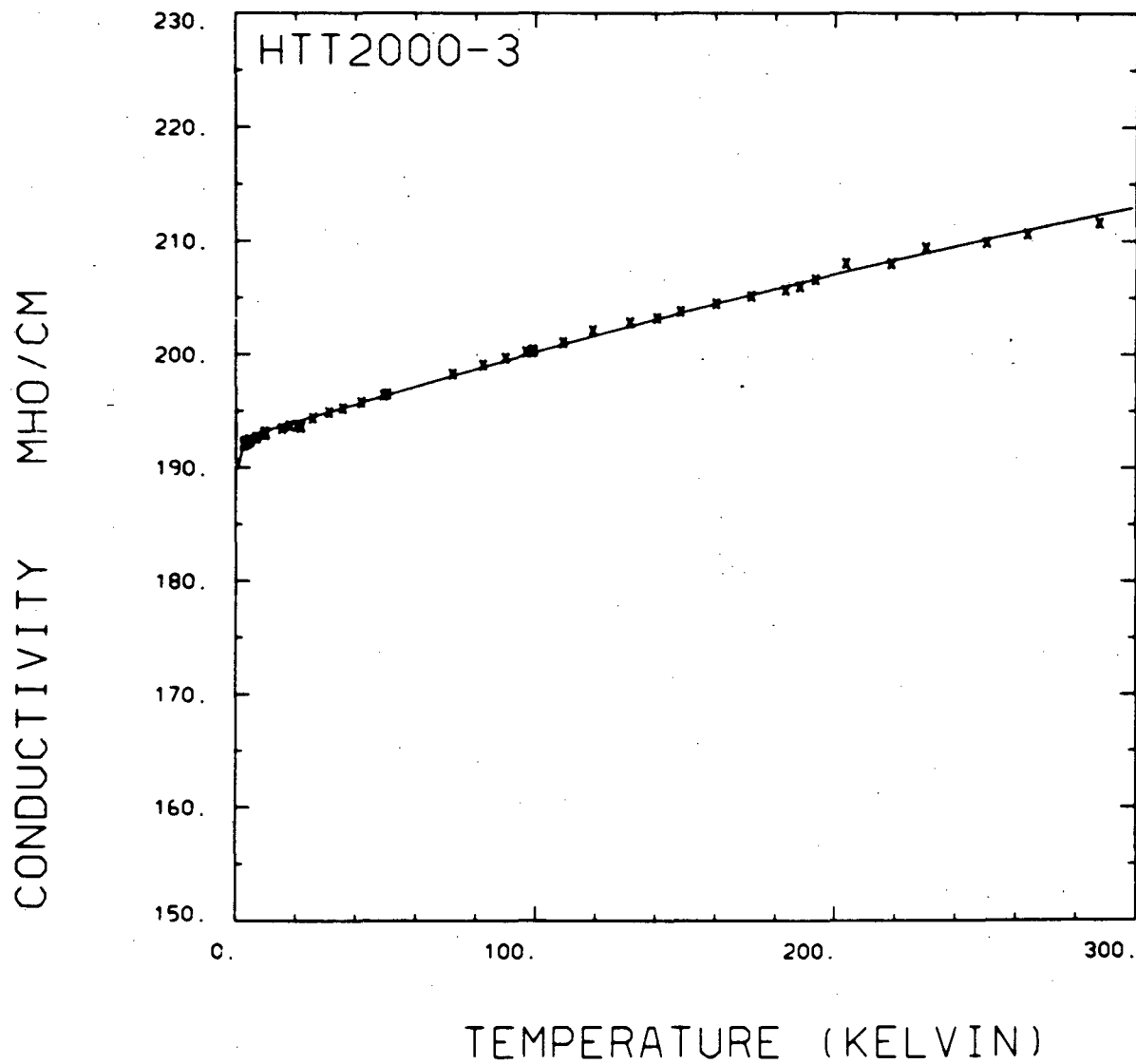
XBL 829-11537

Figure III.14



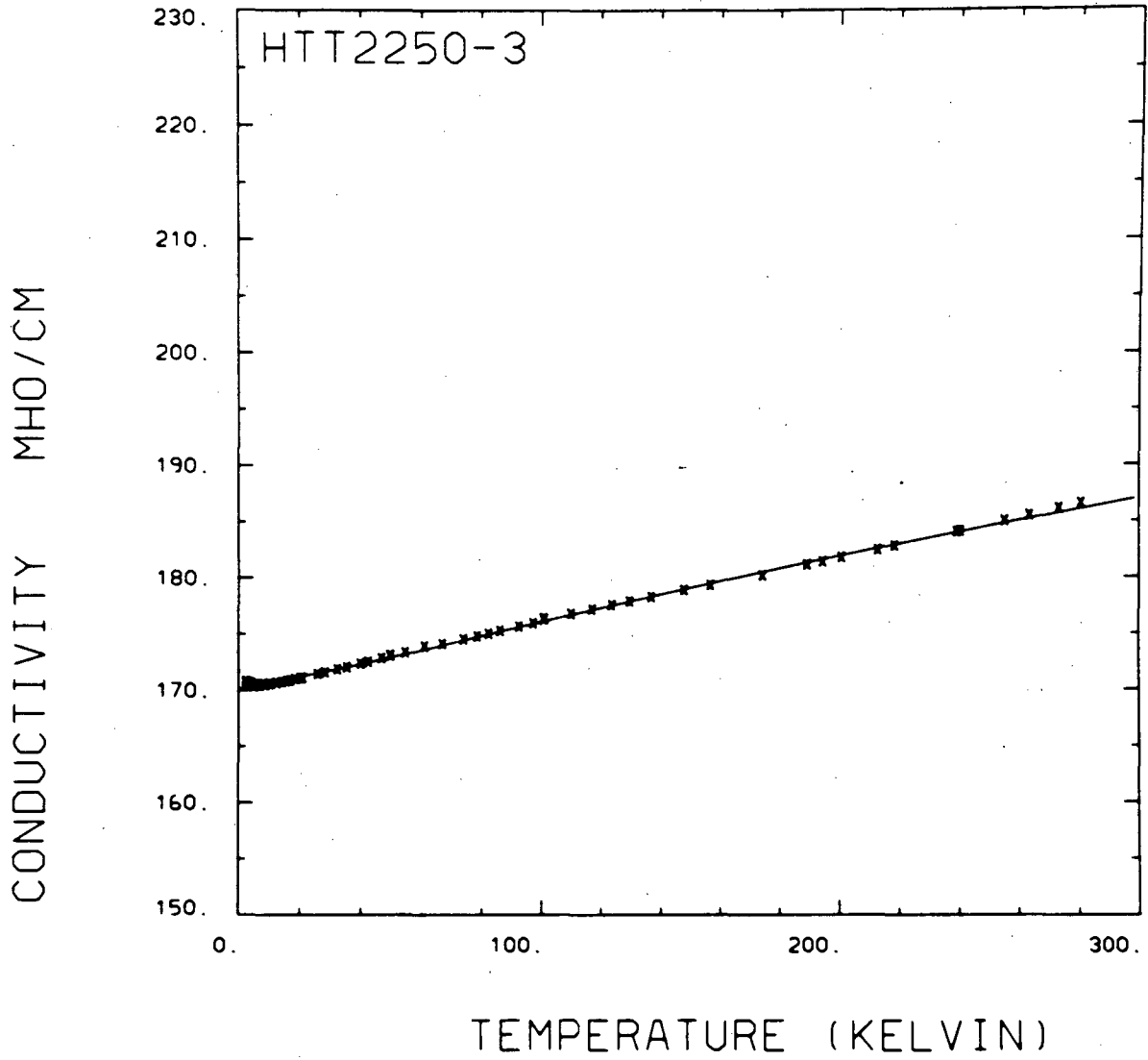
XBL 829-11538

Figure III.15



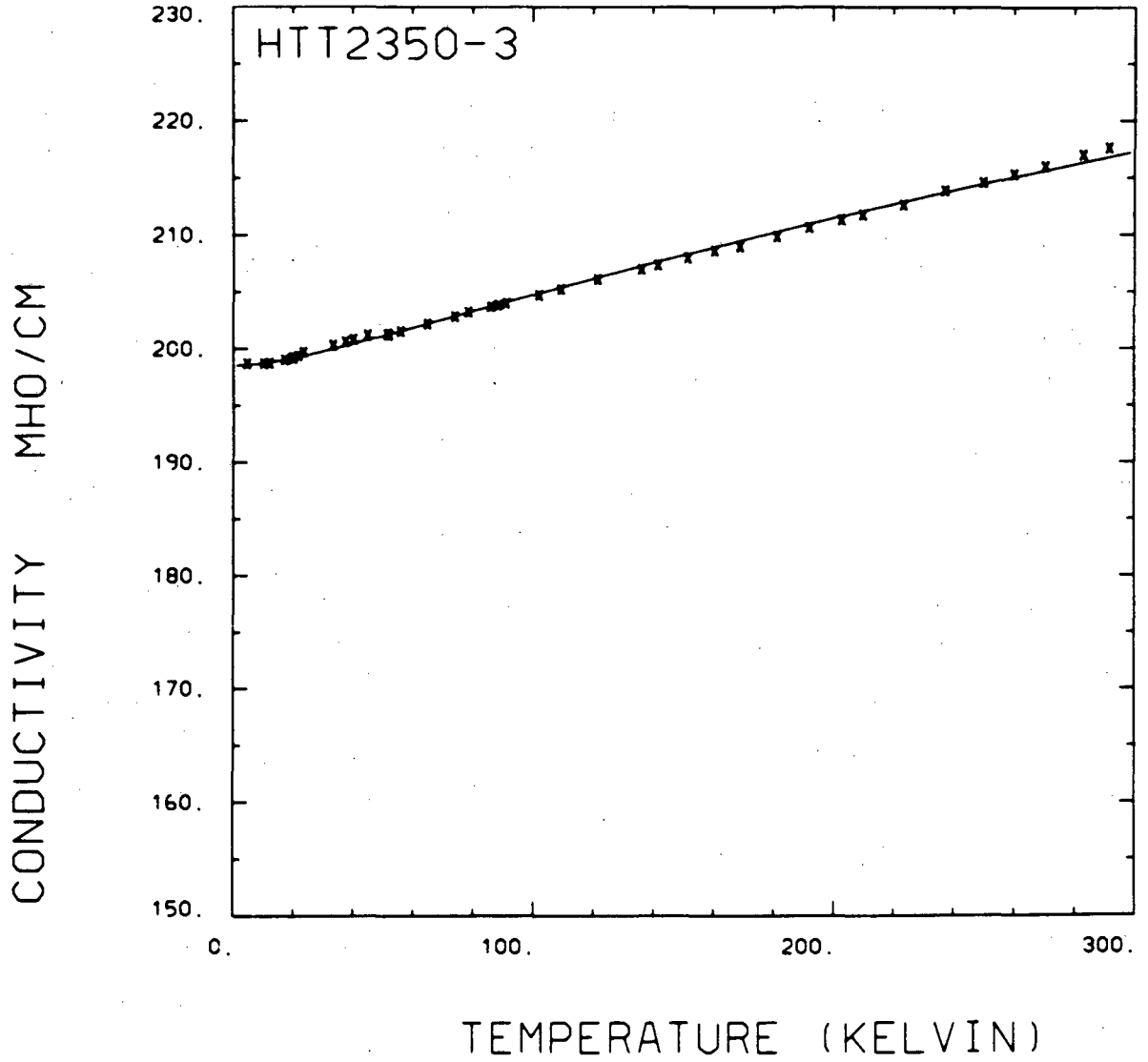
XBL 829-11539

Figure III.16



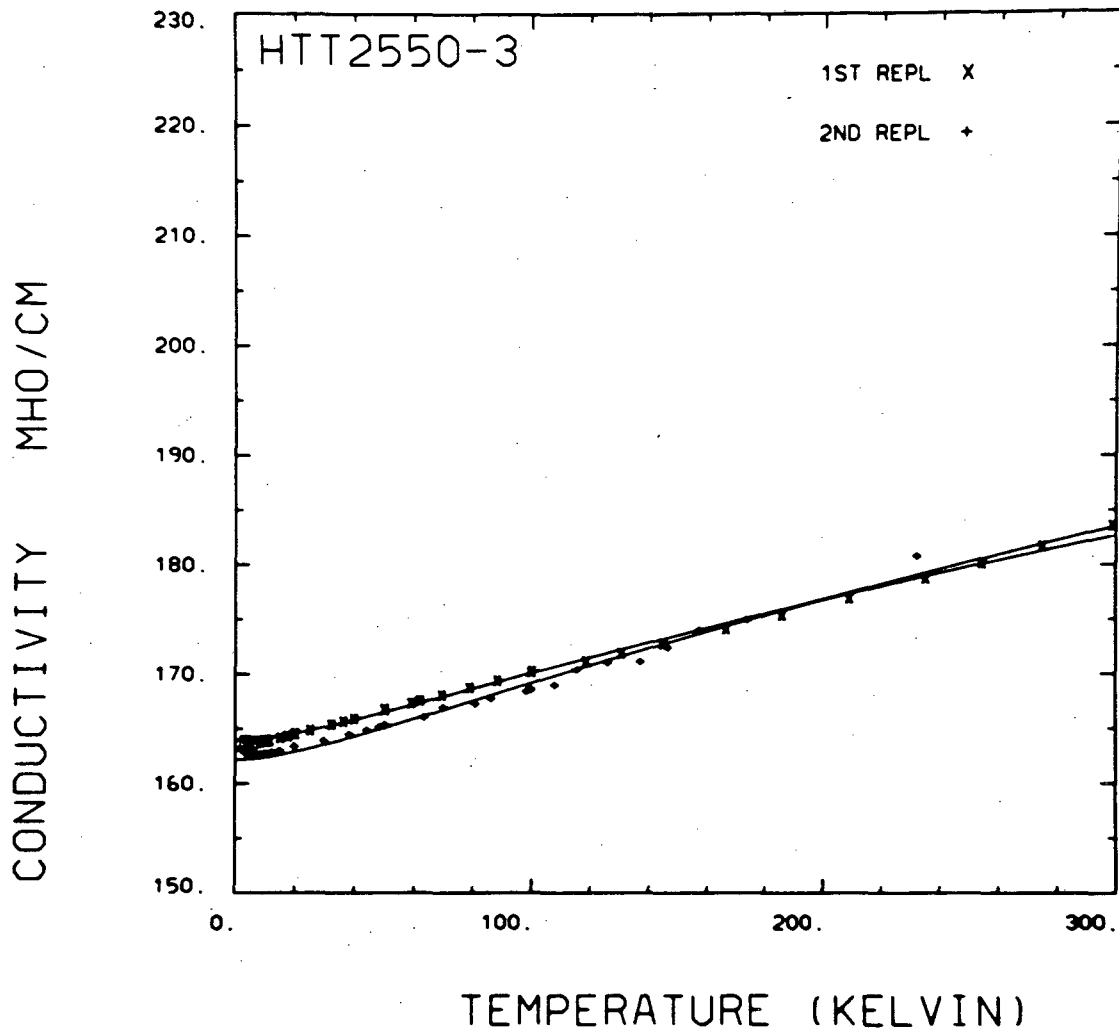
XBL 829-11540

Figure III.17



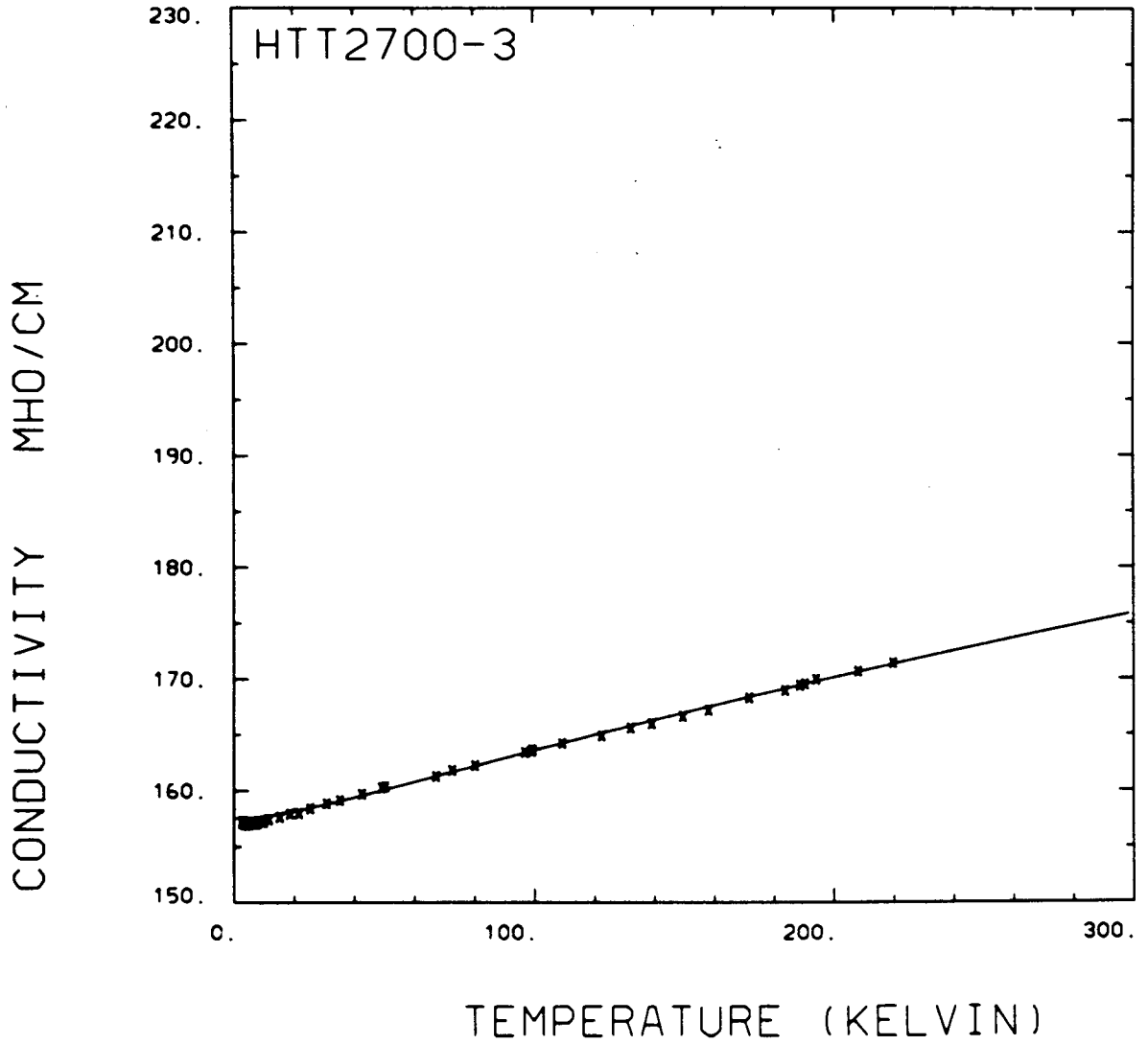
XBL 829-11541

Figure III.18



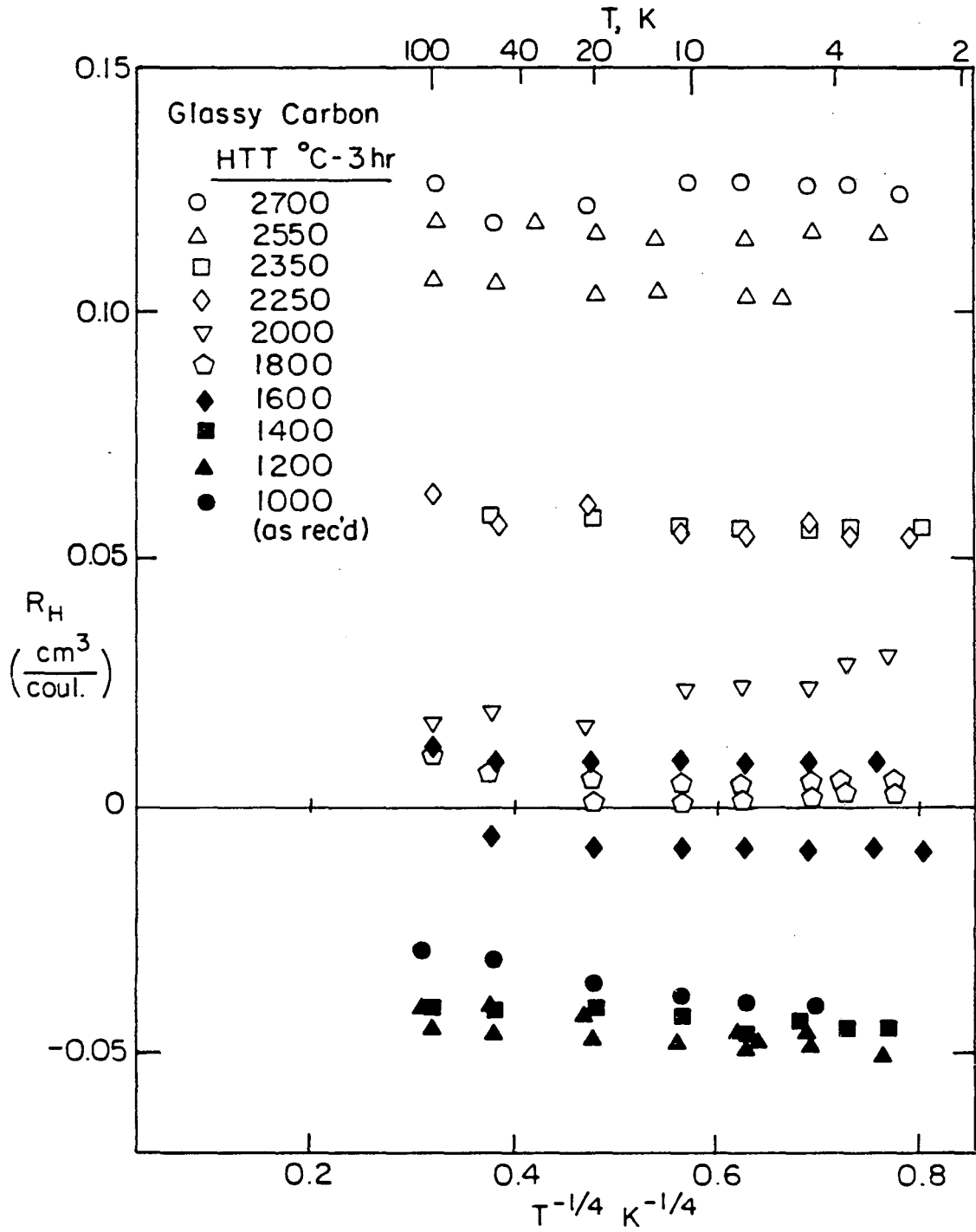
XBL 829-11542

Figure III.19



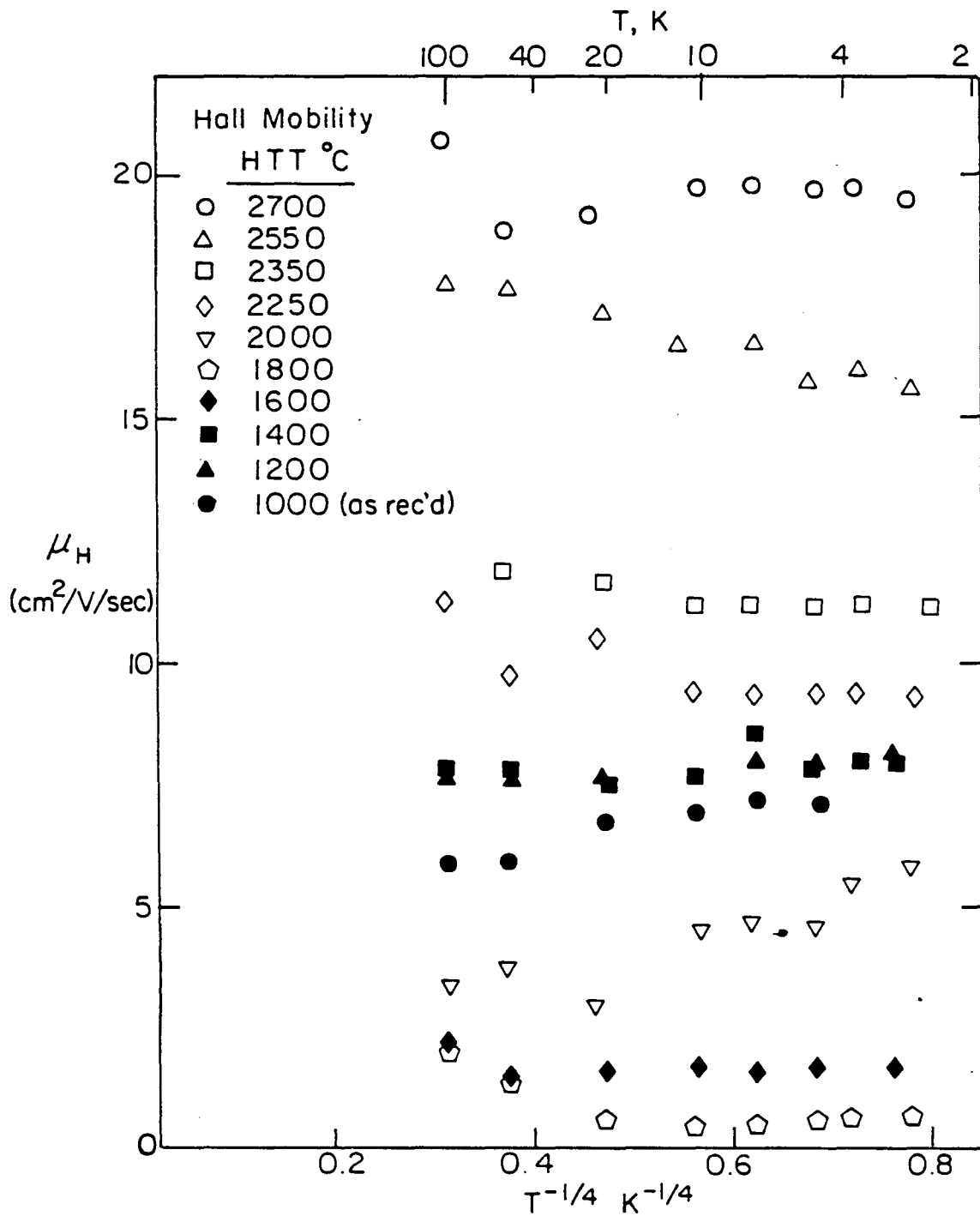
XBL 829-11543

Figure III.20



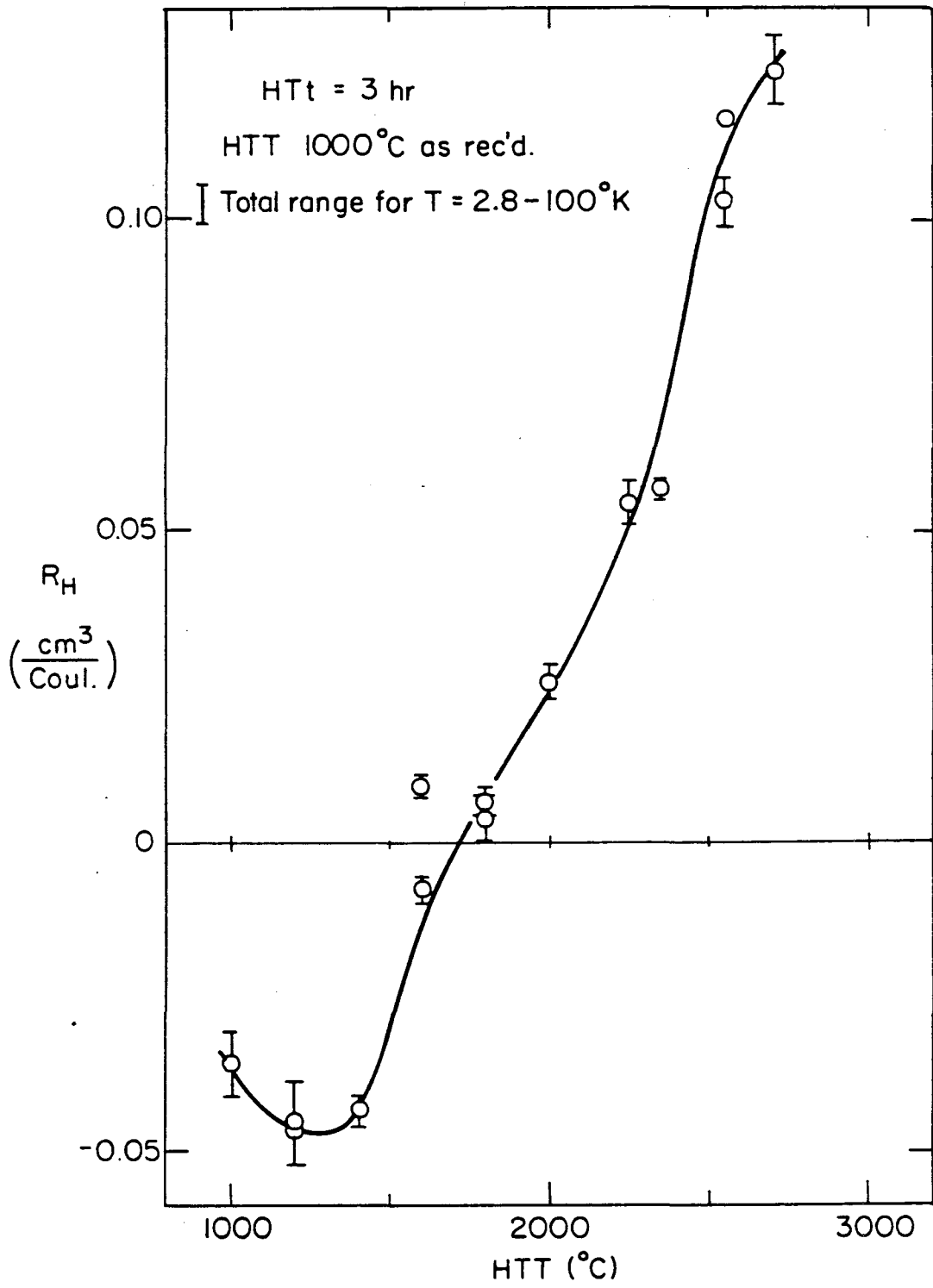
XBL 828-6431

Figure III.21



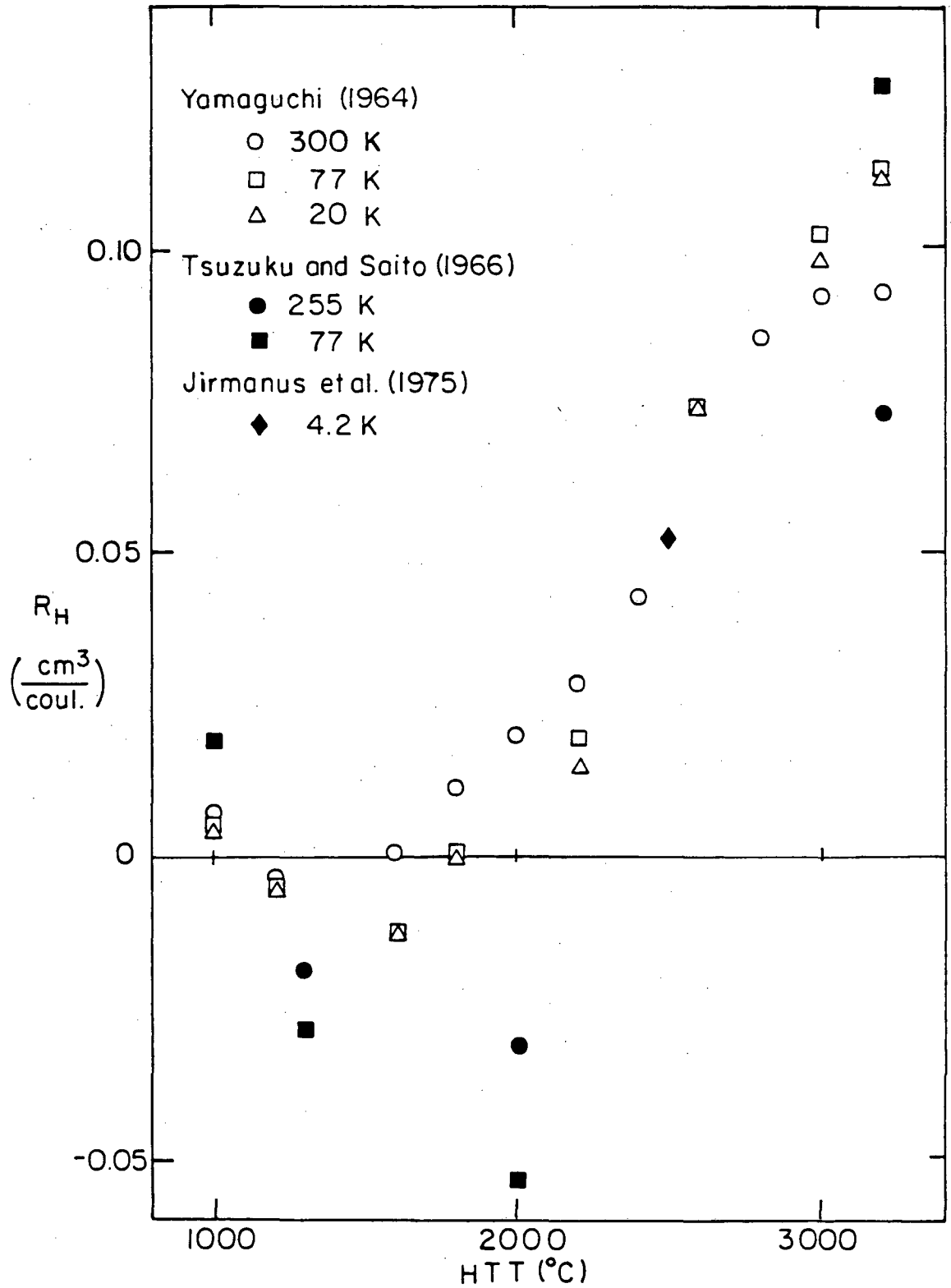
XBL 828-6432

Figure III.22



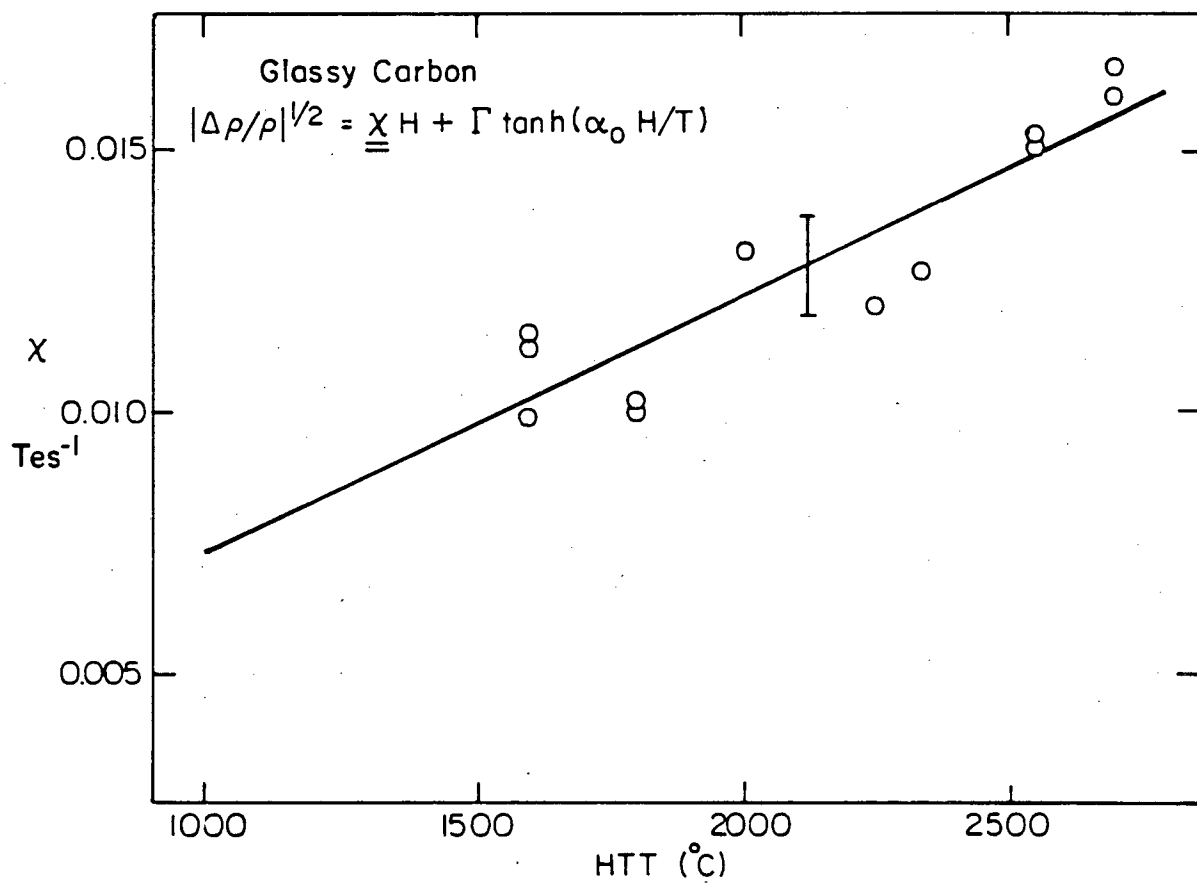
XBL 816-5907A

Figure III.23



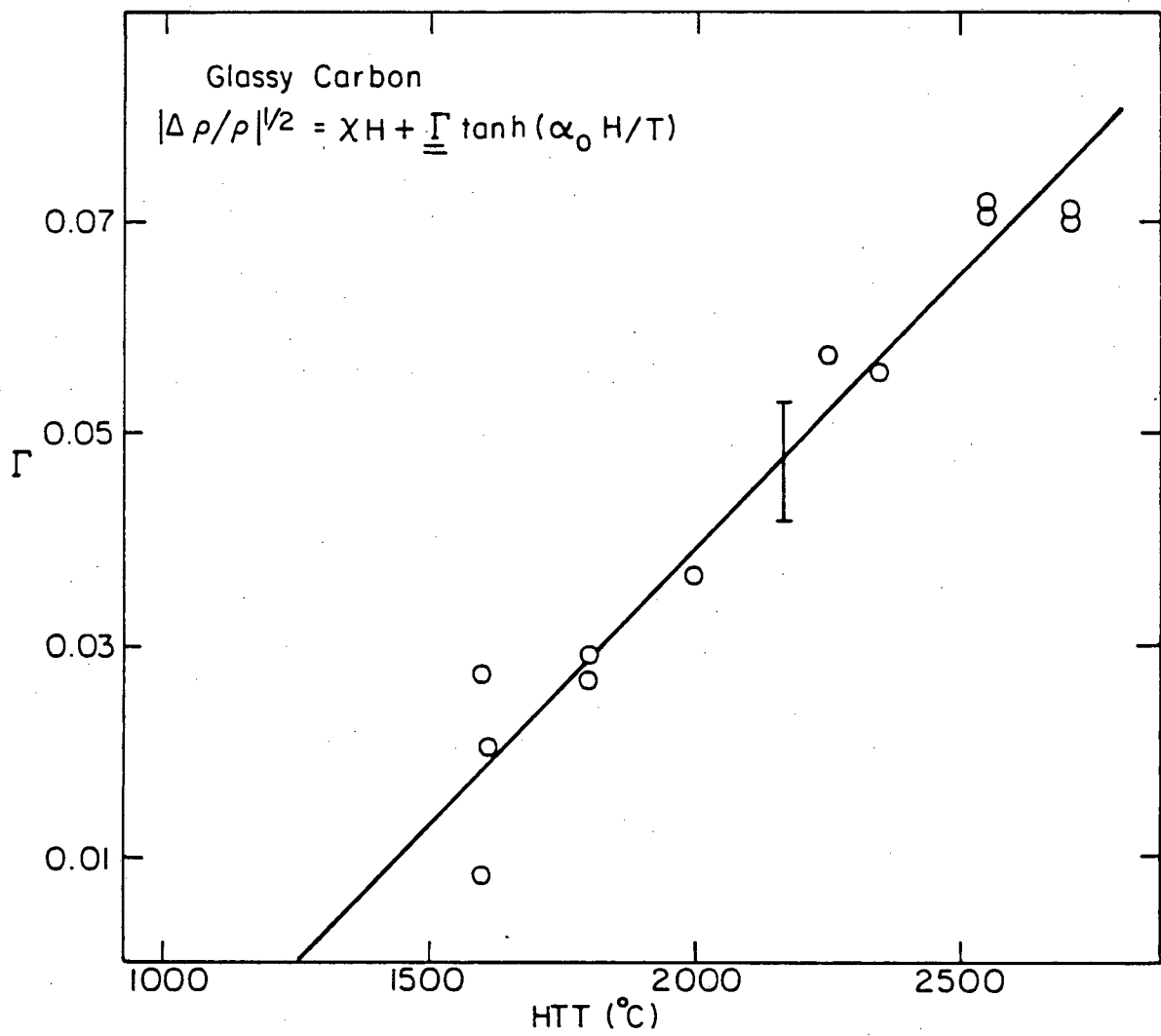
XBL 828-6433

Figure III.24



XBL 828-6437

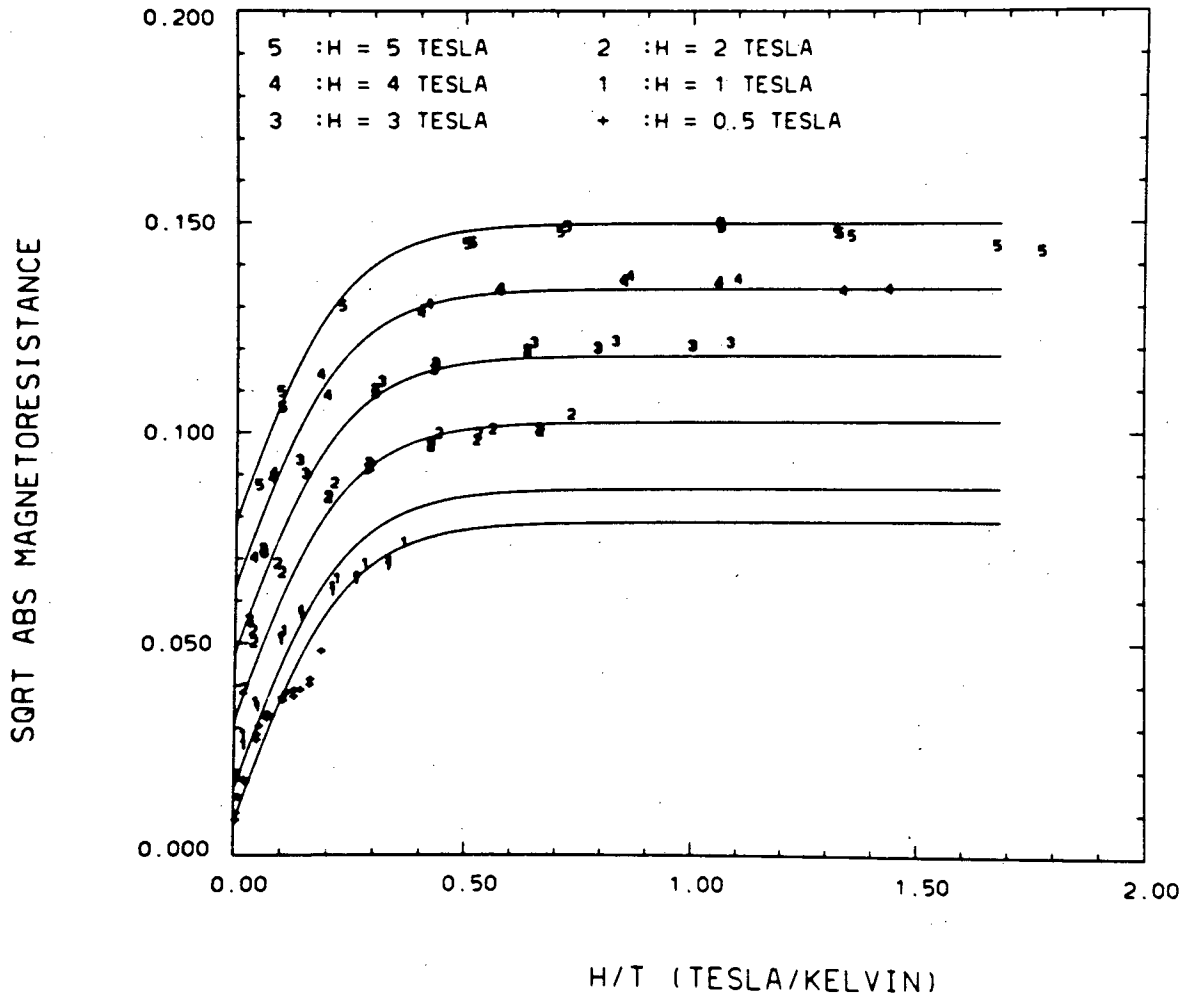
Figure IV.1



XBL 82 8- 6438

Figure IV.2

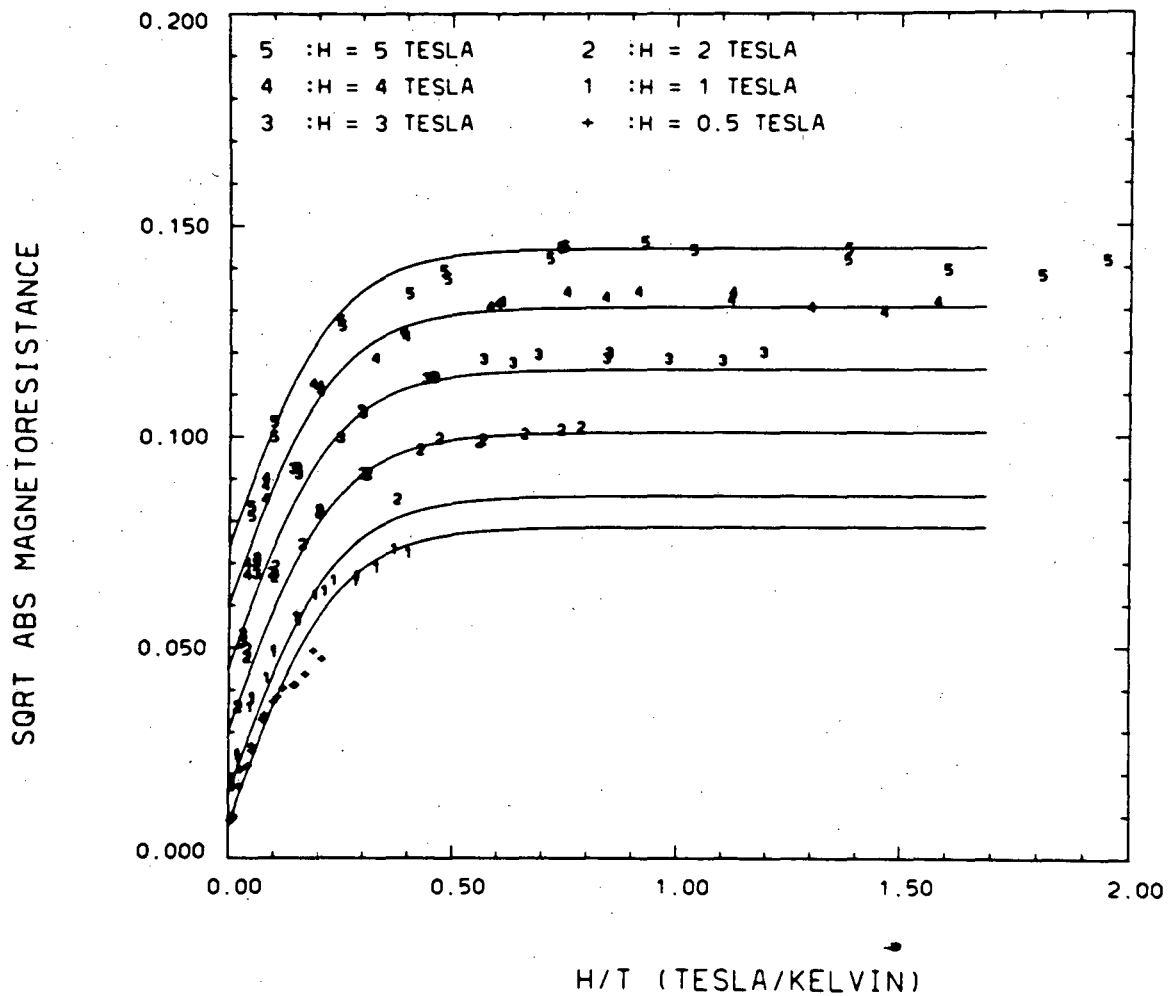
HTT2700-3



XBL 829-11517

Figure IV.3

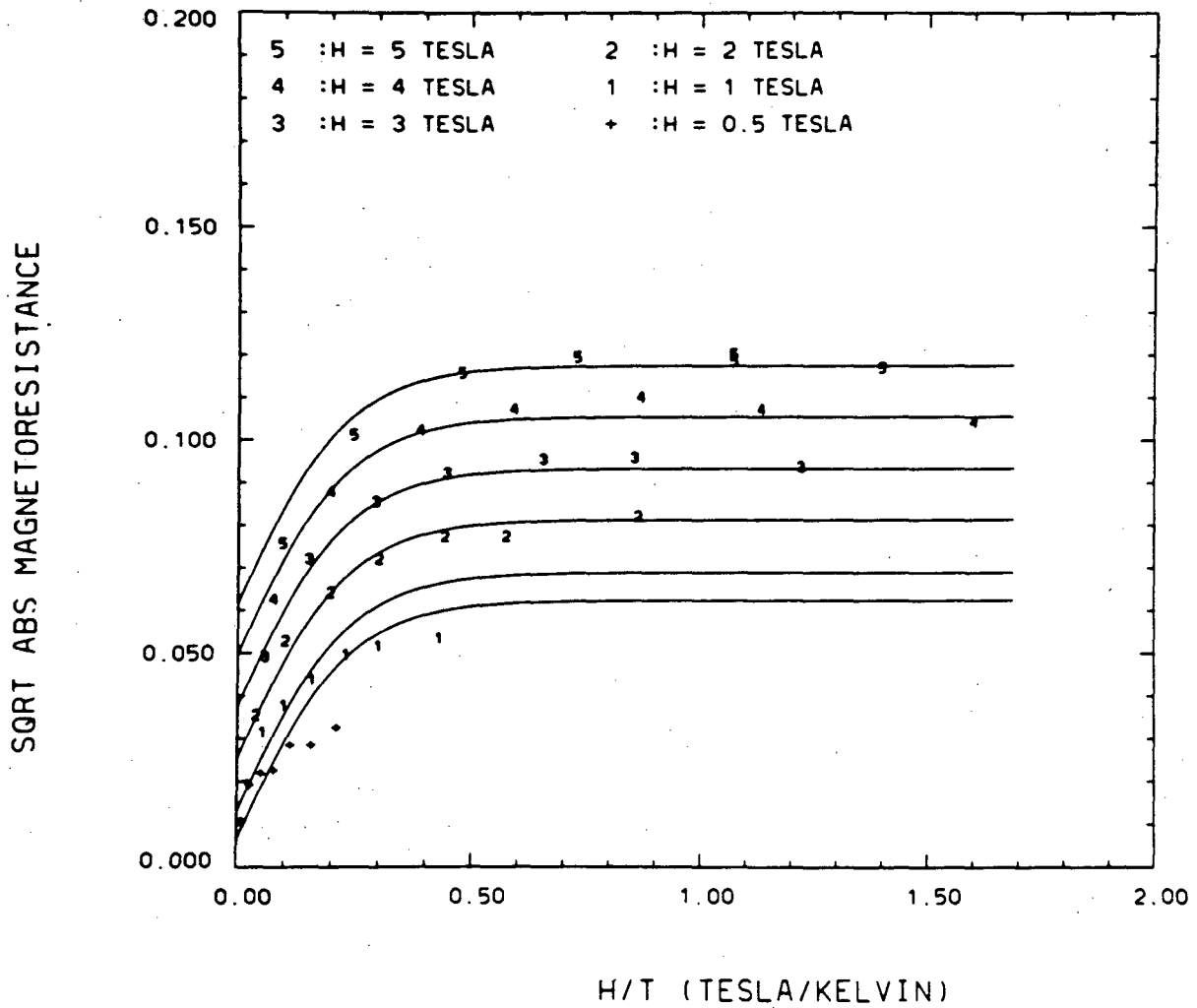
HTT2550-3



XBL 829-11518

Figure IV.4

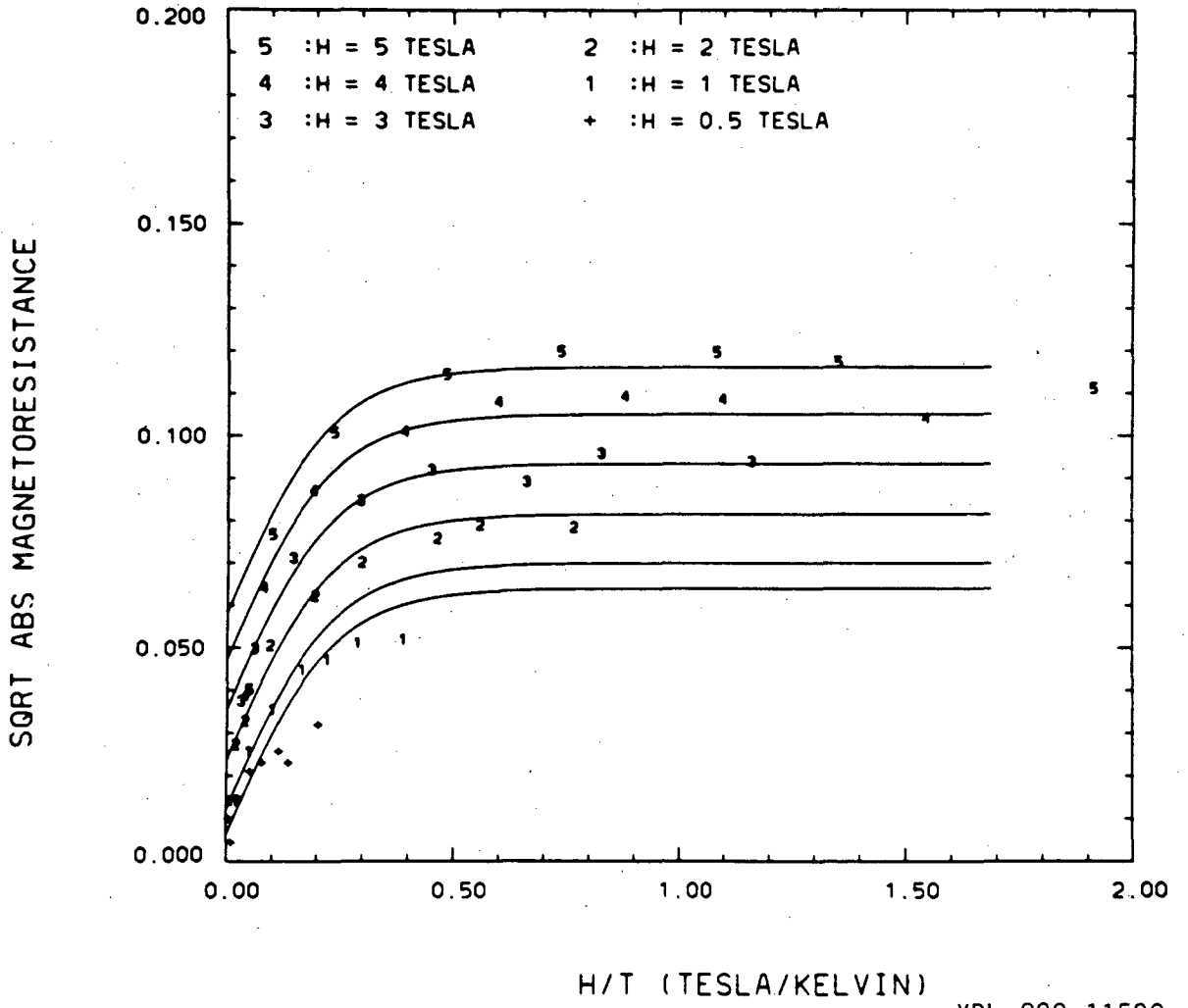
HTT2350-3



XBL 829-11519

Figure IV.5

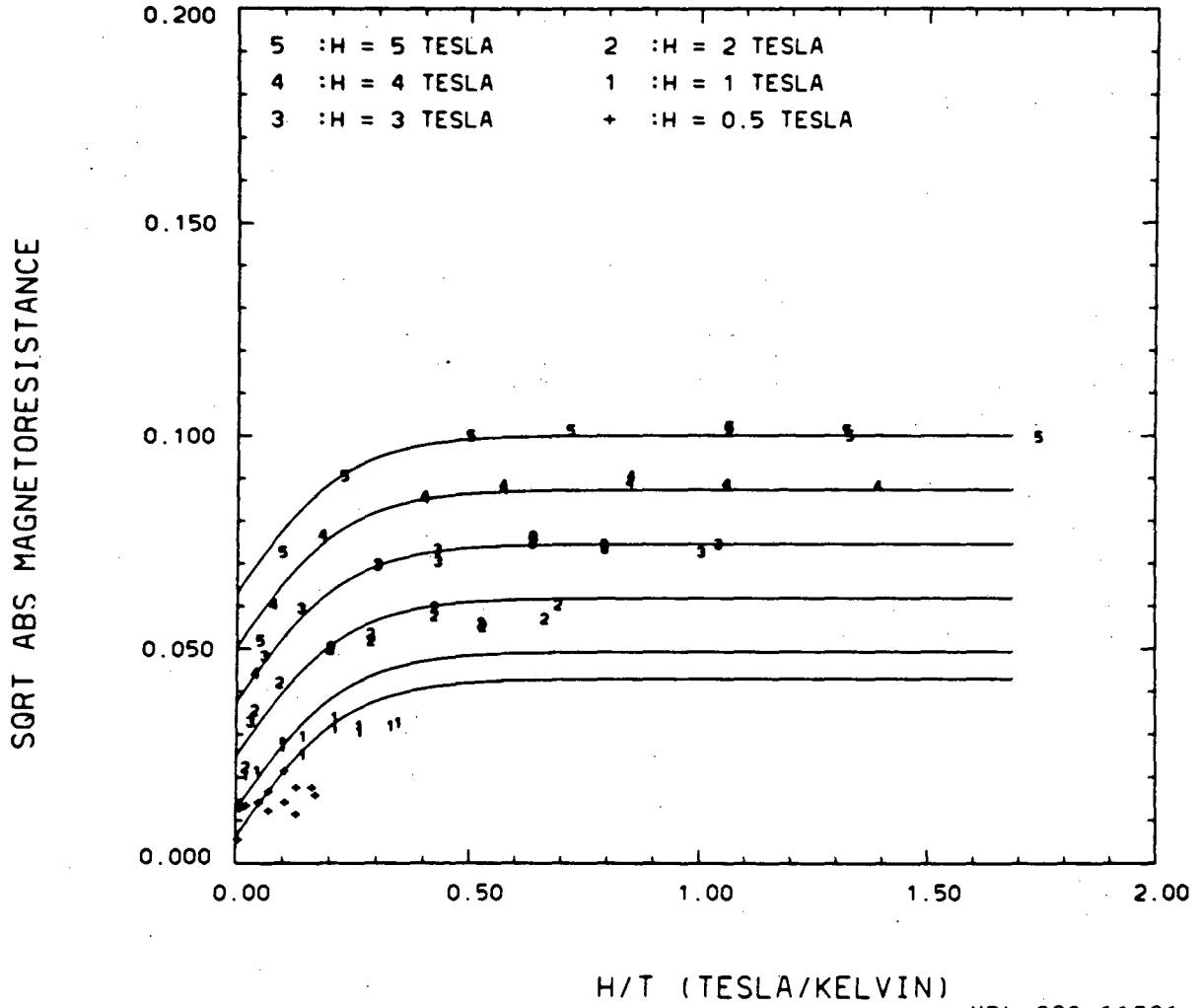
HTT2250-3



XBL 829-11520

Figure IV.6

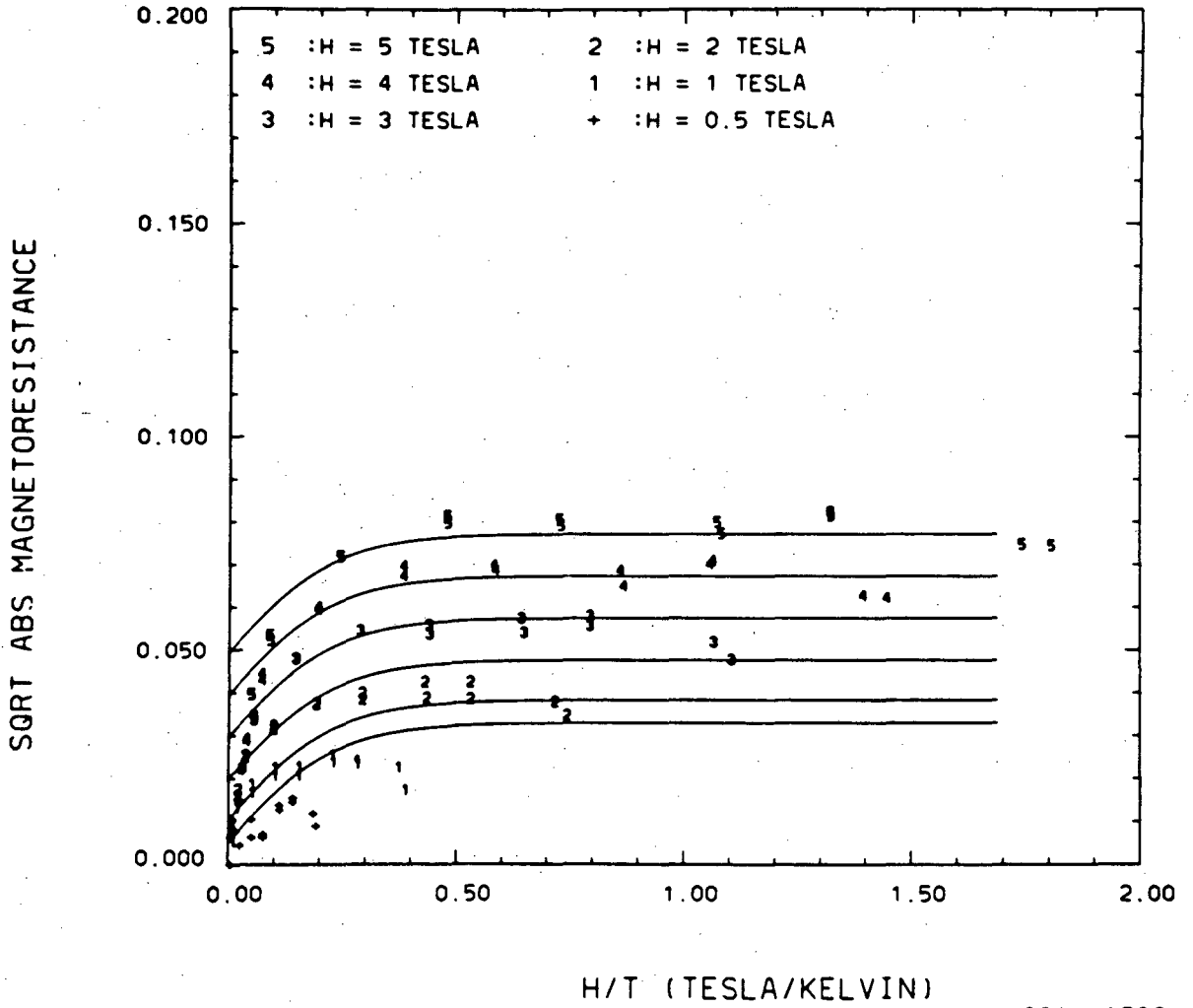
HTT2000-3



XBL 829-11521

Figure IV.7

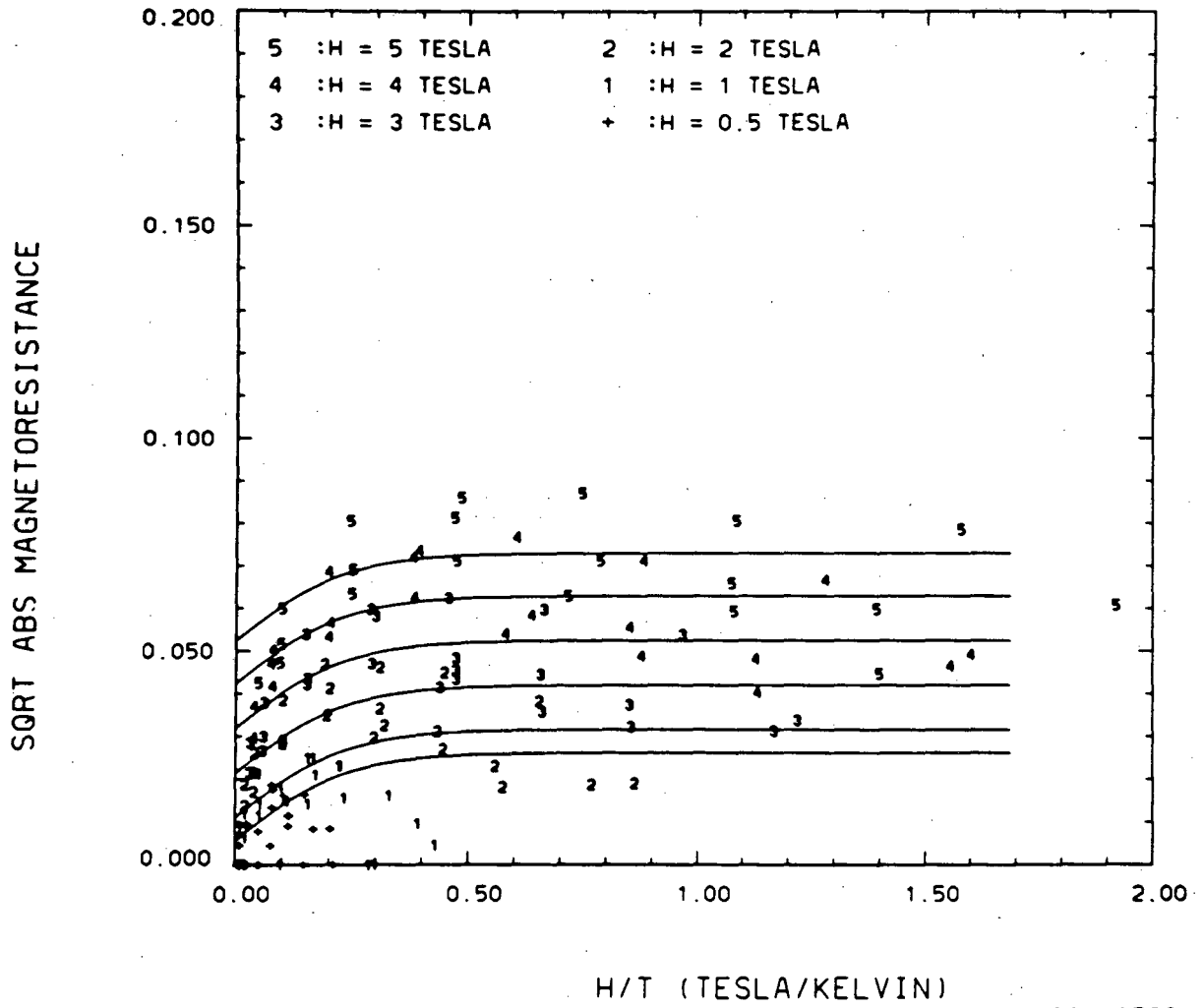
HTT1800-3



XBL 829-11522

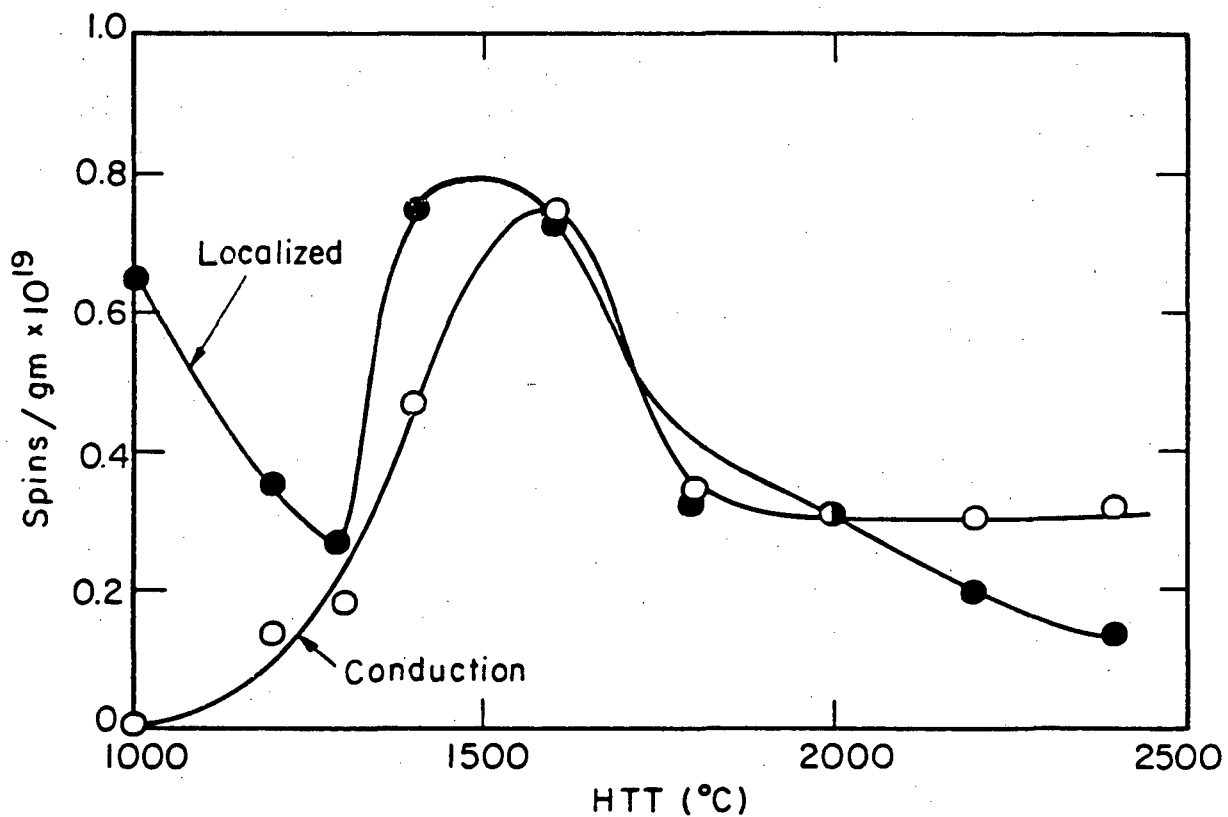
Figure IV.8

HTT1600-3



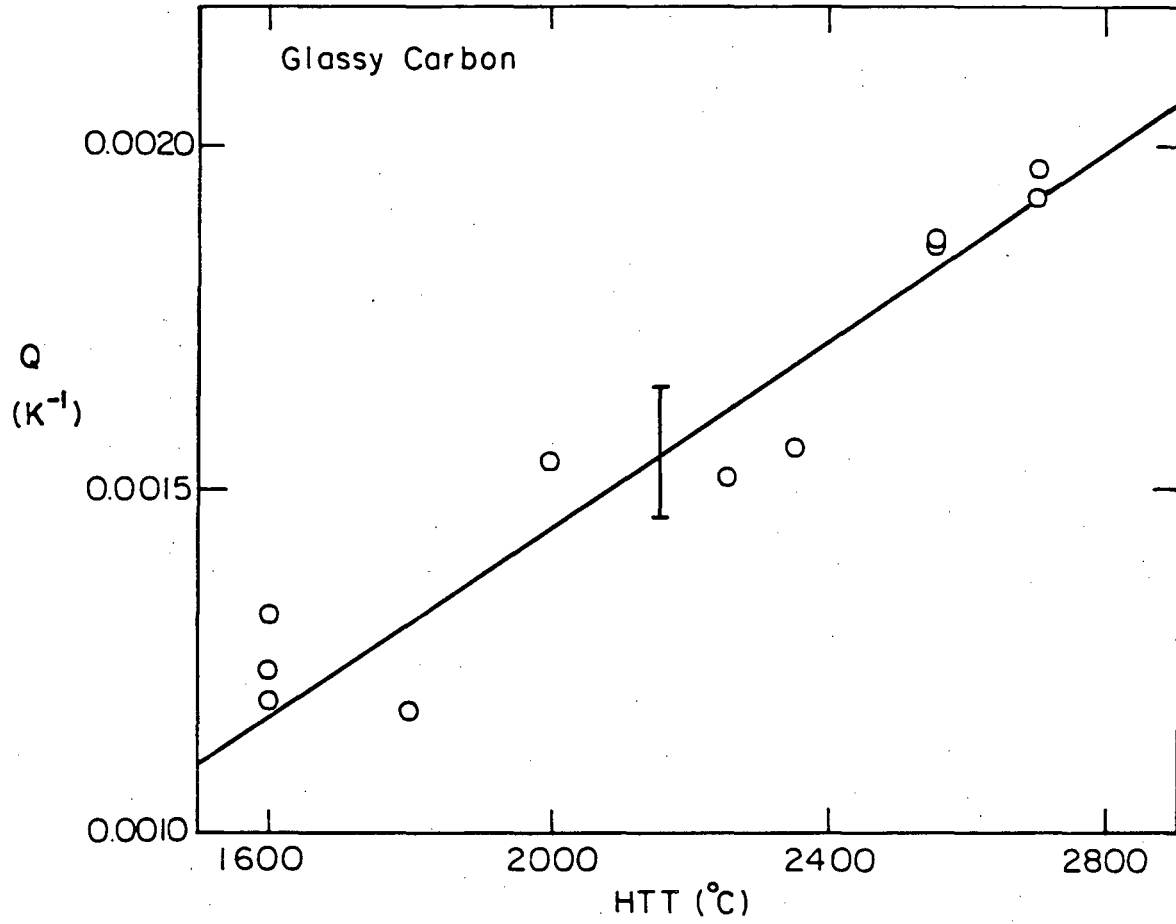
XBL 829-11523

Figure IV.9



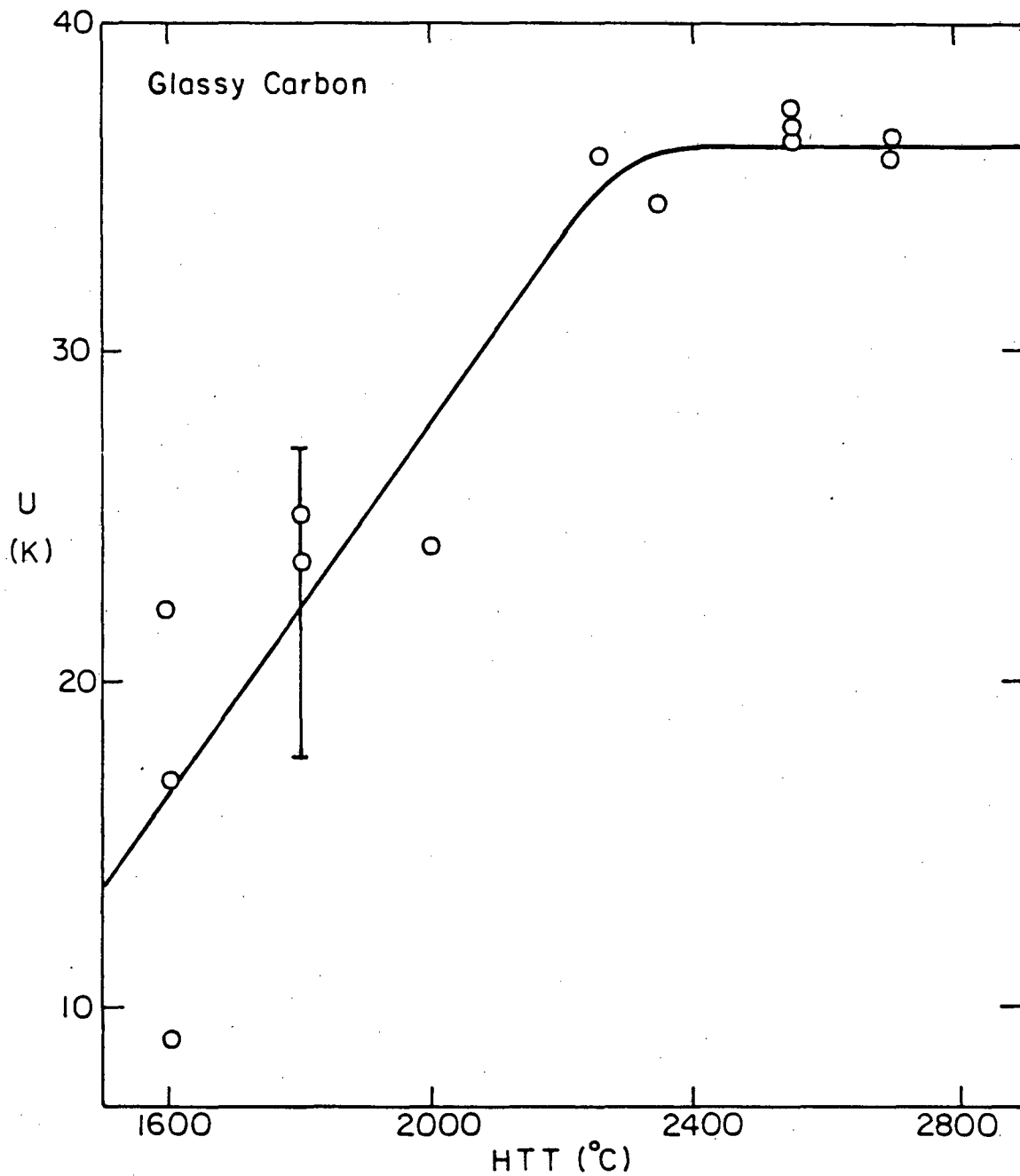
XBL 765-6929

Figure IV.10



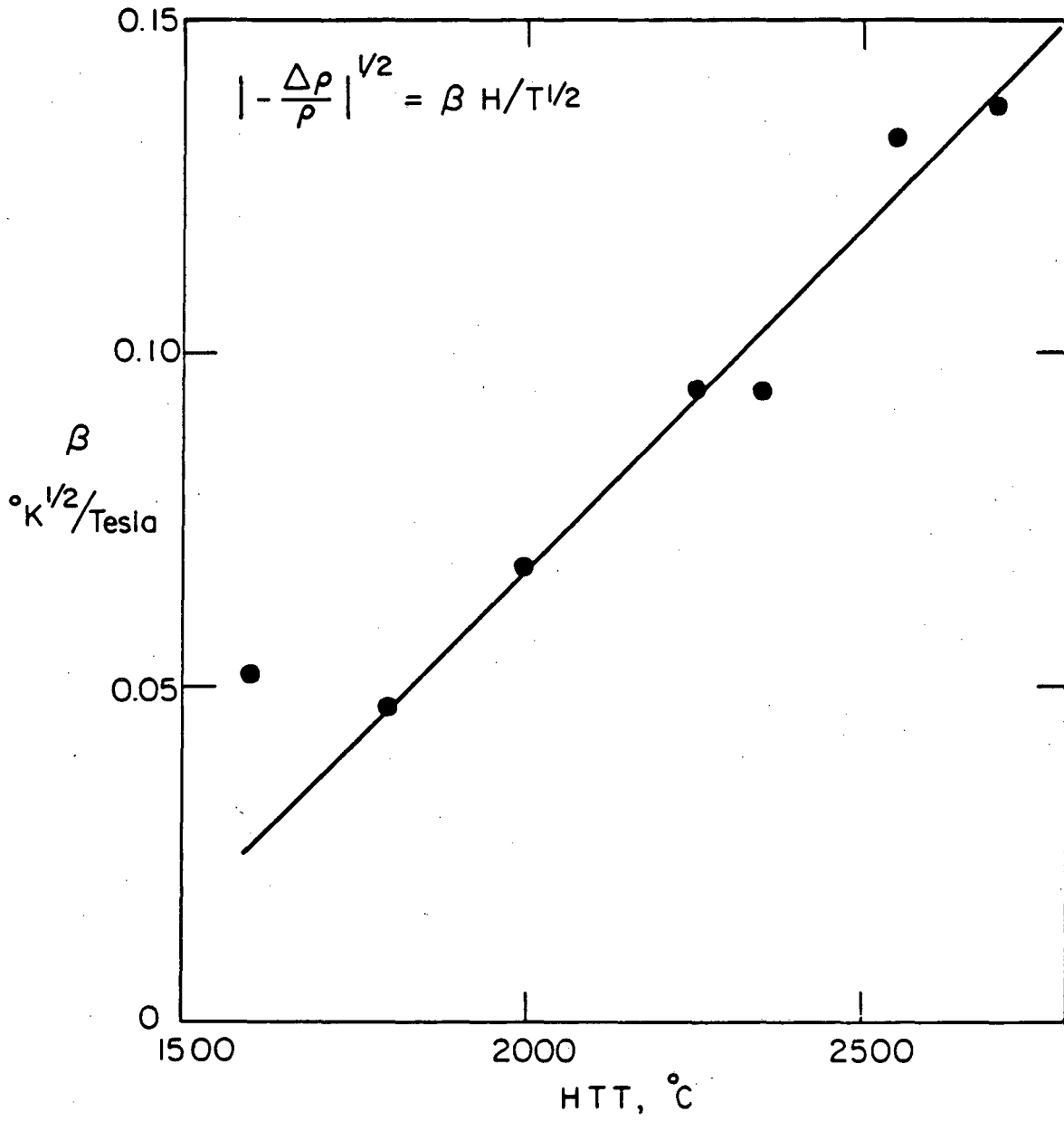
XBL 828 - 6439

Figure IV.11



XBL 828-6440

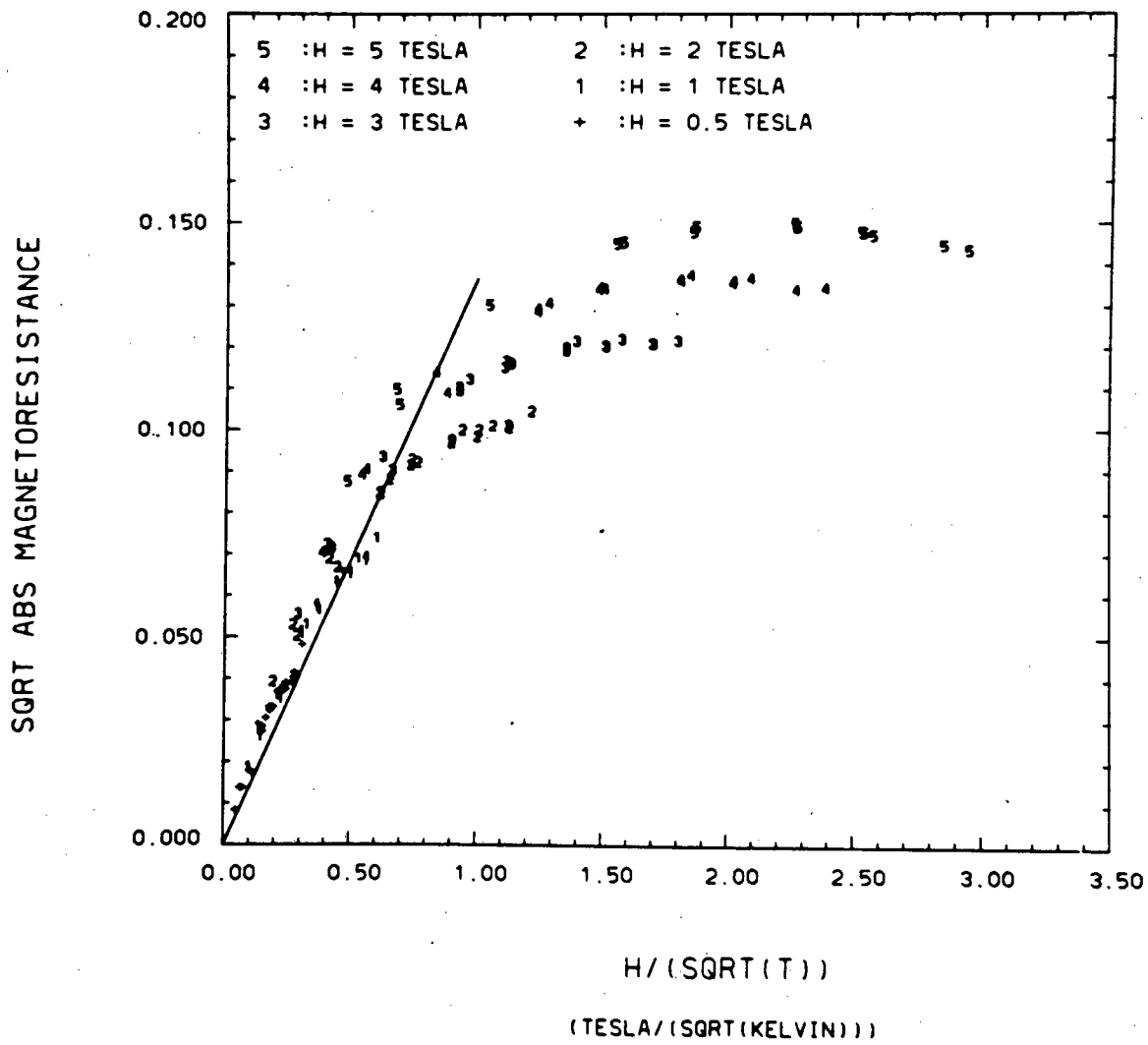
Figure IV.12



XBL 8110-6697

Figure IV.13

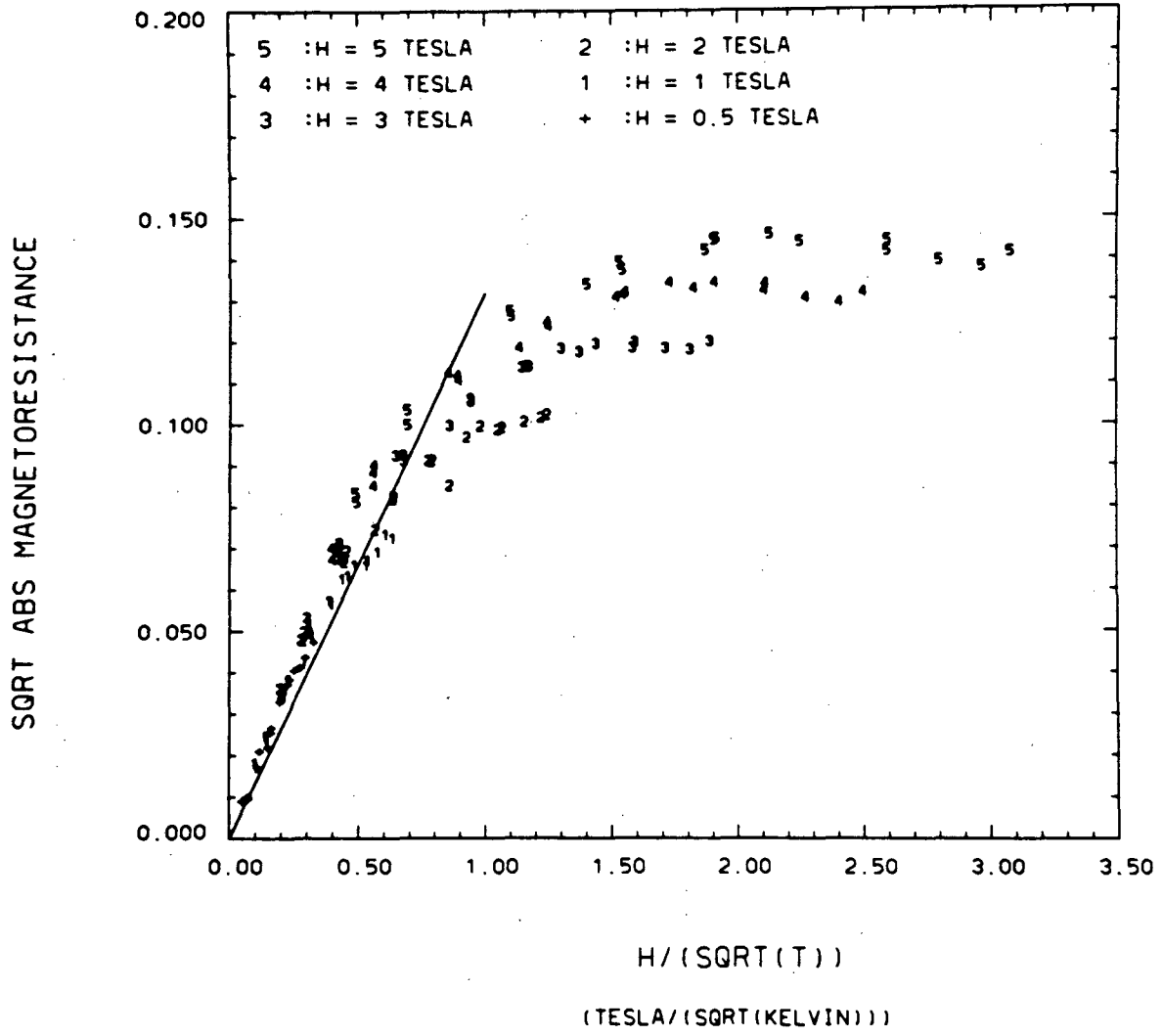
HTT2700-3



XBL 829-11511

Figure IV.14

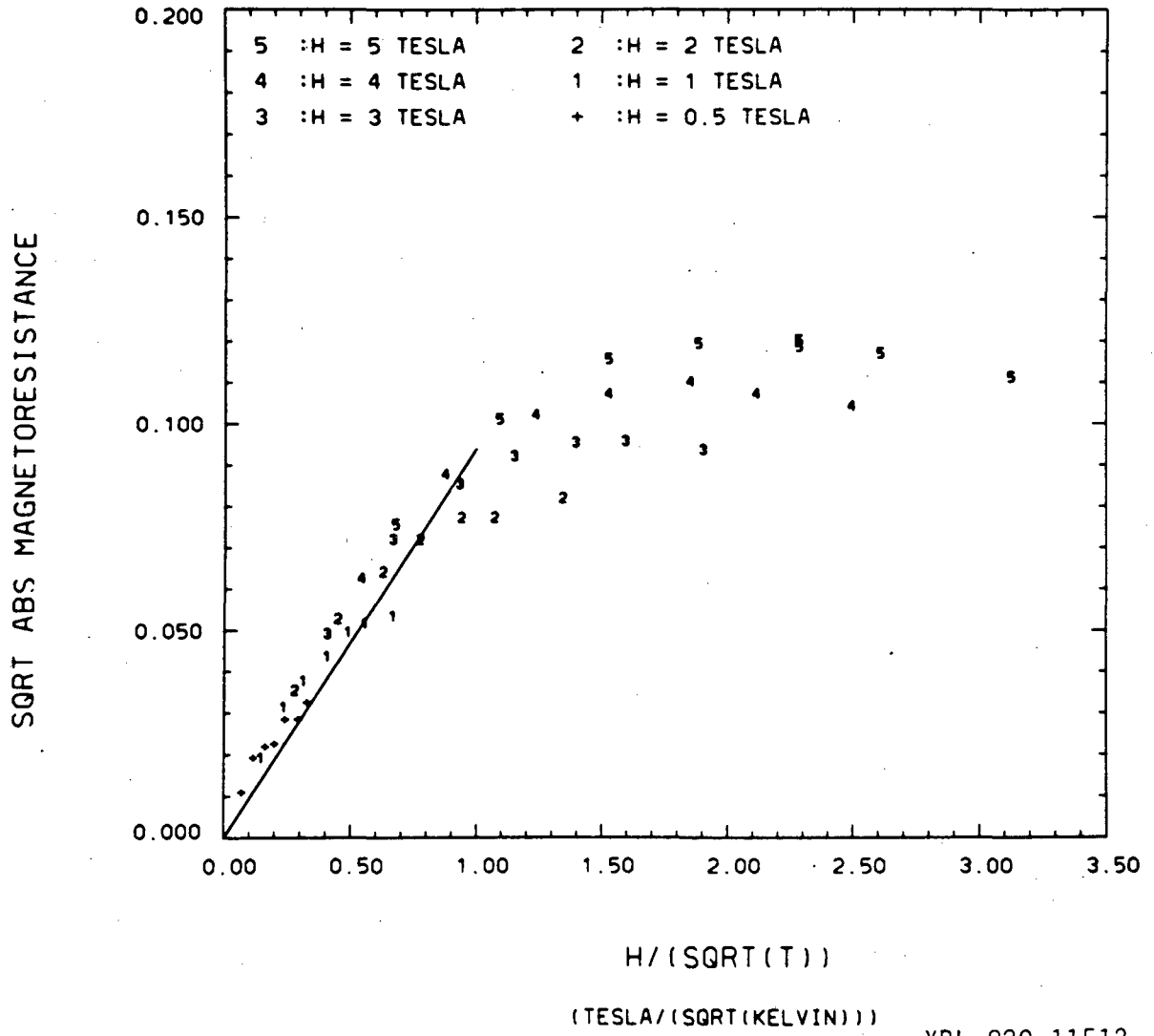
HTT2550-3



XBL 829-11510

Figure IV.15

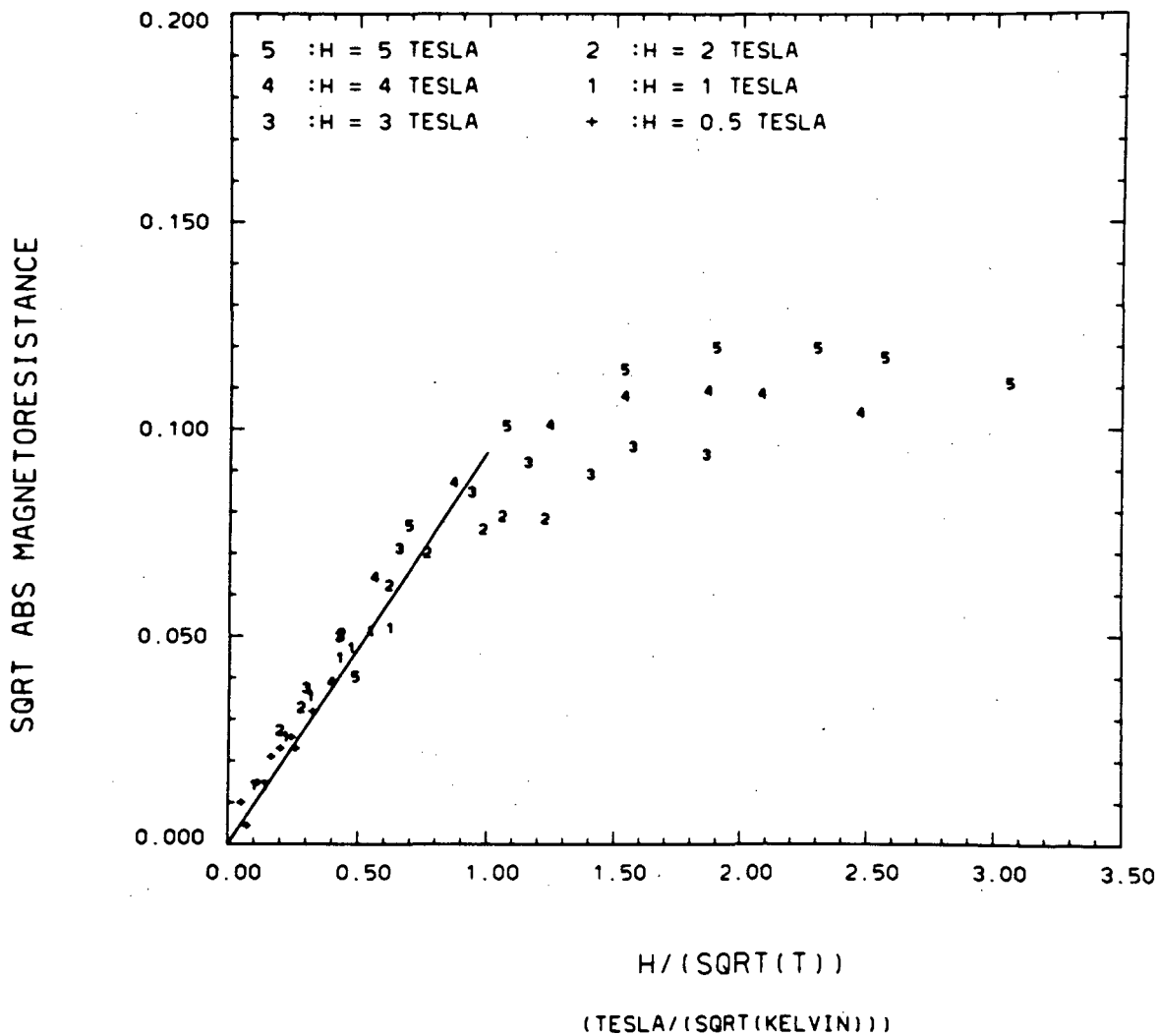
HTT2350-3



XBL 829-11512

Figure IV.16

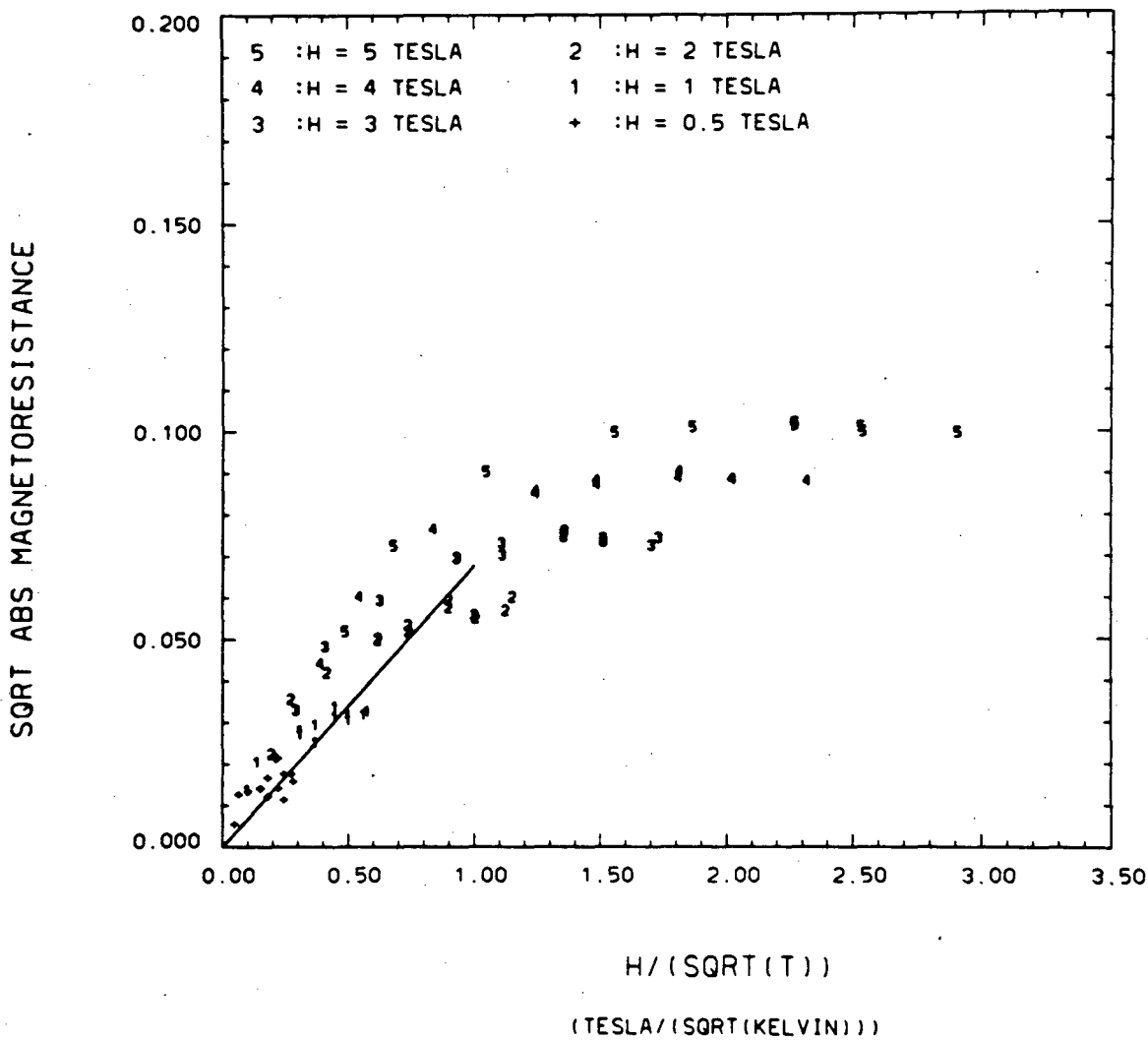
HTT2250-3



XBL 829-11514

Figure IV.17

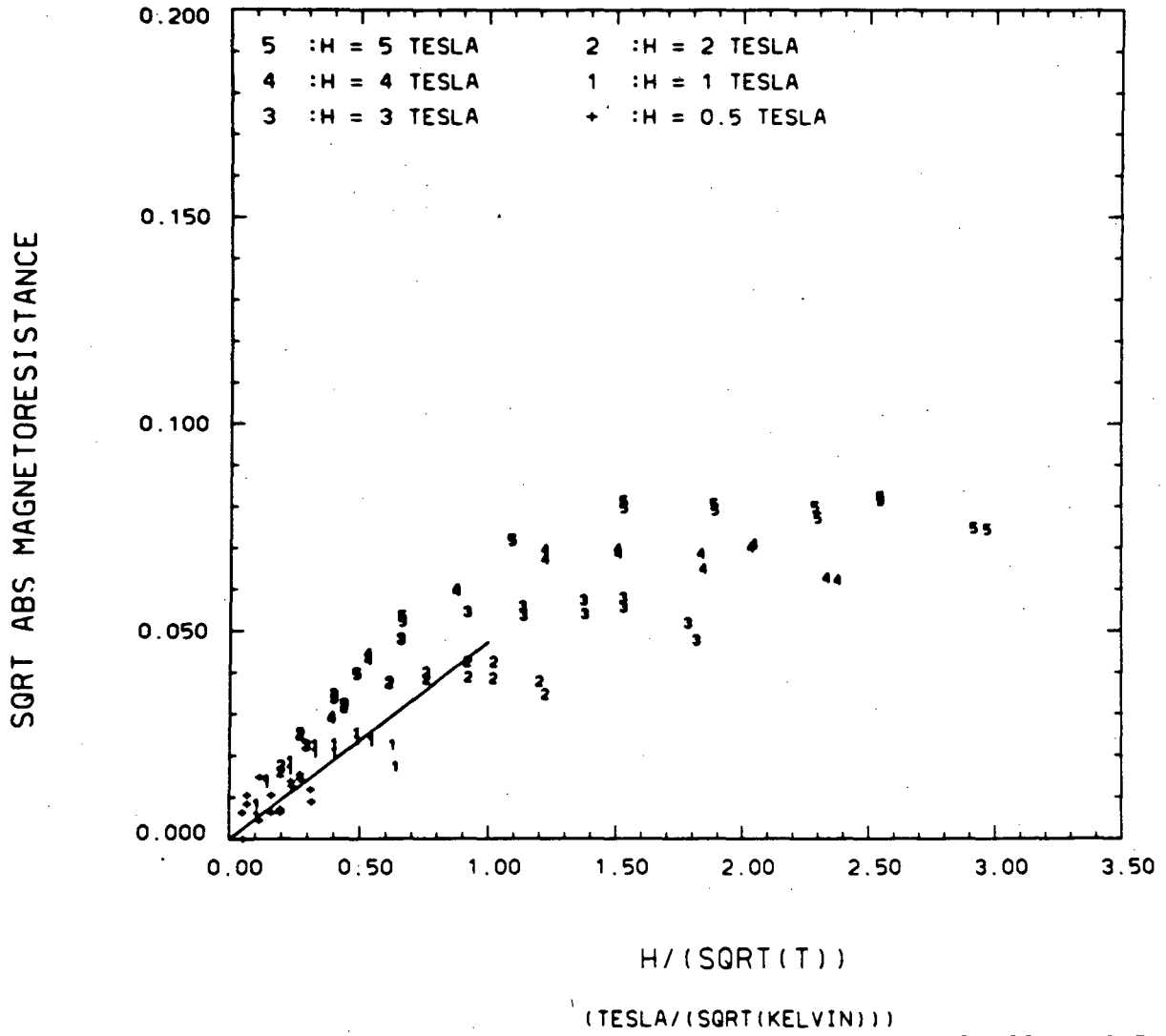
HTT2000-3



XBL 829-11513

Figure IV.18

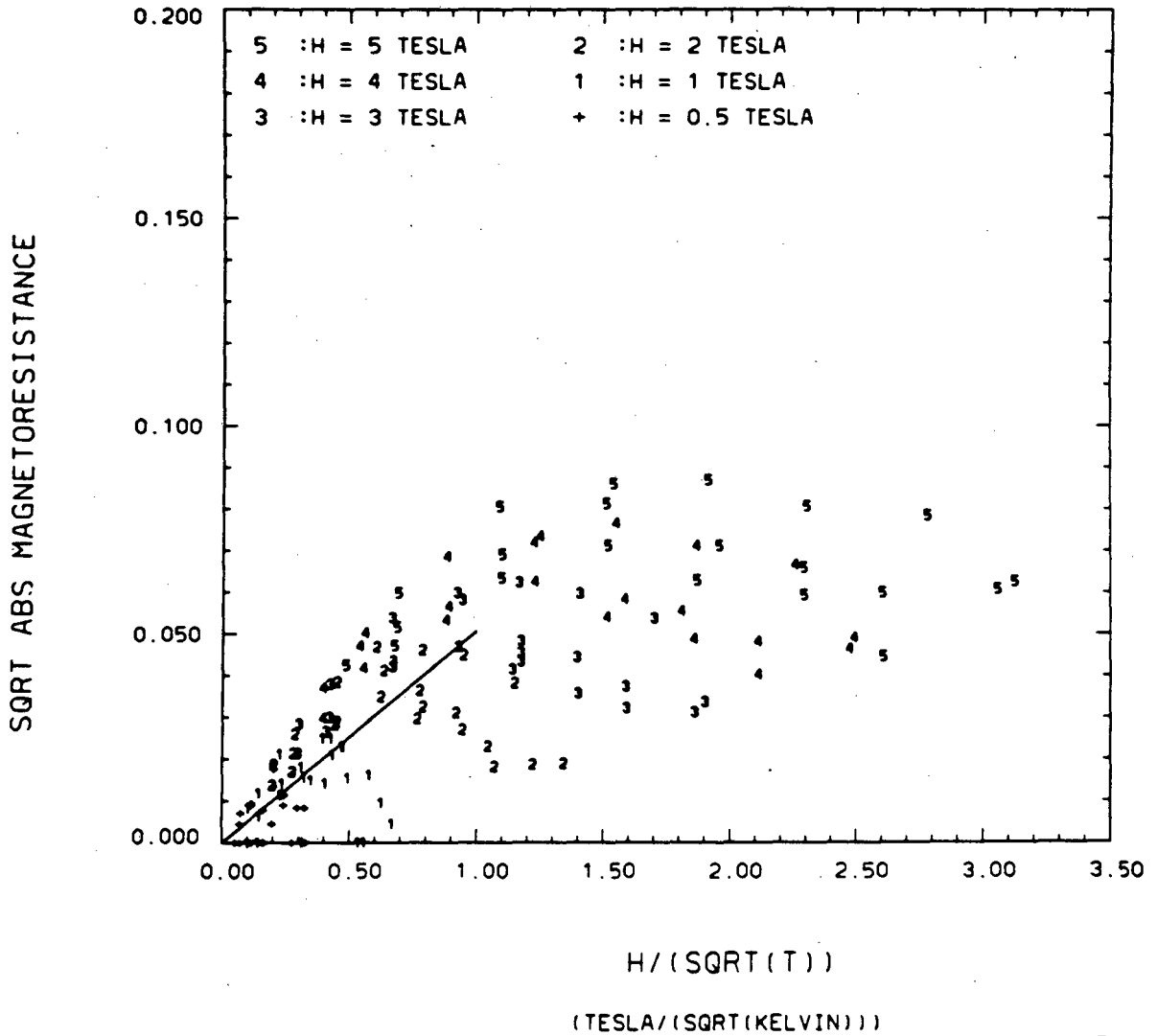
HTT1800-3



XBL 829-11515

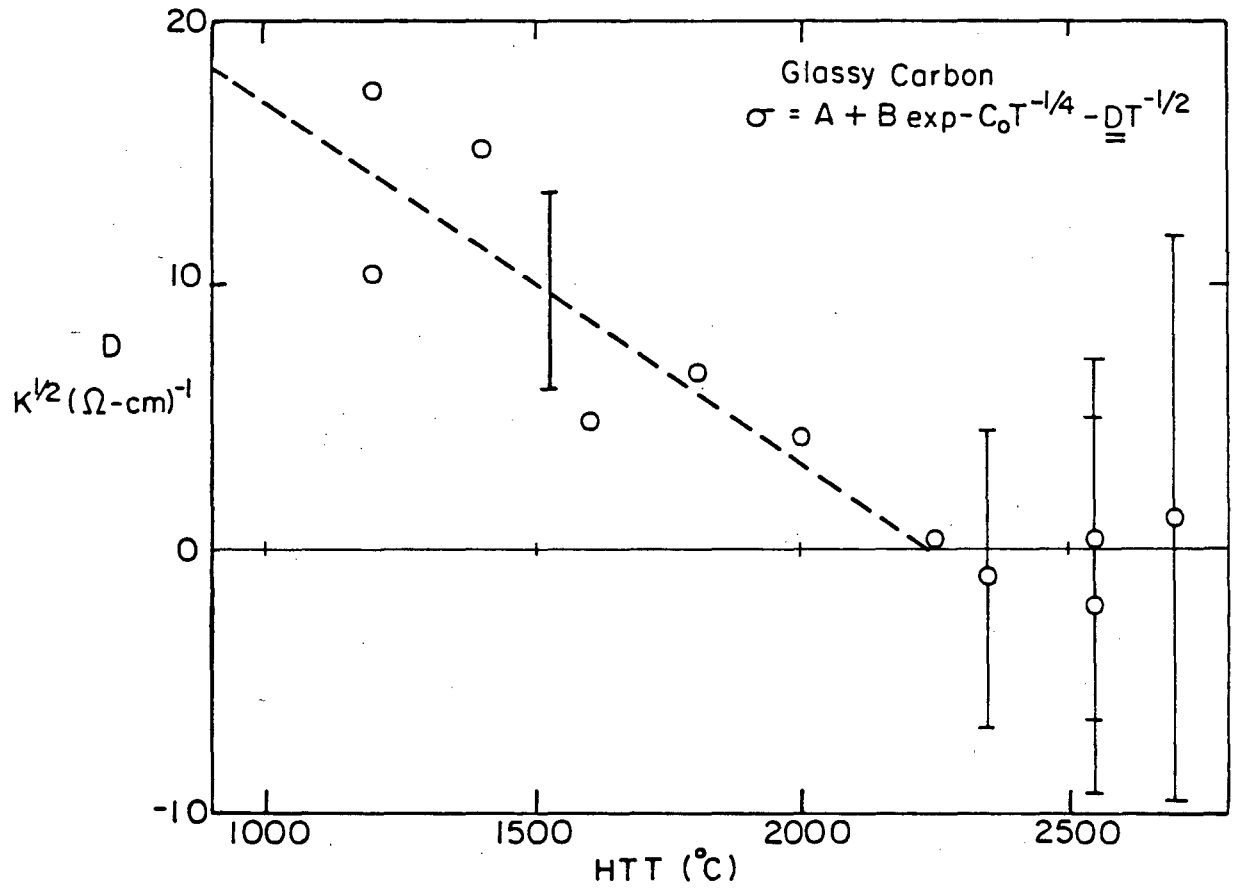
Figure IV.19

HTT1600-3



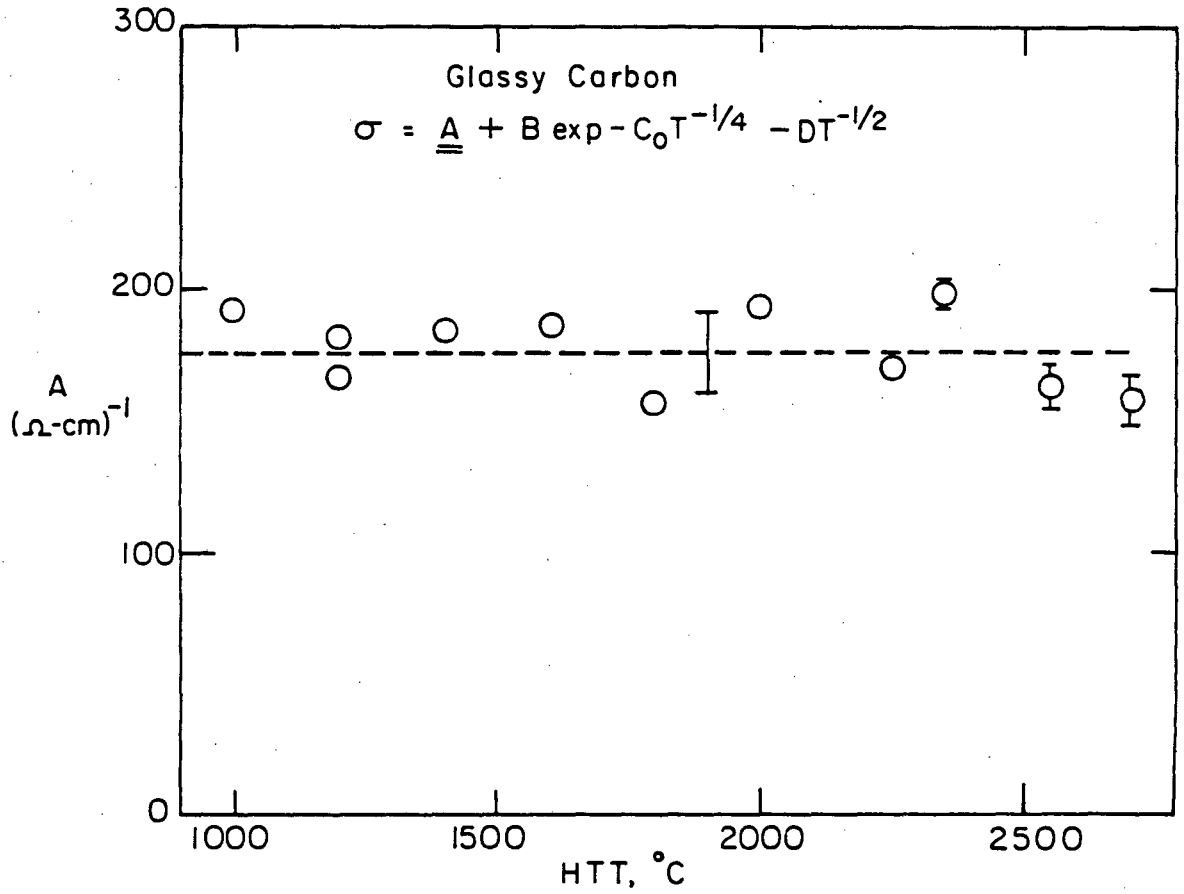
XBL 829-11516

Figure IV.20



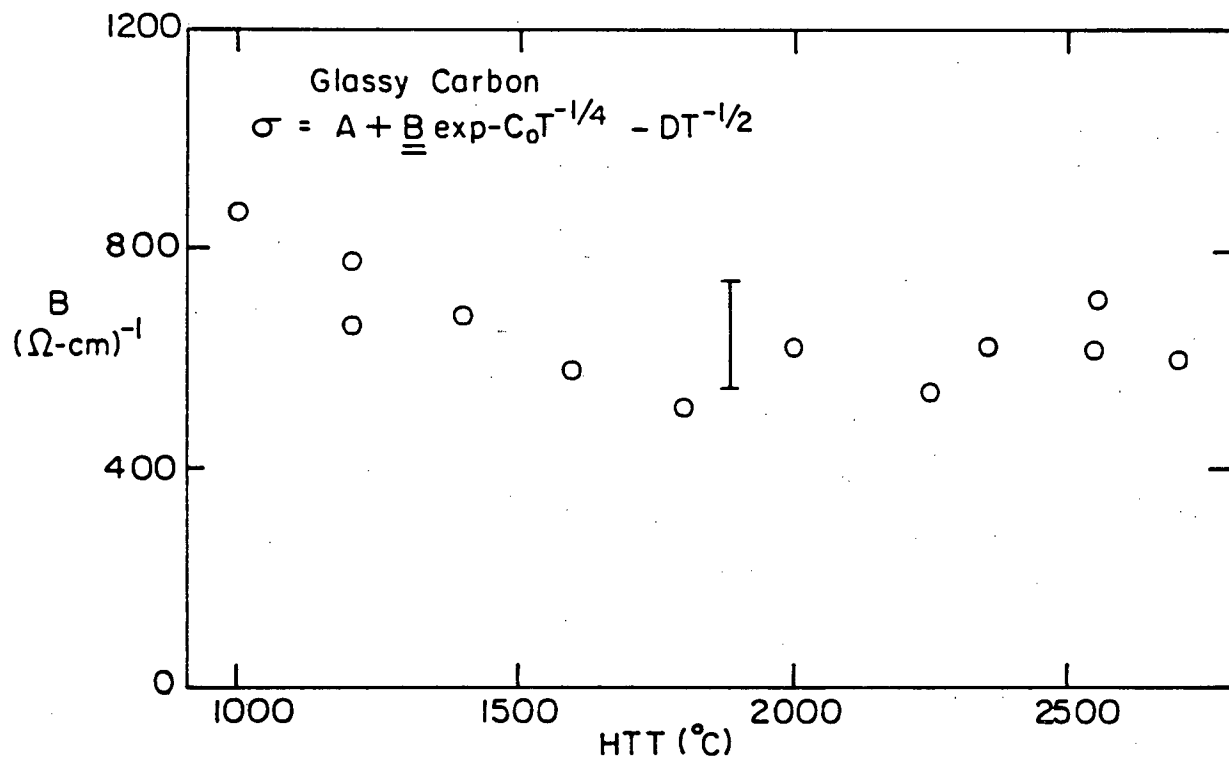
XBL 828-6436

Figure IV.21



XBL 828-6434

Figure IV.22



XBL 828-6435

Figure IV.23

## APPENDIX A

### Experimental Detail

#### 1. Specimen Preparation

Glassy carbon is produced by pyrolysis of thermosetting resins such as phenol-formaldehyde and polyfurfuryl alcohol. The manufacture of bulk high density ( $\sim 1.5 \text{ g/cm}^3$ ) is a slow expensive process mostly limited by the rate at which gases<sup>1,2</sup> can be evolved from the cured resin. Weight and volume losses during carbonization are high (about 50%). Glassy carbon can be cast in a variety of shapes depending on the shape of the mold in which the resin is hardened, but the wall thickness is limited to about 3 mm. Glassy carbon is nominally pure carbon. The material used in this work was prepared by Polycarbon, Inc., of North Hollywood, CA under license from Lockheed Missiles and Space Corporation, and had received a final heat treatment temperature of  $1000^\circ\text{C}$  for one hour. This temperature is high enough so that all of the aromatics and other easily evolved gases will have been driven out. A comprehensive review of carbonization of polymers including glassy carbon precursors was written by E. Fitzer et. al.<sup>3</sup>

Specimens, nominally 5 cm x 2.5 cm x 2 mm, were weighed, measured and scribed with gage lines before heat treatment in a vertically mounted modified Astro graphite model #2560-1000 furnace so that afterward the density, volume, mass and linear dimension changes could be determined.<sup>4</sup> Specimens were heat treated inside a graphite carousel

turnstile which can be lowered from a much lower, though appreciable, temperature into the hot zone of the furnace. However because the thick (~2 mm) plate specimens fracture when exposed to high heating rates, this rapid insertion feature was not used. After purging with inert gas for half an hour, the specimens were heated directly at 15°C/min below 1000°C, and at 25°C/min above 1000°C under a gas flow of 0.1 cc/min STP. After heat treatment for three hours, a convenient arbitrary time long enough to avoid any transient heating effects, specimens were dropped out of the hot zone through a slot in the bottom hearth into a quench chamber (ambient atmosphere at near room temperature). Argon was used as the inert gas for heat treatment at less than 2000°C and helium was used at temperatures higher than 2000°C because helium is less heat conducting and has a smaller heat capacity than argon.

After heat treatment, the specimen plates are ground down to the approximate thickness (0.6 mm) of the electrical conductivity specimens. The 1" x 2" plates are attached with wax\* on steel plates so they can be mounted on a magnetic chuck. Water is used liberally as the lubricant. Cutting depths should only be 0.0005" to prolong the life of the diamond grinding wheel\*\* and to maintain the surface

---

\*Sticky Wax, Corning Rubber Co.

\*\*MD 180, R100, BD1/8 C1, 4" x 1/4" x 1/2", Elgin.

smoothness of the cut. After approximately half of the material to be removed has been ground away, the plate and specimen must be reheated so that the specimen is freed and can be turned over and reattached. The unground surface is ground so that approximately equal amounts of material have been removed from both sides of the center section of the specimen. This center section is chosen for consistency and because glassy carbon plates ground on only one side invariably warp (surfaces in compression, center in tension). Warped specimens do not easily polish to uniform thickness nor mount on flat plates such that all grinding portions of the specimen will be cut through when the specimens are cut ultrasonically. Specimens were hand polished through 600 grit papers to the thickness tolerance of 0.0001".

The specimen configuration was cut into the wax mounted specimens using a Raytheon Ultrasonic Impact Grinder under moderate power with 120 grit silicon nitride as the abrasive and water as the carrier and lubricant. The specimen should be parallel to the tool die to ensure that it is cut through evenly. Nearly completely cut specimens can be broken away and rough edges smoothed with a fine jeweler's file.

The cross section of the specimen is not ideally rectangular because of wear in the graphite male and female electrodes used to electron discharge machine the tool die and wear in the die itself. The combined effect on the specimen cross section is that it is no longer ideally rectangular, but that it is approximately that as represented in Figure A.1. Because  $a > b \gg c \approx d > t$ , the specimen can still be considered nearly rectangular. Since the tool die wears progressively, the cross section of specimens can be sampled and measured

directly by sectioning and mounting specimens and observing them in a metallurgical optical microscope.

After the specimens have been cut, they are cleaned. Residual wax is removed by dissolving it in tetrachloroethylene in a covered dish for a few hours. The specimen is then washed in acetone, distilled water, and ethyl alcohol, and dried under a hot air blower.

A single coat of a commercial colloidal silver contact paint (Dupont Silver Preparation, electronic grade 4817), butyl acetate thinner is applied with a fine brush to the pads of the specimen (Figure A.2). The paint will dry in about half an hour. The resistance between all the pads should be checked; in glassy carbon specimens it should be of the order of 2 ohms.

The specimens are installed in the probe by loosening all six screws through the Cu-Be contact clamps and then sliding the specimen into place. Poor design has made it necessary that the pads of the specimen pass above the insulator washers for the three sidearms and opposing Hall arm. Alternatively, the single opposing Hall contact can be completely removed and the specimen positioned in place. Once the specimen is in place, the end current contacts should be screwed down to fix the specimen, and then the rest of the contacts. The contacts should be screwed down firmly to maintain good electrical contact, but keeping in mind that the arms of the specimen are easily broken. There should be a short between all the contacts if the specimen has been installed properly. If this condition does not prevail, each contact should be checked to make sure it is not loose and is making contact

with the specimen; and if this fails, it should be ensured that the arm and pad of the specimen are still intact. Hairline fractures of the arm at the beam junction are difficult to observe visually, and can be responsible for the open circuit condition.

## 2. Phenomenological Theory, Experiment Design & Instrumentation

From a discussion of the phenomenological theory of electrical conductivity, magnetoresistance and the Hall effect, the choice of design of the measurement system and its instrumentation is made and thus the accuracy and precision of the experimental quantities measured are deduced. Galvanomagnetic and thermomagnetic phenomena are rigorously derived and described by irreversible thermodynamics. Beginning along the lines used by R. Haase<sup>5</sup> the equation defining the differential entropy is written

$$TdS = dU - \sum_i L_i dX_i - \sum_k \mu_k dn_k \quad (A1)$$

where the first term is the internal energy, the second term is the energy from external sources, and the third term is the chemical energy. When integrated (keeping intensive variables constant) the above equations gives

$$TS = U - \sum_i L_i X_i - \sum_k \mu_k n_k \quad (A2)$$

The second law of thermodynamics gives

$$\Delta S = S_{II} - S_I = \int_I^{II} dS = \Delta_a S + \Delta_i S > 0 \quad (A3)$$

where II refers to the final state, I refers to the initial state,

$$\Delta_a S = \int_I^{II} d_a Q/T \equiv 0 \quad (A4)$$

under adiabatic conditions ( $d_a Q \equiv 0$  for a closed system) and  $\Delta_i S >$

0. In differential form

$$dS = d_a S + d_i S \quad (A5)$$

Differentiating with respect to time

$$\frac{dS}{dt} = \frac{d_a S}{dt} + \frac{d_i S}{dt} \quad (A6)$$

Obviously  $d_i S/dt > 0$ ; this term is called entropy production.

The term  $d_a S/dt = 0$  under thermal isolation, and is a description of entropy flow. Let  $d_i S/dt = \theta$  and  $T\theta = \psi$ , the dissipation function. Then

$$\frac{d_a S}{dt} = \frac{1}{T} \frac{d_a Q}{dt} + \sum_k S_k \frac{d n_k}{dt} \quad (A7)$$

where  $S_k$  is the molar entropy. Also

$$\frac{d_i S}{dt} = \frac{1}{T} \frac{dW_{diss}}{dt} + \frac{1}{T} \sum_k A_k w_k = 0 \quad (A8)$$

where  $W_{diss}$  is the work dissipated,  $A_k$  is the affinity and  $w_k$  is the rate of chemical reaction. Then

$$\psi = \frac{dW_{diss}}{dt} + \sum_k A_k w_k > 0 \quad (A9)$$

For chemically stable systems

$$\psi = \sum_i J_i X_i > 0 \quad (A10)$$

where  $J_i$  is a generalized flux, and  $X_i$  is a generalized force. The linear approximation

$$J_i = \sum_j \alpha_{ij} X_j \quad (A11)$$

known as phenomenological equations are valid for near equilibrium conditions. Thus

$$\psi = \sum_i \sum_j \alpha_{ij} X_i X_j > 0 \quad (A12)$$

The Onsager<sup>6</sup> relations can be easily arrived at. These relations have been expanded upon by Casimir's objection and method<sup>7</sup> and have been formally derived by Mazur and DeGroot<sup>8</sup> for vector and tensorial quantities by considering fluctuations (small reversible reactions in time) above an average. Thus

$$\alpha_{ij}(B) = \alpha_{ji}(-B) \quad (A13)$$

The Onsager's relations stated above hold regardless of material characteristics or lack of crystallographic symmetry. Also the trace elements of the tensor are all even function of the magnetic field induction B, whereas all of the off diagonal elements are odd functions of B.

The phenomenological equations for electric charge and heat flow respectively are

$$J_i = \sigma_{ij}(B) E_j + M_{ij}(B) (\partial T / \partial x_j) \quad (A14)$$

$$q_i = T J_s = N_{ij}(B) E_j + S_{ij}(B) (\partial T / \partial x_j) \quad (A15)$$

Often it is more desirable to measure the electric field than the electric current. In this case the former equation is inverted by multiplying through by the resistivity tensor  $\rho_{ij}$ , the reciprocal of the conductivity tensor  $\sigma_{ij}$ . Thus

$$E_i = \rho_{ij} J_j - \rho_{ij} M_{jk} (\partial T / \partial x_k) \quad (A16)$$

$$q_i = N_{ij} \rho_{jk} J_k - (N_{ij} \rho_{jn} M_{nk} - \delta_{ik}) (\partial T / \partial x_k) \quad (A17)$$

Combining the multiplied tensors

$$E_i = \rho_{ik} J_k - \alpha_{ik} (\partial T / \partial x_k) \quad (A18)$$

$$q_i = \pi_{ik} J_k - K_{ik} (\partial T / \partial x_k) \quad (A19)$$

where  $\alpha_{ik}$  is the Seebeck or thermopower tensor,  $\pi_{ik}$  is the Peltier tensor, and  $K_{ik}$  is the heat conductivity tensor.

These four tensors are used to describe many effects observed under certain experimental conditions. Fieschi<sup>9</sup> lists 14 effects with transverse magnetic field and 4 effects in a longitudinal field. The present work is concerned with only two of these effects, the isothermal electrical resistivity and the isothermal Hall effect. The isothermal electrical resistivity is given by the relation

$$E_x/J_x = R_i^L = \rho_{xx}; J_y = 0, \frac{\partial T}{\partial x} = 0, \frac{\partial T}{\partial y} = 0 \quad (A20)$$

and schematically shown in Figure A.3.a.

The isothermal Hall effect is defined by the relation

$$E_y/J_x = R_i^t, \text{ where } J_y = 0, \frac{\partial T}{\partial x} = 0, \frac{\partial T}{\partial y} = 0. \quad (A21)$$

and is schematically shown in Figure A.3.b. The magnetic field is in the z direction.

Of course the phenomenological equations couple all of these effects together. The experiment was designed with isothermal conditions in mind; that is  $\vec{\nabla}T = 0$ ,  $\vec{J} = J_x \hat{x}$ ,  $J_y = 0$ ,  $J_z = 0$ ,  $\vec{B} = B_z \hat{z}$ . Therefore primarily only the isothermal resistivity and Hall effects and perhaps secondarily the Nernst and Ettinghausen effects can be observed. If less than ideal conditions are prevailing, then of course all of the effects may be operating, coupled by the phenomenological equations. Only the trace of the heat conductivity tensor in isotropic materials is nonzero.<sup>5</sup>

There are contact effects to be dealt with. They are the Peltier effect (an heterogenous defect) and the heterogenous (Seebeck) and homogeneous (in the leads) thermoelectric effects.

The Peltier effect is the heat in addition to the Joule heat adsorbed or expended at a junction of two dissimilar materials when an electrical current flows through it. It is related to the difference in specific entropy of electrons in the two materials.

$$\frac{T}{E} (S)_A - (S)_B = \pi_A - \pi_B = \pi_{AB} \quad (A22)$$

Thus for a current flowing through a specimen through identical contacts, the same quantity of heat is evolved at one contact junction and adsorbed at the other.

The heterogeneous thermoelectric effect is the potential difference between two dissimilar materials at constant temperature and is given by

$$\phi_{AB} = (\phi_A - \phi_B) = (\mu_A - \mu_B)_T / e \quad (A23)$$

where  $\mu_A$  and  $\mu_B$  are chemical potentials. For a voltage measured between two contacts on the sample at the same temperature, this effect cancels out. If the temperatures at the contacts are not the same, then the Seebeck effect is operating. The Seebeck effect is the operating effect in thermocouples.

The homogeneous thermoelectric effect is the potential difference between two points at different temperatures. In differential form with no electric current  $\vec{J}$

$$\vec{\nabla}\phi = \frac{Q}{eT} (\vec{\nabla}T) \quad (\text{A24})$$

$$S = \frac{Q}{T} + S' \quad (\text{A25})$$

where  $Q$  is the heat of transport of electrons,  $S$  is the transported entropy of electrons, and  $S'$  is the partial molar entropy.

All of the phenomena above depend on the electric current  $\vec{J}$  and the thermal gradient  $\vec{\nabla}T$ . If  $\vec{J}$  is made to be sinusoidal then the measured electric field  $\vec{E}$  will have an ac component and a dc component. In the present system, only the ac component is measured by a lockin amplifier. Since  $\vec{\nabla}T$  by the design of the cryostat insert cannot fluctuate about zero more than a few times per minute, all the effects that are driven by the thermal gradient are filtered out. Primarily only the resistivity and the Hall effect remain to be measured. The Nernst and Ettinghausen-Nernst effects may produce a second order alternating electric field because the alternating current through the Peltier, Ettinghausen, and Nernst effects could produce the alternating thermal gradient necessary. In the present system, the magnetic field is constant and  $B_z \gg B_x, B_y$  so that all the longitudinal magnetic field effects are small.

Besides the ac current/dc magnetic field scheme used, there are also the dc current/dc field scheme, which has numerous difficulties associated with the effects discussed; the dc current/ac field scheme; and the ac current/ac field scheme. The advantages of the ac current

methods have been discussed above. The ac field methods take advantage of the fact that off diagonal elements of the tensors in the phenomenological equations are odd functions of B and hence reverse sign when B is reversed.

The rectangular parallelepiped was chosen as the shape of the specimen. There are three basic criterion to consider. First, the specimen length must be at least four times longer than its width so that the Hall voltage will not be shorted out.<sup>10</sup> This is especially important in high mobility materials though apparently not in glassy carbon. Long narrow specimens also assure that the current will flow parallel to the long axis (provided of course that the specimen is homogeneous). The second criterion is that the thickness  $t$  of the specimen should be small, because both the resistance voltage and Hall voltage signals are proportional to  $t^{-1}$ . The third criterion is that  $t$  should be large enough to assure mechanical integrity. The resistance and Hall probe areas (or arms in the present configuration) should be as small as possible and contacts should be ohmic (achieved with silver conduction paint).

Figure A.4 is a schematic of how the experiment was set up electrically. A Princeton Applied Research Model 124 lockin amplifier supplies a potential of 10 volts to drive the specimen excitation current which has a stability of better than 0.01%. The excitation current  $I$  itself is measured by measuring the potential across a resistor  $R_s$  (10,000 ohms) with a Triplet Model 630 voltmeter with an accuracy of 3% and a stability of 0.5%. The current then flows to the large pad at

the extreme right of the specimen sketched in Figure A.2 and the return current flows through the opposite pad back to the locking amplifier and ground. The Hall voltage is measured between the two opposing transverse contact pads and the resistance voltage is measured between the remaining two contact pads. The resistance voltage is measured by a PAR 186 lockin amplifier with an accuracy of 2% but a stability of 0.01%. The Hall voltage is measured with the PAR 124 lockin amplifier with an accuracy of 2% but with a stability of only about 0.2% because the signal voltage is typically about 1  $\mu$ V and the noise (probably due to long 5' leads at room temperature and 4' leads in the sample chamber) is 2 nV.

The temperature is measured by a calibrated GaAs diode with an error of 0.1°K as a worse case but stable to 0.01°K. Magnetic fields less than about 2 tesla affect these readings less than 0.1°K. Measurements at temperatures greater than about 20°K do not have significant errors induced by magnetic fields up to 5 tesla.

The magnetic field is known to an accuracy of 0.7% but is stable to 0.01%. The magnet excitation current is provided by a Hewlett Packard Model 6260B power supply and the current is measured by measuring the voltage across two 1/2% shunts in series such that a reading of 1 mV indicates a current of 1 amp. The magnetic field was determined from previous calibration measurements (9.39 amps = 1 tesla) by the magnet manufacturer and were roughly checked independently.

When the specimens are installed and immediately before measurements commence at LHe temperatures, the phase of the lockin

amplifiers was set, the frequency tuned, and the PAR 124 lockin amplifier calibrated against the PAR 186 lockin amplifier. The ohmic and frequency response of the specimens should be checked also. All contacts should be ohmic and frequency response of the specimens should be nil up to 100 kHz, the limit of the lockin amplifiers.

All of the direct current voltages (lockin amplifier output voltages, GaAs diode voltage, and magnet current voltage) are measured by a Hewlett Packard Model 2401 voltmeter with an accuracy of 0.01% and a stability of 0.002%.

Two parameters are the primary interest in the experiment. They are the resistance voltage  $V_{\rho}$  and the Hall voltage  $V_H$ .

The resistance voltage  $V_{\rho}$  is simply given as follows

$$V_{\rho} = \frac{\rho IL}{wt} \quad (A26)$$

The accuracy of the geometric dimensions length  $L$ , width  $w$  and thickness  $t$  are  $0.0005"/0.260" = 0.2\%$ ,  $0.0005"/0.120" = 0.4\%$  and  $0.0001"/0.020" = 0.5\%$  respectively. The accuracy of the conductivity measurement compounding only the uncertainties affecting the accuracy of the resistance voltage is

$$\frac{\Delta\sigma}{\sigma} = \left[ \left( \frac{\Delta V_{\rho}}{V_{\rho}} \right)^2 + \left( \frac{\Delta I}{I} \right)^2 + \left( \frac{\Delta L}{L} \right)^2 + \left( \frac{\Delta w}{w} \right)^2 + \left( \frac{\Delta t}{t} \right)^2 \right]^{1/2} \quad (\text{A27})$$

$$= 3.7\%$$

If only the relative conductivity is desired, then all the geometric factors in the equation above drop out and the stabilities of the current I and the lockin amplifiers can be used rather than their accuracy. Hence

$$\frac{\Delta\sigma}{\sigma} = 0.01\% \quad (\text{A28})$$

This quantity is also the accuracy of the magnetoresistance.

The measured Hall voltage  $V_H$  consists of two components:

$$V_H = V_H^* + V_{\text{mis}} \quad (\text{A29})$$

$$V_H^* = R_i^t I/t = R_H HI/t \quad (\text{A30})$$

$$V_{\text{mis}} = \rho I \Delta L/wt \quad (\text{A31})$$

$$V_{\text{mis}}(H) = V_{\text{mis}}(0) \left( 1 + \frac{\Delta\rho}{\rho} \right) \quad (\text{A32})$$

The voltage  $V_H^*$  is the actual Hall voltage and is defined using the resistance due to the isothermal Hall effect with a transverse magnetic field,  $R_i^t$ , or the Hall coefficient  $R_H$ . The misalignment voltage  $V_{\text{mis}}$  is a resistance potential appearing due to the misalignment  $\Delta L$

of the Hall probes along the direction of current flow. The behavior of the misalignment voltage  $V_{\text{mis}}$  is the same as for the resistance voltage  $V_{\rho}$ , hence the last equation above is valid. Of course  $V_{\text{H}}(0) = V_{\text{mis}}(0)$  since  $V_{\text{H}}^*(0) \equiv 0$ . The accuracy of  $R_{\text{H}}$  is

$$\frac{\Delta R_{\text{H}}}{R_{\text{H}}} = \left[ \left( \frac{\Delta V_{\text{H}}^*}{V_{\text{H}}} \right)^2 + \left( \frac{\Delta t}{t} \right)^2 + \left( \frac{\Delta I}{I} \right)^2 + \left( \frac{\Delta H}{H} \right)^2 \right]^{1/2} = 3.7\% \quad (\text{A33})$$

The relative precision of  $R_{\text{H}}$  is  $\Delta R_{\text{H}}/R_{\text{H}} = 0.2\%$ . This is higher than for conductivity due to the larger noise to signal ratio.

The galvanomagnetic and thermomagnetic phenomena present in the experimental system have been discussed. It has been shown that all of them can be eliminated from consideration in the measurements except the electrical resistivity and the Hall effect, the phenomena desired to be measured. Considering the parameters of the specimen and instrumentation, the accuracies of the electrical conductivity, the magneto-resistance and the Hall coefficient are 3.7%, 0.01%, and 3.7%, respectively. The relative precisions of the electrical conductivity and the Hall effect are 0.01% and 0.2%.

### 3. Cryogenic Procedures

These are procedures for operating the experiment, mostly having to do with steps and precautions concerning the cryogenic aspects of the system.

Preparatory to making measurements on specimens, the cryostat must be prepared for attaining low temperatures. The procedure is to evacuate and purge with the mechanical pump (Welch Duoseal Model #1402,

5 cfm) the isolation and dewar chambers (Figure A.5) with nitrogen gas several times and then leave evacuated and valved off. This operation is performed primarily to remove any helium left that has diffused in or otherwise has inadvertently been introduced in these chambers so that they can be cryopumped by liquid helium (LHe) in the bath adjacent to these vacuum spaces. This is done because soft chambers (He gas present) do not insulate well and consequently the LHe boil off rate will be greater.

Next the bath and pot are evacuated and backfilled with He gas to eliminate any water, nitrogen or other gases from these chambers because otherwise these species will freeze when LHe is introduced. The most obvious result of failure to do this is that the duct between the pot and bath chambers becomes blocked, making transfer of LHe to the pot impossible. The expansion of water when it freezes is no doubt harmful to the bath wall and the magnet, leads and contacts inside the bath.

The nitrogen jacket can now be filled. While the cryostat is cooling from room temperature to about 95°K as measured in the sample probe (about 48 hours), the dewar and isolation chambers can be pumped on. The sample chamber should be covered, preferably with the flange of the specimen probe when it is inserted. The sample chamber should be evacuated and backfilled with He gas two or three times. The specimen probe may be inserted however only a few hours before electrical measurements commence.

On the day measurements are to be taken, the pot and bath must be pumped out again and backfilled with He gas to remove any nitrogen that

may have leaked in (the bath is not extremely leaktight). The duct between the pot and the bath should be checked to make sure it is clear by leaking He gas through it.

Liquid helium is transferred through a transfer tube (Janis Model FHT) inserted through a port in the support flange into the bath after purging the transfer tube with He gas to remove air that might freeze and restrict the flow of LHe. If liquid nitrogen condenses on the bath exhaust line, LHe is being transferred too fast and is being wasted. Except initially when the hot transfer tube is inserted into the LHe dewar, the pressure measured at the neck of the dewar by the gauge on the transfer line should not exceed three pounds. If such a pressure is maintained, the transfer line is probably blocked and must be thawed out, pumped out and purged again. Most of the 20-25 liters used to cool the cryostat is used to bring the massive (23 pounds copper equivalent) down to LHe temperature. When the magnet is covered, indicated by the superconductivity of the magnet and a carbon resistor LHe level indicator (Oxford Instruments), the transfer line is slowly withdrawn, roughly keeping pace with the LHe level indicator. The bath is full when the last indicator light comes on and when the helium boil off rate increases significantly. Starting from a hot magnet, a normal transfer will take from half to three quarters of an hour. The space above the magnet is usually filled within a few minutes after the magnet is covered.

The most efficient way to bring the sample chamber down to LHe temperature and below is to slowly leak LHe in the pot through the needle valve while slowly pumping on the pot. If the exhaust gas from

the bath is much greater than it is when LHe is not being transferred, the procedure is going too fast. The temperature measured in the sample probe will fall slowly at first (~2 hours) to 20°K but will then rapidly fall to about 5°K. The needle valve is then closed, the pot is evacuated, and then filled with liquid helium. The lowest temperature can be obtained by pumping as rapidly as possible on the full pot with the mechanical pump (all valves full open). When the temperature nears the final equilibrium temperature, approximately 2.5 to 3.0°K, the pumping speed is reduced slightly by partially closing one of the valves on the pumping line. When an equilibrium pressure has been established, the temperature is measured by a calibrated GaAs diode and a set of measurements with constant magnetic fields and constant temperature may be made of the magnetoresistance and Hall effect, making sure that the same pressure is maintained. At these low temperatures the GaAs diode voltage is magnetic field dependent, especially for fields greater than 2 tesla. To obtain the next higher temperature, the pot is valved off, and the temperature and pressure allowed to rise until the next desirable measurement temperature is achieved. Then the pot valve can be cracked to maintain the equilibrium pot pressure and the measurements with nonzero magnetic fields made. Conductivity measurements can be made at nearly any time because the measuring time is relatively quick (1 sec.) and the system is always near equilibrium. This procedure can be used for temperatures up to about 6°K when the sample chamber is evacuated. For temperatures up to about 35°K a thermal conducting medium of cold He gas (from LHe in the bath) must be maintained at an equilibrium pressure in the pot. For temperatures not

less than about 20°K, a small resistance heater can be used as well as the automatic temperature controller (magnetic field induced error is small at high temperatures > 20°K). Eventually as higher temperatures are attained, the pot (as well as the sample chamber) is evacuated and the temperature maintained by the heater only.

After the specimens have reached their final temperature (~300°K), the liquid nitrogen supply to the jacket is turned off and all valved are closed. The specimen probe can be removed any time the specimen temperature is greater than the melting point of nitrogen (63°K), otherwise frozen nitrogen will plug the sample bore. The sample chamber flange should be covered at all times, especially when the system is cold to keep water from condensing inside the sample chamber.

The major consumption of LHe is to cool down the magnet to superconducting temperature, usually about 20-25 liters even after pre-cooling with liquid nitrogen as described previously. About 5 liters is used every time LHe is transferred to fill the bath above the magnet. At the cost of a warm dewar instead of a cold one, some of this consumption can be avoided if the transfer line is cooled by letting cold He gas from a empty LHe dewar flow through the line just before transferring LHe from a full dewar. Obviously if the magnet has to be cooled less often, the less LHe will be required. Thus it is most economical to conduct measurements several days together at a time.

The amount of LHe used by the cryostat depends upon the specimen temperature. It is approximately 1/4 liter per hour at 4.2°K and

1 liter per hour at 100°K without a magnetic field. Magnet usage of LHe is high (by a factor of ~10) compared to specifications especially for high fields greater than 3 tesla. A full bath (2.5 liters) can last through two sets of magnetic field measurements if they are expeditiously made. The pot holds 1 liter of liquid helium.

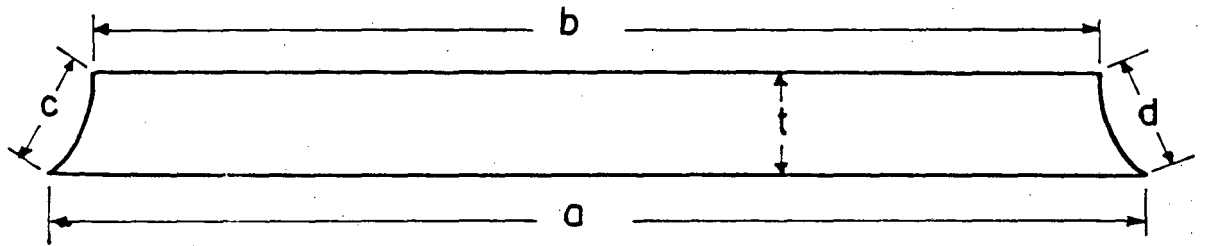
REFERENCES FOR APPENDIX A

1. E. Fitzer, W. Schaeffer, S., Yamada, "The Formation of Glasslike Carbon by Pyrolysis of Polyfurfuryl Alcohol and Phenolic Resin," Carbon 7 643-8 (1969).
2. J. Rautavuori, P. Tormala, "Preparation of Bulky Carbon Bodies from Phenolformaldehyde Resin," J. Mat. Sci. 14 2020-2 (1979).
3. E. Fitzer, R. Mueller, W. Schaefer, "The Chemistry of the Pyrolytic Conversion of Organic Compounds to Carbon," Chemistry and Physics of Carbon, P. Walker, ed., Marcel Dekker, Inc., New York, Vol. 7, pp. 237-303 (1971).
4. B. N. Mehrotra, R. H. Bragg, and A. S. Rao, "The Effect of Heat Treatment Temperature on Density, Weight, and Volume of Glass-Like Carbon," 1st Biennial Conf. on Carbon, Philadelphia, June 1981, Extended Abstracts p. 530; LBL Report #10623 (1981).
5. Rolf Haase, "Thermodynamics of Irreversible Processes," Addison-Wesley, London (1963).
6. Lars Onsager, "Reciprocal Relations in Irreversible Processes. I & II," Phys. Rev. 37 405 (1931) & Phys. Rev. 38 2265 (1931).
7. H. B. G. Casimir, "On Onsager's Principle of Microscopic Reversibility," Rev. Mod. Phys. 17 343 (1945).
8. S. R. DeGroot, P. Mazur, "Extension of Onsager's Theory of Reciprocal Relations. I & II," Phys. Rev. 94 218-224 (1954) & Phys. Rev. 94 224-6 (1954).

9. R. Fieschi, "Thermodynamical Theory of Galvanomagnetic and Thermomagnetic Phenomena," *Nuovo Cimento* 1 Suppl. 1-47 (1955)
10. Albert C. Beer, "Galvanomagnetic Effects in Semiconductors," *Solid State Physics Suppl.* 4, Academic Press, New York, pp. 56-60 (1963).

FIGURE CAPTIONS FOR APPENDIX A

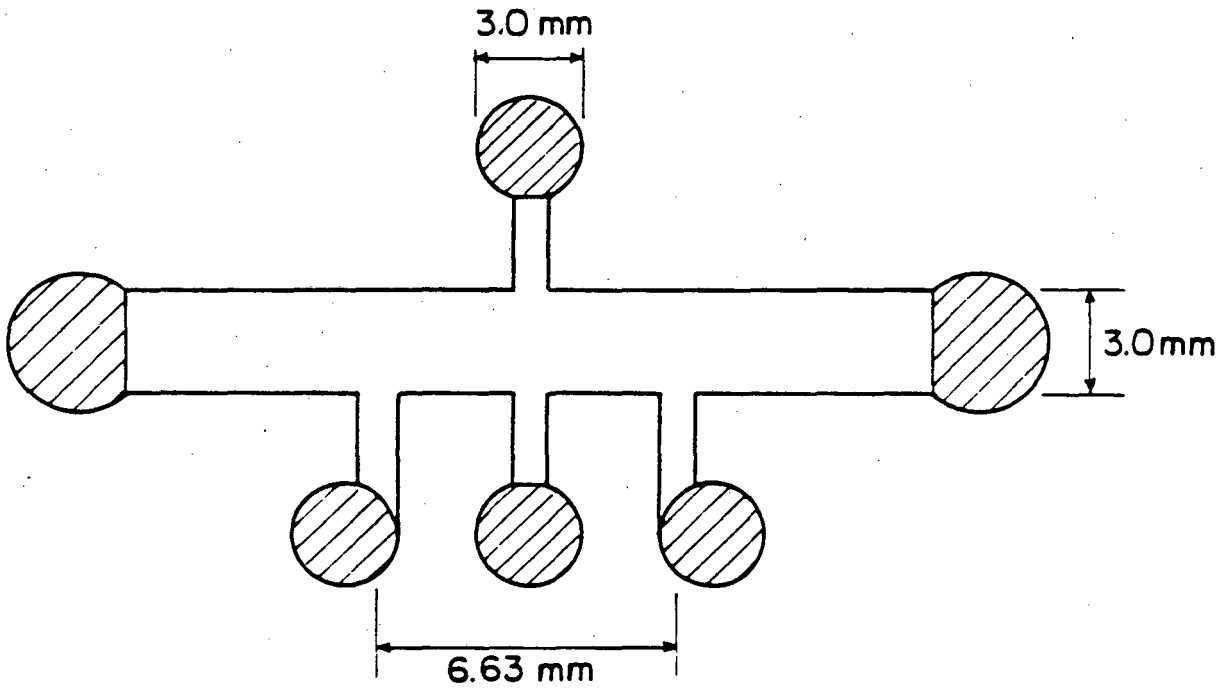
- |   |              |
|---|--------------|
| A.1. Specimen Cross Section   | LBL S24-5490 |
| A.2. Specimen Shape   | LBL S24-5489 |
| A.3. Sketch of Isothermnal<br>Transverse Electrical Resistivity<br>and Isothermal Hall Effect | LBL 824-5491 |
| A.4. Experimental Electrical<br>Schematic   | LBL 824-5492 |
| A.5. Cryostat Schematic   | LBL 766-7042 |



$$a > b \gg c \approx d > t$$

XBL 824-5490

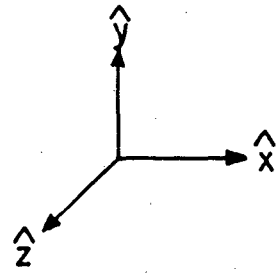
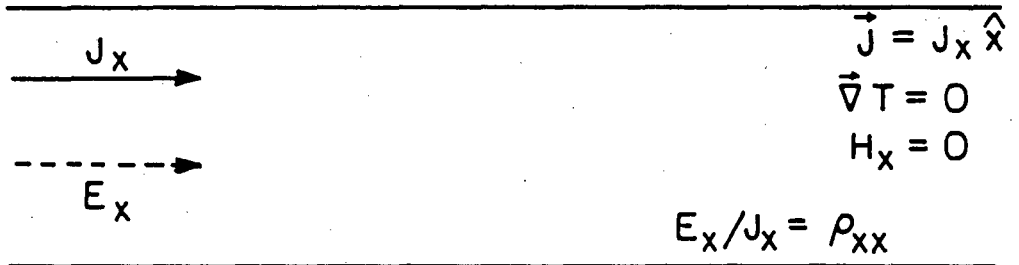
Figure A.1



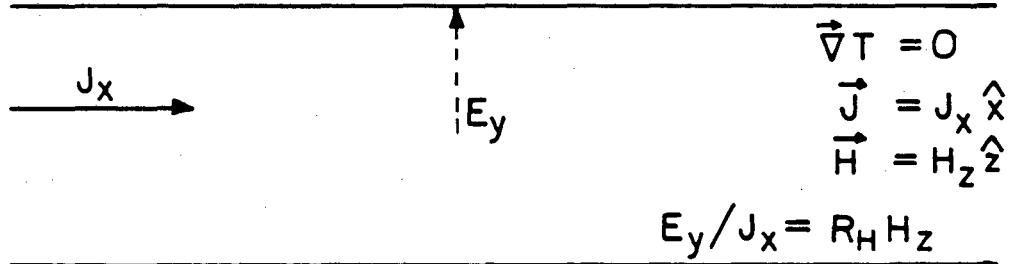
XBL824-5489

Figure A.2

Isothermal Transverse  
Electrical Resistivity (Magneto resistance)

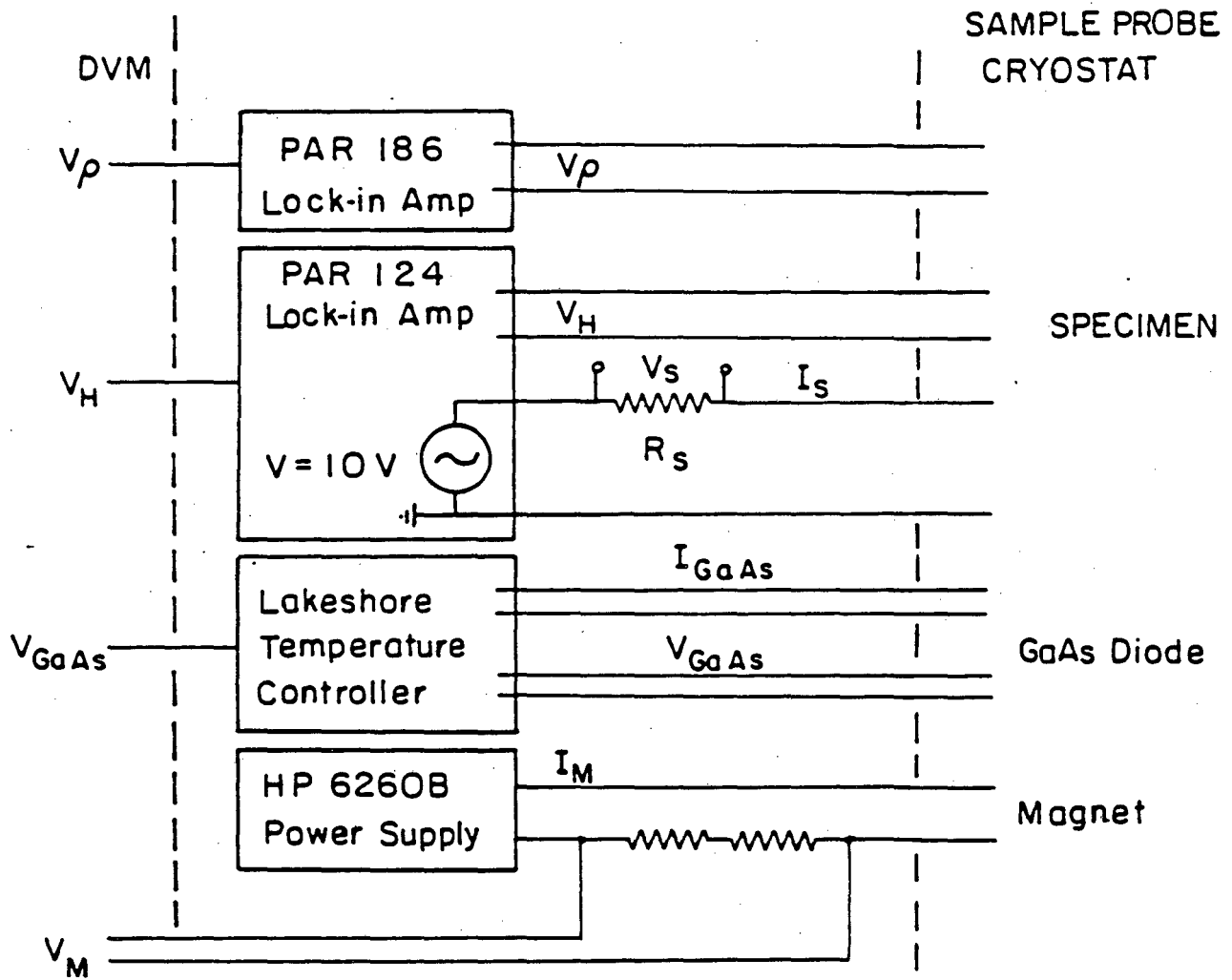


Isothermal  
Hall Effect



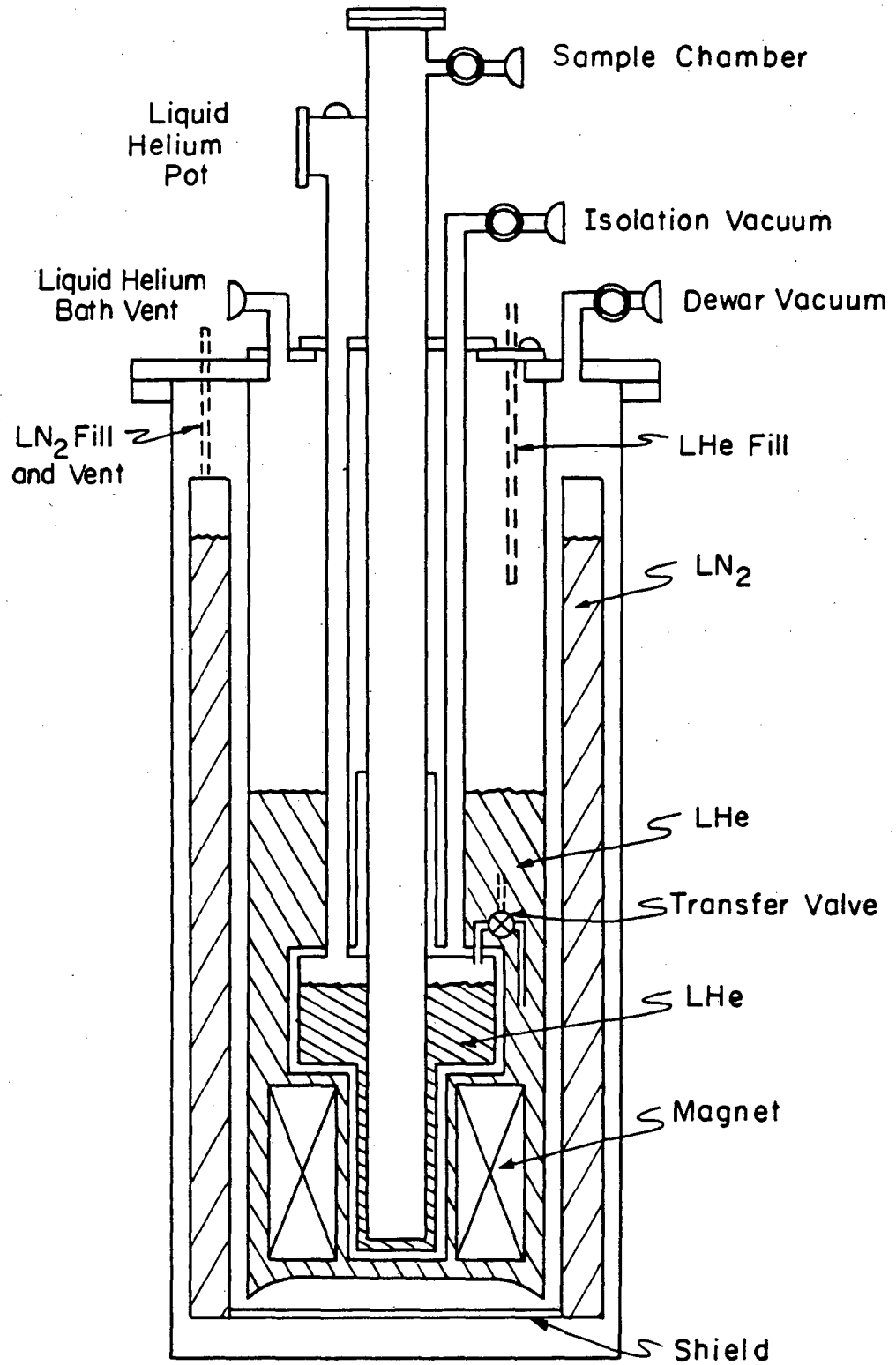
XBL824-5491

Figure A.3



XBL824-5492

Figure A.4



XBL 766-7042

Figure A.5

APPENDIX B

Electrical Conductivity Mechanisms

1. Metallic Conductivity

The largest term of the electrical conductivity of glassy carbon has been attributed to strongly scattering metallic conduction between extended states. The conductivity in three dimensions is given as

$$\sigma = S_F e^2 L / 12\pi^3 \hbar, \quad (B1)$$

where  $S_F$  = Fermi surface area and  $L$  = mean free path. This formula has been derived in a number of ways. It was derived by Ziman<sup>1,2</sup> in his work with liquid metals, by application of the Kubo-Greenwood formula<sup>3,4,5,6</sup> and also the Boltzman equation.<sup>5,6</sup> If the mean free path  $L$  becomes shorter, the conductivity can be legitimately written

$$\sigma = S_F e^2 L_z / 12\pi^3 \hbar \quad (B2)$$

where  $L_z$  is called the Ziman mean free path and is related to the actual mean free path  $L$  by  $L = L_z/g^2$ , where  $g$  is the ratio of the density of states at the Fermi level to the density of states at the Fermi level for free electrons. Of course in the limit that  $L \approx a$ , the conductivity is given by

$$\sigma = S_F e^2 a g^2 / 12\pi^3 \hbar \quad (B3)$$

In two dimensions, the minimum metallic conductivity is universally given by 7,8,9

$$\sigma = 0.12 e^2/h \quad (B4)$$

In one dimension, the conductivity is also about this order of magnitude<sup>9,10,11</sup> but is dependent upon the length and diameter of the wire element.

The term A in the present empirical formula appears to be independent of heat treatment temperature (Figure IV. 22). The "apparent crystallite" size of glassy carbon as reported by x-ray diffraction studies increases monotonically with heat treatment temperatures;<sup>12,13,14</sup> therefore if electrical conductivity of glassy carbon depended on crystallite boundary scattering, the conductivity would be dependent on the "apparent crystallite" size. This is apparently not the case. The conductivity formulae given above are also explicitly independent of temperature.

Application of the metallic conductivity formula for three dimensions using a coarse estimation of the parameters would easily make the metallic term approximate the average experimental value of 176  $(\Omega\text{-cm})^{-1}$ . For example, if the Fermi surface area is made to be the surface of the reciprocal unit cell of graphite, a is the nearest neighbor distance of 1.42 Å, and g is 0.5 (if g is much less than this, there are no extended states<sup>6,15</sup>), then the minimum conductivity predicted is 19  $(\Omega\text{-cm})^{-1}$ . If the mean free path is made larger than

the minimum distance  $a$  to match the average experimental conductivity, the mean free path becomes 13 Å, or 5 unit cells along the basal planes.

## 2. Variable Range Hopping

The second term of the empirical formula found by Saxena and Bragg<sup>16</sup> for the electrical conductivity of glassy carbon was attributed to variable range hopping or Mott scattering. This conduction mechanism has been applied to many systems, notably amorphous and degenerate semiconductors and chalcogenide glasses.<sup>6</sup>

This second term was derived by N. F. Mott,<sup>6,15,17</sup> and has since been refined by others.<sup>18-21</sup> The assumptions are that there are Anderson<sup>22</sup> localized electrons with wave functions given by a decaying exponential with distance  $R$ ,  $\psi = \exp(-\gamma R)$ , and random localization energies. The hopping distance is optimized such that the electron jumps with minimum activation energy to a site of near equivalent energy. This mechanism is known as variable range hopping because this site is not always the nearest neighbor site but some site at a variable range within a maximum distance. Because in the derivation an integral over the set of available sites is performed, Mott scattering is sensitive to the dimensionality of the case. Usually the density of states near the Fermi energy level is assumed to be a constant or slowly varying function with energy. Pollak<sup>23</sup> and Hamilton<sup>24</sup> have calculated a solution for a power dependence of the density of states on energy.

Another more mathematically rigorous approach to explaining Mott scattering is called the percolation method, or sometimes effective medium theory. Miller and Abrahams<sup>25</sup> were the first researchers to propose a resistive network with resistances connecting the nodes of the network dependent on a hopping or jumping rate. These ideas have been extended by many workers<sup>23,26-36</sup> to include the case addressed by Mott and to rigorously obtain his results for the exponential constant temperature dependence.

The results of the theory briefly reviewed above is that the conductivity is given by

$$\sigma = \sigma_p \exp(-S) \quad (B5)$$

Only in the exponential term is there any consensus as to form. It is given for hopping in three dimensions as

$$S = C_3 \left( \frac{\gamma^3}{kTN(E_F)} \right)^{1/4} \quad (B6)$$

and is readily modified for two dimensions to

$$S = C_2 \left( \frac{\gamma^2}{kTN(E_F)} \right)^{1/3} \quad (B7)$$

The constants  $C_3$  and  $C_2$  are dependent on the optimization procedure used. The best consensus values are  $C_3 = 2.0 \pm 0.2$  and  $C_2 = 2.0 \pm 0.4$ . The exponential term for one dimensional hopping is proportional to  $T^{-1/2}$ .

The prefactor term has not yet been fully established. A number of forms with varying temperature dependences between  $T^{-1/2}$  and  $T^{5/4}$  have been advanced;<sup>37</sup> all except one do not have a strong temperature dependence. The prefactor evidently depends on the system parameters, such as the distribution density of sites and the density of states as a function of energy.<sup>30</sup> In most cases involving hopping conduction, the conductivity varies over several orders of magnitude, and consequently the temperature dependence of the prefactor is not very important. However, in glassy carbon, the exponential part of the term is markedly smaller than for most other cases, and hence it may not be possible to ignore the temperature dependence of the prefactor. Because competing theories give both direct and inverse temperature proportionalities, a temperature independent prefactor has been used.

Mott scattering is considered a low temperature process; at higher temperatures electrons jump primarily to the nearest available site rather than to some site within a maximum range and thus the conductivity is thermally activated. Up to room temperature, no activated components of the conductivity were ascertained in glassy carbon, though Hishiyama et. al.<sup>38</sup> claims to have found two activated components and a hopping component at temperatures less than 4°K for glassy carbon treated at 900°C and 1000°C. Several authors<sup>39-42</sup> have proposed multi-phonon-electron interaction models to extend the range of

$\exp(-T^{-1/4})$  conductivity behavior and as another means of explaining the transition to high temperature activated conductivity.

In many materials where hopping conduction takes place, there is a significant ac component of the conductivity. None was found in glassy carbon in this work.

Though the  $\exp(-T^{-1/4})$  relation for the hopping component of the conductivity was established by fitting the experimental data to the model by the method of least squares, such a relationship does not guarantee absolute certainty that the conduction mechanism is variable range hopping.<sup>6,43</sup>

The exponential part in the hopping term yields a temperature constant

$$T_0 = \frac{16 \gamma^3}{k N(E_F)} = 4.5 \times 10^4 \text{ } ^\circ\text{K.} \quad (\text{B8})$$

The constant appears to be valid for all heat treatment temperatures. It is considerably less than that measured for amorphous carbon heated below the nonmetal-metal transition temperature and in silicon and germanium ( $2 \times 10^7 \text{ } ^\circ\text{K}$ ). A reasonable estimate of the density of states puts the localization range,  $\gamma^{-1}$ , in the range of 15 Å or so. As shown by Figure IV.23, the linear hopping term B is not dependent on heat treatment temperature, and thus the whole hopping term is nearly the same for all heat treatment temperatures.

REFERENCES FOR APPENDIX B

1. J. M. Ziman, "Principles of the Theory of Solids," Cambridge University, Cambridge, 2nd ed., Ch. 7, p. 211 (1972).
2. J. M. Ziman, "Models of Disorder, The Theoretical Physics of Homogeneously Disordered Systems," Cambridge University Press, Cambridge, Ch. 10, p. 387 (1979).
3. N. K. Hindley, "Random Phase Model of Amorphous Semiconductors, I. Transport and Optical Properties," J. Non-Cryst. Sol. 5 17 (1970).
4. L. Friedman, "Hall Conductivity of Amorphous Semiconductors in the Random Phase Model," J. Non-Cryst. Sol. 6 329 (1971).
5. N. F. Mott, "Conduction in Non-Crystalline Systems IV. Anderson Localization in a Disordered Lattice," Phil. Mag. 22 7 (1970).
6. N. F. Mott, E. A. Davis, "Electronic Processes in Non-Crystalline Materials, 2nd ed., Clarendon Press, Oxford, (1979).
7. D. C. Licciardello, D. J. Thouless, "Conductivity and Mobility Edges for Two-Dimensional Disordered Systems," J. Phys. C 8 4157 (1975).
8. D. C. Licciardello, D. J. Thouless, "Conductivity and Mobility Edges in Disordered Systems, II. Further Calculations for the Square and Diamond Lattice," J. Phys. C 11 925 (1978).
9. M. Pepper, "The Anderson Transition in Silicon Inversion Layers: The Origin of the Random Field and the Effect of Substrate Bias," Proc. Roy. Soc. A353 225 (1977).
10. D. J. Thouless, "The Effect of Inelastic Electron Scattering on

- the Conductivity of Very Thin Wires," Sol. St. Comm. 34 683-5 (1980).
11. D. J. Thouless, "Resistance and Localization in Thin Films and Wires," J. Non-Cryst. Sol. 35&6 3-7 (1980).
  12. F. Rousseaux, D. Tchoubar, "Structural Evolution of a Glassy Carbon as a Result of Thermal Treatment Between 1000 and 2700°C--I. Evolution of the Layers," Carbon 15 55-61 (1977).
  13. F. Rousseaux, D. Tchoubar, "Structural Evolution of a Glassy Carbon as a Result of Thermal Treatment Between 1000 and 2700°C--II. Tridimensional Configuration of a Glassy Carbon," Carbon 15 63-68 (1977).
  14. Ram R. Saxena, Robert H. Bragg, "Kinetics of Graphitization in Glassy Carbon," Carbon 16 373-6 (1978).
  15. N. F. Mott, "Conduction in Non-Crystalline Materials, III. Localized States in a Pseudogap and Near Extremities of Conduction and Valence Bands," Phil. Mag. 19 835 (1969).
  16. Ram R. Saxena, Robert H. Bragg, "Electrical Conduction in Glassy Carbon," J. Non-Cryst. Sol. 28 45-60 (1978).
  17. N. F. Mott, "Conduction in Glasses Containing Transition Metal Ions," J. Non-Cryst. Sol. 1 1-17 (1968).
  18. N. Apseley, H. P. Hughes, "Temperature- and Field-Dependence of Hopping Conduction in Disordered Systems," Phil. Mag. 30 963-72 (1974).
  19. H. Bottger, V. V. Bryksin, "Hopping Conductivity in Ordered and Disordered Solids (I)," Phys. Stat. Sol. (b) 78 9-56 (1976).

20. R. M. Hill, A. K. Jonscher, "DC and AC Conductivity in Hopping Electronic Systems," J. Non-Cryst. Sol. 32 53-69 (1979).
21. M. Ortuno, "Variable-Range Hopping Including Correction Between Energies and Positions," J. Phys. C 14 L421-5 (1981).
22. P. W. Anderson, "Absence of Diffusion in Certain Random Lattices," Phys. Rev. 109 1492-505 (1958).
23. M. Pollak, "A Percolation Treatment of dc Hopping Conduction," J. Non-Cryst. Sol. 11 1-24 (1972).
24. E. M. Hamilton, "Variable Range Hopping in a Non-Uniform Density of States," Phil. Mag. 26 1043-5 (1972).
25. A. Miller, E. Abrahams, "Impurity Conduction at Low Concentrations," Phys. Rev. 120 745-55 (1960).
26. V. Ambegaokar, S. Cochran, J. Kurkijarvi, "Conduction in Random Systems," Phys. Rev. B8 3682-8 (1973).
27. V. Ambegaokar, B. I. Halperin, J. S. Langer, "Hopping Conductivity in Disordered Systems," Phys. Rev. B4 2612-20 (1971).
28. P. N. Butcher, "Calculation of Hopping Transport Coefficient," Phil. Mag. B42 799-824 (1980).
29. P. N. Butcher, J. A. McInnes, "Analytical Formulae for D. C. Hopping Conductivity: r-Percolation in 3D," Phil. Mag. B37 249-53 (1978).
30. P. N. Butcher, K. J. Hayden, J. A. McInnes, "Analytical Formulae for D. C. Hopping Conductivity," Phil. Mag. 36 19-32 (1977).
31. J. A. McInnes, P. N. Butcher, "D. C. Hopping Conductivity," Phil. Mag. B39 1-11 (1979).

32. K. Maschke, H. Overhof, P. Thomas, "On Variable Range Hopping Near the Fermi Energy," Phys. Stat. Sol. (b) 62 113-22 (1974).
33. B. Movaghar, W. Schirmacher, "On the Theory of Hopping Conductivity in Disordered Systems," J. Phys. C 14 859-80 (1981).
34. B. Movaghar, B. Pohlmann, W. Schirmacher, "Theory of Electronic Hopping Transport in Disordered Materials," Phil Mag. B41 49-63 (1980).
35. B. Movaghar, B. Pohlmann, G. W. Sauer, "Theory of AC and DC Conductivity in Disordered Hopping Systems," Phys. Stat. Sol. (b) 97 533-40 (1980).
36. C. H. Seager, G. E. Pike, "Percolation and Conductivity: A Computer Study II," Phys. Rev. B10 1435-46 (1974).
37. F. R. Allen, C. J. Adkins, "Electrical Conduction in Heavily Doped Germanium," Phil. Mag. 26 1027 (1972).
38. Y. Hishiyama, Y. Kaburagi, A. Ono, "Variable-Range Hopping Conduction and Negative Magnetoresistance of Disordered Carbons at Low Temperatures," Carbon 17 265-76 (1979).
39. D. Emin, "Phonon-Activated Jump Rate in Noncrystalline Solids," Phys. Rev. Lett. 32 303-7 (1974).
40. E. Gorham-Bergeron, D. Emin, "Phonon-Assisted Hopping Due to Interaction with Both Acoustical and Optical Phonons," Phys. Rev. B15 3667-80 (1977).

41. G. Ahmed, J. A. Blackman, "Influence of Defect Phonon Modes on Hopping Conduction, I. Formalism," Phil. Mag. B42 517-28 (1980).
42. G. Ahmed, J. A. Blackman, "Influence of Defects Phonon Modes on Hopping Conduction, II. Numerical Results," Phil. Mag. B42 529-550 (1980).
43. R. M. Hill, "Hopping Conduction in Amorphous Solids," Phil. Mag. 24 1307 (1971).

## APPENDIX C

### Hall Effect Mechanisms

The Hall effect in glassy carbon is insensitive to temperature, and is not a function of magnetic field up to five tesla, but is a strong function of heat treatment temperature.

As mentioned in the introduction, the Hall effect for most carbon materials is sensitive to many variables, among them temperature, magnetic field, strain, impurities, and defect structure. There is no theory that adequately describes the Hall effect in perfect single crystal graphite, and therefore much less so in heavily defective carbons. In the following discussion of the Hall effect, the Hall effect for each of the transport mechanisms responsible for electrical conduction are addressed, beginning with the strongly scattering metallic conductivity.

Friedman<sup>1,2,3</sup> has worked out the Hall coefficient and Hall mobility for a random phase model (RPM). This model applies for conductivity by extended states where the scattering length approaches the lattice or nearest neighbor spacing. He writes that the Hall coefficient

$$R_H = \frac{6\bar{nz}}{ecW N(E_F)} \quad , \quad (C1)$$

the Hall mobility  $\mu_H$

$$\mu_H = 4\pi(ea^2/h)(a^3 JN(E_c))(\eta \bar{z}/z) \quad , \quad (C2)$$

and the ratio of the Hall mobility to the drift mobility is

$$\mu_H/\mu_D = \frac{6kT}{J} (\eta \bar{z}/z) \quad (C3)$$

where  $W$  is the bandwidth,

$z$  is the number of nearest neighbors

$\bar{z}$  is the number of closed loops about a site

$N(E_F)$  is the density of states/ev at the Fermi level and

$\eta$  is a constant less than unity and

$J$  is the transfer energy integral between sites.

It should be noted that  $R_H$  is inversely proportional to  $N(E_F)$ ; for a judicious choice of constants it is given as

$$R_H = \frac{C}{necg} \quad (C4)$$

where  $g = N(E_F)/N(E_F)$  free electrons and  $C \approx 0.7$ . Similar results have been found by Kaneyoshi,<sup>4</sup> Ziman,<sup>5</sup> and Straub et al.<sup>6</sup>

The Hall mobility and coefficient for hopping conduction are not well known.<sup>7,8</sup> Proposed forms for the mobility range from constant<sup>9,10</sup> to weakly activated as the hopping conductivity<sup>11,12</sup> proportionality constant ( $\exp(-T^{-1/4})$ ), to thermally activated.<sup>13</sup> However, in most cases, the Hall coefficient and mobility are small, and are expected to be minor components in the present case.

The Hall coefficient for the low temperature one dimensional wire correction has not been predicted, but is expected to be small especially if the dominant mechanism is localization diffusion.

The Hall effect cannot in general be used to predict the density of carriers or even whether the majority carriers are electrons or holes. This sign anomaly is dependent not only on the number of nearest neighbor sites, but also on the transfer integral or bonding between sites.<sup>7,8,9,14,15,16</sup> A number of authors have commented on the anomaly of carrier sign between the Hall coefficient and thermopower in chalcogenide glasses, and amorphous germanium and silicon.<sup>17</sup>

As Figure III.23 shows, the Hall coefficient in glassy carbon is a strong function of heat treatment temperature, having a minimum at about 1200°C and crossing over from negative to positive with increasing temperature at about 1700°C. This is an indication that there is a change in the microstructure occurring with increasing heat treatment temperature, but due to the ambiguities cited above, the exact nature of the microstructural transformation cannot be deduced from the Hall coefficient. Figure III.21&22 show that the Hall coefficient and mobility are nearly constant with measurement temperature; no clear trends are observed. The Hall effect is not a function of the magnetic field up to 5 tesla; Jirmanus et al.<sup>18</sup> detected no magnetic field dependence up to 15 tesla in the Hall measurements that they made.

If it is assumed that the measured Hall coefficient is due entirely to contribution from the random phase metallic model and the formula  $R_H = C/neg$  holds, then for glassy carbon heated at 2700°C, which shows the largest Hall coefficient for material in this study and for which the model assumption should be most justified, the predicted

number of carriers is  $7 \times 10^{19}/\text{cm}^3$ . Through electron spin resonance Orzeszko and Yang<sup>19</sup> measured  $5 \times 10^{18}$  spins/ $\text{cm}^3$  in their high heat treatment temperature glassy carbon.

The thermopower of glassy carbon should at least give a reliable indication of the majority carrier. However, only sketchy data has been collected in the heat treatment temperature range of interest. Yamaguchi<sup>20</sup> found that the thermopower at room temperature is positive and increases similarly to the Hall coefficient for heat treatment temperatures greater than about  $2000^\circ\text{C}$ . Tsuzuku and Saito<sup>21</sup> found in their glassy carbon that the thermopower follows fairly well the Hall coefficient they measured for similar measurement temperatures. A survey of the thermoelectric effect in the glassy carbon in this work at room temperature showed that the thermopower remained positive for all heat treatment temperatures.

The Hall effect data show that the constancy of the Hall coefficient with measurement temperature observed by earlier investigators is observed for much lower temperatures than  $20^\circ\text{K}$  down to  $3^\circ\text{K}$ . The theoretical basis for the Hall effect in glassy carbon is thought to be due to a random phase model applicable to strongly scattering metals, with minor components attributed to hopping conductivity and any low temperature corrections. Unfortunately, except perhaps at the highest heat treatment temperatures, no other parameters such as carrier concentration can be derived from the measurements. The calculated carrier concentration for glassy carbon heat treated at  $2700^\circ\text{C}$  is  $7 \times 10^{19}$  holes/ $\text{cm}^3$ .

REFERENCES FOR APPENDIX C

1. L. Friedman, "Hall Conductivity of Amorphous Semiconductors in the Random Phase Model," J. Non-Cryst. Sol. 6 329-341 (1971).
2. L. Friedman, "The Hall Effect in Ordered and Disordered Systems," Phil. Mag. 38 467-476 (1978).
3. L. Friedman, "Hall Conductivity in the Random-Phase Model," Phil. Mag. 41 347-50 (1980).
4. T. Kaneyoshi, "Hall Coefficient in a Narrow Band: Random Phase Model," J. Phys. C 5 L247-9 (1972).
5. J. M. Ziman, "The Electron Transport Properties of Pure Liquid Metals," Advan. Phys. 16 551 (1967).
6. W. D. Straub, H. Roth, W. Bernard, S. Goldstein, J. E. Mulhern, Jr., "Galvanomagnetic Investigation of the Metal-Nonmetal Transition in Silicon," Phys. Rev. Lett. 21 752 (1968).
7. H. Bottger, V. Bryskin, "A Theory of the Hall Effect in the Hopping Region in Disordered Systems I. Rate Equation in the Presence of Electrical and Magnetic Fields," Phys. Stat. Sol. (b) 80 569-578 (1977).
8. H. Bottger, V. Bryskin, "Hopping Conductivity in Ordered and Disordered Solids (II)" Phys. Stat. Sol. (b) 78 415-451 (1976).
9. P. N. Butcher, A. A. Kumar, "The Hall Mobility of Carriers Hopping in an Impurity Band," Phil. Mag. B42 201-12 (1980).
10. P. N. Butcher, "Calculation of Hopping Transport Coefficients," Phil. Mag. B42 799-824 (1980).

11. L. Friedman, M. Pollak, "The Hall Effect in the Variable-Range-Hopping Regime," *Phil. Mag.* B44 487-507 (1981).
12. M. Gruenewald, H. Mueller, P. Thomas, D. Wuertz, "The Hopping Hall Mobility - A Percolation Approach," *Sol. St. Comm.* 38 1011-4 (1981).
13. L. Friedman, T. Holstein, "Studies of Polaron Motion - Part III: The Hall Mobility of the Small Polaron," *Ann. Phys.* 21 494 (1963).
14. D. Emin, "Sign of the Hall Effect in Hopping Conduction," *Phil. Mag.* 35 1189-98 (1977).
15. R. W. Munn, W. Siebrand, "Sign of the Hall Effect for Hopping Transport in Molecular Crystals," *Phys. Rev.* B2 3435 (1970).
16. J. Holstein, "Theory of Transport Phenomena in an Electron-Phonon Gas," *Ann. Phys.* 27 410-535 (1964).
17. N. F. Mott, E. A. Davis, "Electronics Processes in Non-Crystalline Materials," 2nd ed., Clarendon Press, Oxford, Ch. 5-9 (1979).
18. M. Jirmanus, H. H. Sample, L. J. Neuringer, "Low Temperature Specific Heat of Glassy Carbon," *J. Low Temp. Phys.* 20 229-40 (1975).
19. A. Orzeszko, K. T. Yang, "Electron Spin Resonance in Glassy Carbon," *Carbon* 12 493-8 (1974).
20. T. Yamaguchi, "Thermoelectric Power of Glassy Carbon at High Temperature," *Carbon* 1 535-6 (1964).
21. T. Tsuzuku, K. Saito, "Electric Conduction in Glassy Carbons," *Japan. J. Appl. Phys.* 5 738-9 (1966).

APPENDIX D

Curie-Pauli Negative Magnetoresistance Parameters

Negative magnetoresistance data was fitted by least squares to the Curie-Pauli moment model. The following master model equation was generated for all heat treatment temperature (HTT °C) by fitting the parameters  $\chi$  and  $\Gamma$  for each set of data using a common  $\alpha_0$ :

$$\left| \frac{\Delta\rho}{\rho} \right|^{1/2} = \chi H + \Gamma \tanh(\alpha_0 H/T)$$

$$\left| \frac{\Delta\rho}{\rho} \right|^{1/2} = ((4.86 \times 10^{-6} \text{ HTT} + 0.00248) \pm 0.00057) H$$

$$+ ((5.19 \times 10^{-5} \text{ HTT} - 0.0645) \pm 0.0052) \tanh(\alpha_0 H/T)$$

H = magnetic field induction

T = measurement temperature

$\alpha_0 = 4.33 \pm 0.07^\circ\text{K/tesla}$

The fitted parameters are listed below and plotted in Figures IV.1 and 2.

Heat Treatment Temperature °C	$\chi$ tesla <sup>-1</sup>	$\Gamma$	st. dev. $\left  \frac{\Delta\rho}{\rho} \right ^{1/2}$
1600	.01116 ±.00026	.0084 ±.0043	.0068
1600	.00989 ±.00030	.0206 ±.0043	.0089
1600	.01143 ±.00017	.0270 ±.0026	.0047
1800	.01021 ±.00017	.0266 ±.0025	.0048

1800	.01007 ±.00016	.0287 ±.0022	.0036
2000	.01309 ±.00010	.0369 ±.0012	.0034
2250	.01197 ±.00017	.0578 ±.0022	.0046
2350	.01266 ±.00171	.0559 ±.0018	.0034
2550	.01526 ±.00108	.0705 ±.0017	.0049
2550	.01514 ±.00016	.0704 ±.0012	.0036
2550	.01492 ±.00015	.0718 ±.0002	.0040
2700	.01648 ±.00013	.0709 ±.0001	.0034
2700	.01595 ±.00010	.0713 ±.0001	.0030

APPENDIX E

Kobayashi Model Parameters

The square root of the absolute value of the negative magnetoresistance was modeled as proportional to the paramagnetic moment as derived by Kobayashi et al.

$$\left| \frac{\Delta\rho}{\rho} \right|^{1/2} = Q \ln \frac{\cosh X + Z}{\cosh X - Z} ;$$

$$Q = \frac{N(0)g\mu_B \sinh X}{\beta Z}$$

$X = \beta g \mu_B H$  ;  $\beta = (kT)^{-1}$   $T =$  Temperature,  $k =$  Boltzman's Constant

$\mu_B =$  Bohr magneton

$g =$  effective number of Bohr magnators =  $6.2 \pm 0.1$

$H =$  Magnetic field induction

$Z = (\cosh^2 X - P)^{1/2}$

$P = e^{-U/T}$ ;  $U =$  intra-state correlation energy/ $k$

The parameters of  $Q$  and  $U$  were fitted by least squares keeping the number of Bohr magnetons constant. Figures IV.11 and 12 are plots of the tabulated values of  $Q$  and  $U$  below as a function of heat treatment temperature (HTT °C).

$$Q = (6.77 \times 10^{-7}/^\circ\text{K} \times \text{HTT}) + 9.0 \times 10^{-5} \text{ } ^\circ\text{K}^{-1};$$

standard error of estimate =  $.00096 \text{ } ^\circ\text{K}^{-1}$

$$U = (0.0283 \text{ } ^\circ\text{K} \times \text{HTT}) - 28.7 \text{ } ^\circ\text{K} \text{ (HTT} < 2200 \text{ } ^\circ\text{C});$$

standard error of estimate =  $4.7 \text{ } ^\circ\text{K}$

$$U = 36.2 \pm 0.9 \text{ } ^\circ\text{K} \text{ (HTT} > 2200 \text{ } ^\circ\text{C)}$$

Heat Treatment Temperature °C	Q °K <sup>-1</sup>	U °K	st. dev $\left  \frac{\Delta\rho}{\rho} \right ^{1/2}$
1600	.001236 ±.000027	9.057 ±.020	.0072
1600	.001189 ±.000027	16.954 ±.027	.0094
1600	.001317 ±.000016	22.084 ±.014	.0052
1800	.001174 ±.000014	23.629 ±.012	.0049
1800	.001176 ±.000012	24.991 ±.008	.0036
2000	.001537 ±.000007	24.057 ±.005	.0033
2250	.001514 ±.000010	35.935 ±.007	.0046
2350	.001559 ±.000009	34.465 ±.006	.0034
2550	.001865 ±.000010	36.820 ±.005	.0056
2550	.001852 ±.000013	37.448 ±.008	.0052
2550	.001864 ±.000012	36.449 ±.007	.0052
2700	.001960 ±.000008	35.837 ±.005	.0047
2700	.001919 ±.000010	36.453 ±.006	.0042

APPENDIX F

Bright Model Parameter

The linear parameter  $\beta$  for the Bright model, fitted by least squares for each heat treatment temperature using only the low field (less than 1.5 tesla) negative magnetoresistance data. The tabulated parameters below are plotted in Figure IV.13.

$$\left| \frac{\Delta\rho}{\rho} \right|^{1/2} = \beta H/T^{1/2}$$

Heat Treatment Temperature °C	$\beta$ °K <sup>1/2</sup> tesla <sup>-1</sup> st. dev.	$\left  \frac{\Delta\rho}{\rho} \right ^{1/2}$
1600	.0507 ±.0035	.0081
1800	.0473 ±.0023	.0052
2000	.0679 ±.0021	.0051
2250	.0845 ±.0022	.0042
2350	.0941 ±.0037	.0061
2550	.1320 ±.0020	.0063
2700	.1267 ±.0020	.0061

APPENDIX G

Electrical Conductivity Model Parameters

The electrical conductivity was modeled according to the equation

$$\sigma = A + B \exp(-C_0 T^{-1/4}) - DT^{-1/2}$$

Using a common  $C_0$ , all of the data was fitted by least squares simultaneously. When the parameters A, B, and D, tabulated below, are considered as functions of heat treatment temperature (Figures IV.22, 23, and 21), the following master equation was developed as an approximation:

$$\begin{aligned} \sigma(\Omega\text{-cm})^{-1} &= 176 \pm 15 + (652 \pm 101) \exp(-C_0 T^{-1/4}) \\ &- ((-0.0137 \times \text{HTT}) + 30.7) \pm 3.7 T^{-1/2} \end{aligned}$$

HTT = heat treatment temperature °C if less than 2200°C

= 0 otherwise

$C_0 = 14.5 \pm 0.3^\circ\text{K}^{1/4}$

st. dev. = 0.28 (ohm-cm)<sup>-1</sup>

The standard deviations increase significantly for high heat treatment temperatures because the third parameter D is ill-conditioned and should be set identically to zero.

Heat Treatment Temperature °C	A ( $\Omega\text{-cm}$ ) <sup>-1</sup>	B ( $\Omega\text{-cm}$ ) <sup>-1</sup>	D ( $\Omega\text{-cm-}^\circ\text{K}^{1/2}$ ) <sup>-1</sup>
1000 (as received)	191.58 ±.04	872.98 ±.04	35.637 ±.034
1200	181.51 ±.04	783.67 ±.04	10.462 ±.039
1200	166.67 ±.04	658.08 ±.04	17.425 ±.042
1400	185.23 ±.04	680.73 ±.04	15.149 ±.042
1600	186.54 ±.24	580.92 ±.24	4.769 ±.044
1800	157.28 ±.26	513.90 ±.26	6.592 ±.256
2000	194.36 ±.27	623.38 ±.27	4.173 ±.268
2250	170.66 ±.29	545.69 ±.54	0.255 ±.282
2350	198.31 ±5.71	626.54 ±6.76	-1.199 ±5.654
2550	163.94 ±7.00	619.55 ±7.11	.336 ±6.901
2550	161.76 ±7.47	719.69 ±8.73	-2.152 ±7.199
2700	157.67 ±10.97	603.71 ±13.92	1.193 ±10.078

This report was done with support from the Department of Energy. Any conclusions or opinions expressed in this report represent solely those of the author(s) and not necessarily those of The Regents of the University of California, the Lawrence Berkeley Laboratory or the Department of Energy.

Reference to a company or product name does not imply approval or recommendation of the product by the University of California or the U.S. Department of Energy to the exclusion of others that may be suitable.

TECHNICAL INFORMATION DEPARTMENT  
LAWRENCE BERKELEY LABORATORY  
UNIVERSITY OF CALIFORNIA  
BERKELEY, CALIFORNIA 94720